

**Genomic, transcriptomic and phenotypic analysis
of the plant growth promoting and phosphate
solubilizing *Paenibacillus riograndensis* SBR5**

DISSERTATION

Submitted by

Luciana Fernandes de Brito

for the degree of Doctor of Science

Bielefeld University,

Department of Biology

-Bielefeld, June 2017-

For my dear grandparents, Vicente e Ozita

The practical work of this thesis has been performed at Bielefeld University in the Institute of the Genetics of Prokaryotes, from October 2013 until May 2017 under the supervision of Prof. Dr. Volker F. Wendisch.

Examiners

Prof. Dr. Volker F. Wendisch
Chair of Genetics of Prokaryotes
Faculty of Biology & CeBiTec, Bielefeld University

Prof. Dr. Trygve Brautaset
Department of Biotechnology and Food Science
Norwegian University of Science and Technology

Parts of this thesis have been published in:

Brito LF, Bach E, Kalinowski J, Rückert C, Wibberg D, Passaglia LM, et al. Complete genome sequence of *Paenibacillus riograndensis* SBR5, a Gram-positive diazotrophic rhizobacterium. *J. Biotechnol.* 2015;207:30–1.

Brito LF, Irla M, Kalinowski J, Wendisch VF. Detailed transcriptome analysis of the plant growth promoting *Paenibacillus riograndensis* SBR5 using RNAseq technology. *BMC Genomics* [submitted].

Brito LF, Irla M, Walter T, Wendisch VF. Magnesium aminoclay-based transformation of *Paenibacillus riograndensis* and *Paenibacillus polymyxa* and development of tools for gene expression. *Appl. Microbiol. Biotechnol.* 2017;735–47.

Erklärung

Die hier vorgelegte Dissertation habe ich eigenständig und ohne unerlaubte Hilfe angefertigt. Ich versichere, dass ich keine anderen als die angegebenen Quellen und Hilfsmittel benutzt, sowie Zitate kenntlich gemacht habe. Die Dissertation wurde in der vorgelegten oder in ähnlicher Form noch bei keiner anderen Institution eingereicht. Ich habe bisher keine erfolglosen Promotionsversuche unternommen.

Bielefeld, den 02.06.2017

Luciana Fernandes de Brito

Abstract

Food production increases concomitantly with the world's population, therefore the impact caused by the over fertilization of soil, especially with nitrogen and phosphate, in order to improve the crops productivity will only increase in importance. One of the putative strategies to establish more sustainable agricultural production is the use of biofertilizers which are based on plant growth promoting properties of some microorganisms. Therefore, the inoculation of crops with plant growth promoting rhizobacteria (PGPR) has emerged as relevant concept in agriculture. *Paenibacillus riograndensis* is a Gram-positive, rod-shaped, endospore forming, motile rhizobacterium. The strain SBR5 was isolated from the rhizosphere of wheat plants cultivated in Rio Grande do Sul, Brazil. In addition to nitrogen fixation, SBR5 is capable of producing the phytohormone indol-3-acetic acid and antagonistic compounds against phytopathogens and therefore is an interesting candidate for crop inoculation. However, this organism has not been characterized regarding other plant growth promoting characteristics, e. g. phosphate solubilization and production of vitamins.

In order to improve the knowledge on the metabolism and plant growth promoting activity of *P. riograndensis* SBR5, its genome was re-sequenced, assembled and fully annotated. The genome of SBR5 consists of one circular chromosome with 7,893,056 bps, containing 6,705 protein coding genes, 87 tRNA and 27 rRNA genes. Genes for biotin biosynthesis such as *bioWAFDBI* are absent from the genome of SBR5. Based on the complete genome sequence of *P. riograndensis* SBR5, a detailed transcriptome analysis of this organism was performed using RNAseq technology. To this end, *P. riograndensis* SBR5 was cultivated under 16 different growth conditions and RNA was isolated from samples collected during growth experiments and combined in order to analyze an RNA pool representing a large set of expressed genes. The resultant RNA pool was used to generate two different libraries, one enriched in 5'-ends of the primary transcripts and the other representing the whole transcriptome. Both libraries were sequenced and analyzed to identify the conserved sequences of ribosome binding sites and translation start motifs, and to elucidate operon structures present in the transcriptome of *P. riograndensis*. Sequence analysis of the library enriched in 5'-ends of the primary transcripts was used to identify 1,173 TSSs belonging to 5' UTRs of annotated genes and 1,082 belonging to novel transcripts. This allowed the determination of promoter consensus sequence and regulatory sequences in 5' untranslated regions including riboswitches.

A new transformation protocol based on physical permeation through mixing the cell suspension with a plasmid-aminoclay solution was established for *P. riograndensis* SBR5. Transformation was shown by plasmid isolation and re-transformation as well as by heterologous production of a fluorescent reporter protein. Furthermore, the *gfpUV* reporter gene was used to test rolling-circle and theta-replicating

plasmids for constitutive and inducible gene expression. Flow cytometry verified the versatility of the developed expression vectors for constitutive and graded inducible expression. These gene expression systems could be transferred to another *Paenibacillus* species, *Paenibacillus polymyxa* DSM365. In addition, rolling circle inducible gene expression was applied to metabolic engineering of *P. riograndensis*, when the heterologous expression of the biotin biosynthesis operon from *B. subtilis* *bioWAFDBI* rendered *P. riograndensis* SBR5 biotin prototrophic. Further, the developed tools for gene expression served to characterize a putative thiamine pyrophosphate (TPP) dependent riboswitch upstream of the thiamine biosynthesis gene *thiC*. This was achieved by translational fusion to a fluorescent reporter gene lacking a promoter and a ribosome binding site. The switch was shown to function as TPP “off” switch in *P. riograndensis* SBR5.

Finally, the differential gene expression analysis associated to functional study was performed aiming to evaluate the process of phosphate solubilization SBR5. SBR5 was cultivated in two distinct conditions, with NaH_2PO_4 or hydroxyapatite, which are soluble and insoluble phosphate sources, respectively. Total RNA of SBR5 cultivated in these two conditions was isolated and submitted to sequencing. The sequences underwent DESeq analysis that lead to discovery that the expression of 42 genes was upregulated and 15 genes downregulated in insoluble phosphate condition. The differential gene expression analysis showed that the expression of genes involved in glucose metabolism, including those coding for 2-oxoglutarate dehydrogenase, was downregulated in insoluble phosphate condition. Associated to that, organic acids production in the two conditions was determined, resulting in the finding that the metabolic channeling of glucose towards the tricarboxylic acid cycle is negatively regulated by insoluble phosphates. Moreover, as flagellin encoding gene was downregulated in insoluble condition, cell motility was evaluated by the means of flow cytometry revealing that motility of SBR5 cells is reduced as a response to phosphate depletion. Finally, SBR5 was able to solubilize hydroxyapatite, which suggests that this organism is a promising phosphate solubilizing bacterium.

All the information gathered here, starting from the genome, serves as groundwork for the characterization of a very promising PGPR, *P. riograndensis*. The present thesis provides insight into the *P. riograndensis* SBR5 transcriptome at the systems level and was a valuable basis for differential RNAseq analysis of this organism regarding one plant growth promoting characteristic. Moreover, the gene expression tools here developed will allow the characterization of this organism and other member of *Paenibacillus* species, because this technology is transferrable to DSM-365. However, a larger effort is still to be done in the field of characterization of plant growth promotion features in SBR5. The phosphate solubilization process for instance still needs to be studied in depth; my findings showed that SBR5 possibly changes its metabolic channeling of glucose to perform PS, which is an interesting first step for the study of this feature.

Abbreviations

PGPR	Plant growth promoting rhizobacteria
PSB	Phosphate solubilizing bacteria
BNF	Biological nitrogen fixation
IAA	Indole-3-acetic acid
OD₆₀₀	Optical density at 600 nm
MES	2-(N-morpholino)ethanesulfonic acid
MOPS	3-Morpholinopropane-1-sulfonic acid
TAPS	3-[[1,3-Dihydroxy-2-(hydroxymethyl)propan-2-yl]amino]propane-1-sulfonic acid
LB	Lysogeny broth
PbMM	<i>Paenibacillus</i> minimal medium
CDS	Coding DNA sequences
TLS	Translation start sites
TSS	Transcription start sites
RBS	Ribosome binding site
RPKM	Reads per kilobase per million mapped reads
BLAST	Basic local alignment search tool
5'UTR	5' Untranslated region
TPP	Thiamine pyrophosphate
CFU	Cell forming units
PS	Phosphate solubilization
TCA	Tricarboxylic acid
2-OGDH	2-Oxoglutarate dehydrogenase

Common (biological) abbreviations, units, and gene names are not included. Abbreviations are introduced in parentheses the first time they are used within the text and abbreviations only used in the figures are explained in each figure, but not included here.

Contents

1. INTRODUCTION.....	1
1.1. <i>Impact and importance of agriculture</i>	1
1.1.1 <i>Phosphorus dynamics in soil and impact of phosphate fertilization on the environment</i>	2
1.2. <i>Active rhizosphere: the role of plant growth promoting rhizobacteria (PGPR) in sustainable agriculture</i>	4
1.2.1. <i>Solubilization of phosphates as strategy to improve plant nutrition and growth</i>	6
1.2.2. <i>Bacillus and Paenibacillus spp. as potential PGPR</i>	8
1.2.3. <i>Paenibacillus riograndensis SBR5: a promising candidate for crop inoculation</i>	9
1.3. <i>Genome-based functional analysis of microorganisms</i>	11
1.3.1. <i>Genome-based identification of biosynthesis pathways: biotin biosynthesis pathway in microorganisms</i>	12
1.3.2. <i>Transcriptome-based identification of regulatory elements: gene regulation by riboswitches</i>	14
1.4. <i>Molecular biology tools for functional study of PGPR features</i>	17
1.5. <i>Objectives</i>	18
1.6. <i>References</i>	18
2. RESULTS.....	30
2.1. <i>Complete genome sequence of Paenibacillus riograndensis SBR5^T, a Gram-positive diazotrophic rhizobacterium</i>	30
2.1.1. <i>Abstract</i>	30
2.1.2. <i>Results and Discussion</i>	30
2.2.3. <i>References</i>	33
2.2. <i>Detailed transcriptome analysis of the plant growth promoting Paenibacillus riograndensis SBR5 using RNAseq technology</i>	35
2.2.1. <i>Abstract</i>	35
2.2.2. <i>Background</i>	36
2.2.3. <i>Materials and Methods</i>	37
2.2.4. <i>Results</i>	43
2.2.5 <i>Discussion</i>	54
2.2.6. <i>Conclusions</i>	59
2.2.7. <i>References</i>	60
2.3. <i>Magnesium aminoclay-based transformation of Paenibacillus riograndensis and Paenibacillus polymyxa and development of tools for gene expression</i>	66

2.3.1. Abstract	66
2.3.2. Introduction.....	66
2.3.3. Materials and Methods.....	68
2.3.4. Results	73
2.3.5. Discussion	83
2.3.6. References	87
2.4 Differential gene expression of phosphate solubilizing-bacterium <i>Paenibacillus riograndensis</i> SBR5 cultivated in two distinct phosphate sources.....	91
2.4.1. Abstract	91
2.4.2. Introduction.....	92
2.4.3. Materials and Methods.....	93
2.4.4. Results and Discussion.....	96
2.4.5. Conclusion.....	107
2.4.6. References	108
3. DISCUSSION	113
3.1. Basis for the characterization of <i>Paenibacillus riograndensis</i> SBR5: complete genome sequence and genome-wide transcriptome analysis	113
3.2. Transformation method and the use of genomic data to develop genetic tools for <i>P. riograndensis</i> SBR5	114
3.3 Application of the omics and gene expression toolbox in <i>P. riograndensis</i> SBR5: analysis of two B-group vitamins	118
3.3.1 Characterization of biotin auxotrophy in <i>P. riograndensis</i> SBR5	119
3.3.2. A functional thiamine pyrophosphate riboswitch present in <i>P. riograndensis</i> SBR5	121
3.4. First insights on the phosphate solubilization process in <i>P. riograndensis</i> SBR5.....	123
3.5. Final Remarks	127
3.6. References	128
4. APPENDIX	138

1. INTRODUCTION

1.1. Impact and importance of agriculture

In the past years, the demand for agricultural commodities has grown extensively. Main factors that drive increasing food demand are population growth, expanding urbanization and rise in income. With regard to the first point, human population size is projected to grow up by 34% by 2050, reaching 9.1 billion people [1]. Food production has increased over the past years and is predicted to grow further while the area of cultivated land expands at a slow rate (Table 1). Moreover, it is to be noted, that in the future the total demand for agricultural commodities may significantly exceed the demand for food and feed because of the expansion of technologies enabling the conversion of agricultural biomass into biofuels [1]. Furthermore, arable land resources are limited and significant portions of world's agricultural lands are currently being converted from food to fuel crop production. Due to the growing human population (Table 1) and the rising demand for biofuels, the major food competitor for land use, the crops yields must increase.

Table 1. Global progress in food production, population, cultivated land, CO₂ emissions caused by agriculture and fertilizer consumption over the years. Total food production (mega tones- Mt); world's population (in 1,000 people - both sexes); cultivated lands (hectares- ha); global emissions of CO₂ caused by agriculture (in Gg of CO₂eq); and world's total consumption of fertilizers in agriculture (tones - t) in 1960, 2000 and the prediction for the 2030 decade. Data adapted from Vance et al [2], FAO [1] and FAOstat [3].

Item	1960	2000	2030 –2040
Food production (Mt)	1.8×10^9	3.5×10^9	5.5×10^9
Population	3.0×10^6	6.1×10^6	9.1×10^6
Cultivated land (ha)	1.3×10^9	1.5×10^9	1.8×10^9
CO ₂ emissions (Gg)	2.7×10^6	4.6×10^6	-
fertilizer consumption (t)	3.3×10^7	4.0×10^8	-

There are many strategies in the modern agronomy that lead to sharp increase of yields from crop cultivations: development of agrochemicals and fertilizers, plant breeding technologies, techniques of soil management and development of agricultural machinery. Yet, while the advance in the agronomical field is an imperative to support the global demand for food, it has caused substantial negative impact on human health, for example the human poisoning caused by pesticides which has been reported since the 1960 decade [4]. The environmental hazards caused by the advances in agriculture are also an important factor; one of the indicators of this impact is the global CO₂ emissions caused by agriculture, which had a

Introduction

crescent tendency (Table 1). Moreover, the fertilizer application on soil causes significant water and soil contamination, not only by the accumulation of excessive fertilizer amounts in soil and groundwater, but also by the fertilizer-derived radioactivity and heavy metal contamination [5,6]. The occurrence of those incidents may increase if the fertilizer consumption keeps the rising tendency observed in the past decades (Table 1).

1.1.1 Phosphorus dynamics in soil and impact of phosphate fertilization on the environment

Phosphorus (P), together with nitrogen and potassium, is an essential element for plant and animal growth and is necessary to maintain sustainable crop and livestock production. This element is involved in processes of energy generation, photosynthesis, glycolysis, respiration, membrane synthesis and stability, enzyme activation and inactivation, redox reactions, signaling and nitrogen fixation, and it is a component of the structure of carbohydrate esters, phospholipids, coenzymes and nucleic acids. The concentration of P in plants varies from 0.05 to 0.5% of the dry weight and it is known that P availability influences the development of plants and their fruits [2]. In general, P deficiency causes chlorosis in older plant leaves followed by necrosis in the leaf margins, while stressed younger leaves present a curled shape. This effect can be observed for example in the economically relevant soybean culture [7].

Figure 1 shows that, in the soil, P exists in various chemical forms, either inorganic: secondary P minerals precipitated with calcium (CaP) manganese (MnP), iron (FeP) and aluminum (AlP), or organic: as inositol phosphates (phytates), phosphonates (PN), and organic polyphosphates (OPP) [8]. P in the soil is formed in the process of weathering of primary minerals, which is slow and depends on several conditions, rarely naturally occurring in the soil. As an example, the release of P during the dissolution of apatite rocks (CaP) is controlled by diverse factors, such as soil pH and composition, temperature, and surface area [9]. In long-term, P can also be released to the soil from microbe, plant and animal remains and manure [10]. However, the concentration of soluble P in soil is usually very low: less than 0.1% of the P exists in its labile form (free in soil solution as orthophosphate ions HPO_4^{-2} and $\text{H}_2\text{PO}_4^{-1}$) which can be taken up by plants [11]. It is a general knowledge that substantial part of the P present in the soil is immobilized, adsorbed in soil colloids or chemically precipitated as CaP or AlP depending on the soil pH [12]. The desorption of the P adsorbed in soil colloids exist mostly due to a complex equilibrium with soil solution, while the mineralization or dissolution of immobilized and precipitated P, respectively, is mostly performed by the soil microbiota [8].

Introduction

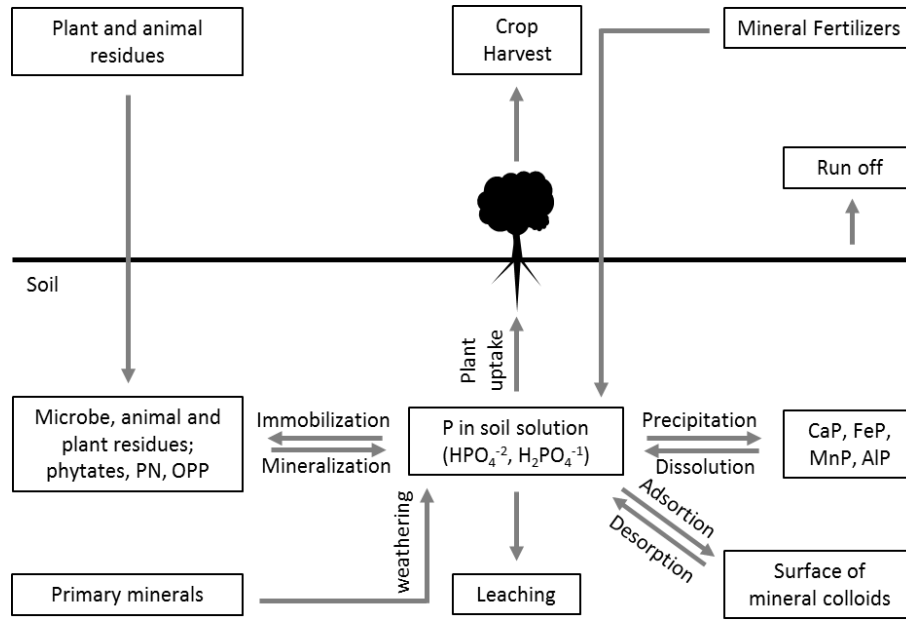


Figure 1. P dynamics in the soil-plant continuum. PN- phosphonates, OPP-organic polyphosphates, CaP- calcium phosphates, FeP- iron phosphates, MnP- manganese phosphates, AIP- aluminum phosphates.

The availability of P in the soil is a critical factor for plant growth, and the application of P fertilizers is a major problem of intensive agriculture. It has been documented that relevant cultivated plants demonstrate high demand for phosphate source for growth: to yield of up to 9 t ha^{-1} , maize crop requires an uptake of 50 kg P ha^{-1} ; the production of approximately 3 t ha^{-1} of small grains takes up 22 kg P ha^{-1} ; soybean plants demand 25 kg P ha^{-1} [13]. However, it is estimated that only 20% of the P applied in soil is taken up by plants due to its retention by the soil [14]. The low rate of P uptake by plants leads to the overload of P fertilizer into the soil by the farmers. Hence, the P fertilizer utilization increased substantially over the years (Figure 2). This scenario leads to the occurrence of the main environmental hazard caused by P fertilization, eutrophication of lakes and marine estuaries, mainly caused by the run-off of the remaining P from fertilized agricultural land [2]. Moreover, rock phosphates are a non-renewable resource and can be used up in a near future due to mining exploration (estimation of approximately 60 years) [2].

Introduction

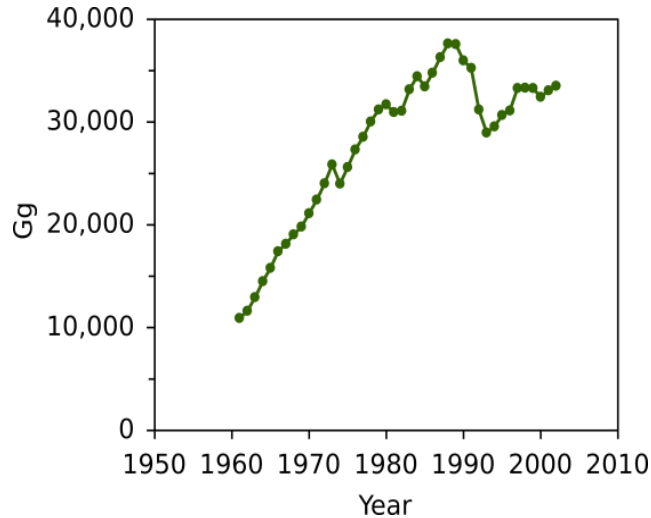


Figure 2. Global annual consumption of phosphate fertilizers. The consumption of phosphate fertilizers is represented in Gg, since 1961 to 2004. Data adapted from FAOstat [3].

In the present, as the society requires more of agricultural resources to feed expanding populations, impact of phosphate to improve the crop productivity will only increase in importance. Hence, sustainable methods to increase the labile P content in the soil must be developed. One of the putative strategies to establish more sustainable agricultural production is the use of biofertilizers which are based on plant growth promoting properties of some microorganisms. The global biofertilizer market is dominated by biofertilizers designated to the nitrogen fixation process, covering around 77% thereof. Despite the big difference in number, the biofertilizers designated to enhance phosphate solubilization occupy the second place in this market, with around 14% of the share [15].

1.2. Active rhizosphere: the role of plant growth promoting rhizobacteria (PGPR) in sustainable agriculture

Currently, the biofertilizer market occupies 5% of global fertilizer market [15]. The interaction between plants and microbes (e. g. PGPR, mycorrhizal fungi or rhizobia) is essential for plant growth. PGPR are the group of bacteria (which does not include rhizobia) inhabiting the root surroundings and are directly or indirectly involved in promoting plant health, growth and development via production and secretion of several regulatory chemicals and enzymes [16]. The application of PGPR to benefit crops is a potential way to reduce the environmental impact caused by the conventional agriculture. In the recent years, the use of biofertilizers has emerged as relevant component in agriculture, especially due to the biological nitrogen fixation (BNF). The association between plants and PGPR starts by the phenomenon called “rhizosphere effect”. It involves the attraction and establishment of a microbiota around the plant

Introduction

root at the time of the seed germination, due to the liberation of organic metabolites [17]. The microbial migration towards the rhizosphere is a key factor for plant-microbe association and the microbial motility increases the probability of plant-microbe interaction in the soil [18]. To maintain the associated microbes, the liberation of components such as root exudates, lysates and mucilage by the plant is needed [19]. Generally, 40% of the plant photosynthates are allocated to the rhizosphere [20]. These components contain a large variety of chemicals beneficial for microbes such as amino acids, sugars, flavonoids, vitamins and organic acids, which are utilized for microbial growth [18]. Moreover, surface proteins and polysaccharides are released by plants to promote the adherence of some rhizobacteria to the plant root [21].

There are many benefits emerging from the rhizosphere microbiota in exchange to the components produced by plants. Many PGPR species are well characterized as non-legume nitrogen fixing bacteria, such as *Azospirillum*, *Gluconacetobacter*, *Herbaspirillum*, *Burkholderia*, *Klebsiella* and *Pseudomonas* [22]. Non-symbiotic BNF is carried out by a diverse group of PGPR that enzymatically reduce atmospheric dinitrogen (N_2) to ammonia. The biological reduction of N_2 is catalyzed by an enzymatic complex, nitrogenase [23]. Although the concentration of fixed nitrogen by PGPR is not as high as that measured in legumes nodulated by rhizobia, their BNF contribution to plant growth in field conditions (determined by $^{15}N_2$ incorporation studies and nitrogenase activity assays) have been reported foremost for sugarcane and rice [24] and recently for maize [25].

Moreover, PGPR produce metal-chelating agents called siderophores that possess the ability to solubilize and bind iron from soil precipitates, making this element available for the plant uptake [26,27], which leads to an increased percentage of seed germination and induction of the plant growth [28]. Bacterial cells mainly produce siderophores under iron starvation conditions, because they need such substances to improve their own iron uptake [29]. Among the siderophore-producing bacteria, the siderophore production by *Pseudomonas* spp. is well documented [30–32], but can also be observed in *Klebsiella* [33], *Azotobacter* [34] and bacilli [35,36].

Plant hormones have a major role in regulation of a plant growth. Many rhizobacteria are able to produce phytohormones which are structurally unrelated small molecules. Phytohormones produced by bacterial communities improve plant health and immunity by influencing regulatory processes [37]. The phytohormone-producing PGPR promote beneficial effects on plant health and growth, suppress phytopathogens and accelerate nutrient availability and assimilation. Phytohormones may regulate many aspects of plant growth, such as apical dominance, root gravitropism, root hair, lateral root, leaf, and flower formation, and plant vasculature development [38,39]. Examples of compounds that are classified as phytohormones are indole-3-acetic acid (IAA), and other auxins, abscisic acid, cytokinin, gibberellin and ethylene [40]. It is documented that inoculation with the IAA producing strains of *Pseudomonas aeruginosa* leads to the increased yield of sesame plants by approximately 40% [41].

Introduction

Furthermore, rhizospheric halotolerant IAA producing bacterium *Kocuria turfanensis* is able to promote growth of peanut both in non-saline and saline soils [42].

The PGPR can act as biocontrol agents and reduce the use of synthetic chemicals for controlling plant pathogens such as bacteria, fungi, oomycetes, protozoa, nematodes and also weeds [43,44]. The biocontrol activity can be mediated by the competition for rhizosphere colonization area. As the rhizosphere is a significant carbon sink [18], there is a variety of nutrient-rich niches in this environment which attract great diversity of microorganisms, including plant pathogens. The promoted competition for these niches is a known mechanism by which PGPR protects plants from pathogens colonization [45]. A diverse group of PGPR, including *Pseudomonas fluorescencens*, *Bacillus subtilis* and *Streptomyces libani* [46–48], can also promote biocontrol by releasing antibiotics into the environment. Antibiosis between bacteria is very broad, including production of phenazines, phloroglucinols, pyoluteorin, pyrrolnitrin, cyclic lipopeptides (all of which are diffusible) and hydrogen cyanide (which is volatile) for control of root diseases [49]. The production of lytic enzymes [50], induction of systemic resistance (e. g. activation of $[+]\text{-}\delta\text{-cadinene}$ synthase in cotton against *Spodoptera exigua*; [51]), production of IAA and small chelating components such as the above-mentioned also contribute to bacterial biocontrol activity.

Lastly, some PGPR has the ability to promote the solubilization of immobilized phosphates in soil [52]. Although the physiology of phosphate solubilization has not been studied thoroughly, some scientific insights on this process have been published and are presented in the following chapter.

1.2.1. Solubilization of phosphates as strategy to improve plant nutrition and growth

Phosphate solubilizing bacteria (PSB) possess the ability to solubilize the immobilized P from soil. PSB serve as efficient biofertilizer candidates for improving the P nutrition of crop plants [53]. The plant growth promoted by PSB has been tested, showing the potential of those organisms to contribute to the P uptake in pea [54] and greengram [16]. The PSB *Pseudomonas putida* along with the nitrogen fixing bacteria *Azospirillum* spp. and *Azotobacter* spp led to significant increase of germination and plant development of artichoke [55]. Furthermore, when co-inoculated with rhizobia, the PSB *Pseudomonas* sp. applied on wheat crop significantly increased the seed yield and the plant P uptake [56]. PSB are greatly abundant in the rhizosphere of non-legume plants [57]. There are different bacterial genera with this capacity such as *Pseudomonas*, *Bacillus*, *Rhizobium*, *Burkholderia*, *Achromobacter*, *Agrobacterium*, *Micrococcus*, *Aereobacter*, *Flavobacterium* and *Erwinia* [52].

The physiology of mineral phosphate solubilization processes in bacteria is not well understood. Nevertheless, as a core phenotype, the phosphate-solubilizing activity of PSB is induced by the exogenous depletion of water soluble phosphates [58]. There are few known strategies for the P solubilization by bacteria e.g. synthesis of organic acids and expression of alkaline/acid phosphatases, phosphonatases and phytases.

Introduction

Synthesis of organic acids has been well recognized and widely accepted as principal P solubilization strategy by bacteria. Organic acids have the potential to increase the availability of P in the soil [59,60]. This event occurs due to the chelating properties of the organic acids [61]. Moreover, the synthesis of organic acids leads to the acidification of the bacterial surroundings; this may promote the solubilization of apatite by proton substitution of H^+ and release of Ca^{2+} [62]. It is known that the phosphate solubilization rate by bacteria depends on the carbon source in the medium [63]. Moreover, the deficiency of soluble phosphate in the medium leads to the change of the metabolic carbon flux in bacteria, altering the profile of secondary metabolites production [64]. Gluconate is predominantly produced by bacteria at low levels of soluble phosphate. For *Pseudomonas frederiksbergensis*, the production of gluconate, tartrate, and oxalate is reduced with the increase of concentration of soluble phosphate in its environment [65]. It is documented that production of gluconate in the reaction catalyzed by glucose dehydrogenase, which requires pyrroloquinoline quinone (PQQ) as cofactor, is a primary mechanism behind phosphate solubilization [63,66]. Different kinds of organic acids (e. g. citrate, gluconate, lactate, succinate and propionate) can be detected in PSB culture broths supplemented with insoluble phosphate as single P source [53]. Moreover, the phosphate solubilization by *Bacillus* sp. is related to production of oxalate and malate [60]. However, the influence of organic acids on phosphate solubilization by bacteria is very complex and need to be studied deeply.

Acid and alkaline phosphatases can act in phosphate solubilization by removing phosphate groups from phosphorylated compounds and catalyzing the hydrolysis of ester-phosphate bonds, leading to the release of free phosphate in the soil, which can be taken up by plants [67]. It was previously shown that plant available P concentration in the rhizosphere, as well as shoot P levels closely mirrored acid and alkaline phosphatase activity in the rhizosphere of several plant species [68]. Moreover, acid phosphatase activity can be observed in acid conditions while alkaline phosphatase is active under neutral or alkaline conditions [69]. Acid phosphatase activity is mainly found in members of *Enterobacteriaceae* [70] while alkaline phosphatase activity can be observed in *Pseudomonas* [71]. The best studied system for the regulation of phosphatases is the *pho* regulon, which is an important two-component regulatory operon acting as a sensor responding to soluble phosphate in signaling processes. This two-component transcriptional factor regulates the expression of several *pho* regulon genes, such as the alkaline phosphatase genes *phoA* and *phoB* and the APase-alkaline phosphodiesterase gene *phoD* [72].

In organic soils, the phosphate solubilization may be mediated by the cleavage of the C-P bond of organophosphonates by phosphonatases (C-P lyases) activity under conditions of phosphate limitation [73,74]. Furthermore, phytase activity can be detected in PGPR, e. g. in *Streptomyces* [75], *Pseudomonas*, *Enterobacter*, and *Pantoea* [76]. Phytases are enzymes which catalyze the hydrolysis of phytate, releasing less phosphorylated *myo*-inositol and plant available phosphate forms [52] and phytase-producing PGPR are interesting targets for organic agriculture.

Introduction

The physiology and molecular basis of phosphate solubilization is not fully elucidated yet and the knowledge on genes expressed in PBS during solubilization of immobilized phosphates remains elusive. Nevertheless, *Bacillus* and *Paenibacillus* species are prominent examples of PGPR candidates which are interesting for further phosphate solubilization studies [77].

1.2.2. Bacillus and Paenibacillus spp. as potential PGPR

This thesis focused on characterization of a promising candidate for PGP use, *Paenibacillus riograndensis* SBR5, which belongs to *Paenibacillus* genus. Members of the genera *Bacillus* and *Paenibacillus*, which belong to the phylum Firmicutes, are Gram-positive, facultatively aerobic and endospore forming bacteria [78]. They formerly belonged to the same genus; however, members of the group 3 within the genus *Bacillus* were transferred to the genus *Paenibacillus*, by the proposal of Ash et al. [79], in which *Paenibacillus polymyxa* was suggested as the new genus type species. Multiple species of these two genera can promote plant growth and health in a variety of ways. Most species of *Bacillus* and *Paenibacillus* are globally widespread and have been isolated from rhizosphere soils and plant tissues [80–82]. They are interesting candidates to use as biofertilizers due to their PGP features such as, N₂ fixation properties, synthesis of phytohormones, biocontrol of plant pathogens and P solubilization.

Many isolates of *Paenibacillus* species, are able to fix nitrogen [83–86]. The presence of *nif* genes, related to nitrogenase activity, is highly conserved in the majority of the *Paenibacillus* nitrogen fixing species [87]. Likewise, *B. subtilis* and *Bacillus amyloliquefaciens* present nitrogenase activity [88]. Moreover, inoculation of maize plants with *Bacillus pumilus* contributed to the development of plants and led to the N₂ fixing contribution of around 30% of total N uptake [89]. *Bacillus* and *Paenibacillus* species can also contribute indirectly to N₂ fixation when applied during the co-inoculation with legume symbionts; they increase plant development by stimulating the signaling between plant host and symbiont [90]. Moreover, the co-inoculation of PSB *Paenibacillus polymyxa* and *Bacillus megaterium* with rhizobia increased the growth and P uptake of common beans [77]. Finally, soybean plants produced longer roots and shoots than those of control plants when inoculated with the non-symbiont *Bacillus aryabhatai* [91].

Furthermore, many *Bacillus* and *Paenibacillus* species are able to produce plant phytohormones. *B. subtilis* and *B. amyloliquefaciens* isolated from rhizosphere of cucumber produce high levels of IAA [92]. Furthermore, inoculation of *B. amyloliquefaciens* into tomato plants increased the plant development and fruit size [93]. Occurrence of *Bacillus* and *Paenibacillus* species was observed in the rhizosphere of sunflower and its isolates could produce up to 100 µg of indolic compounds per mL of culture medium [94]. Rice inoculation with *Bacillus* species led to considerable impact on different growth parameters of this plant including germination percentage, shoot and root growth and chlorophyll content as compared to negative control, due to the influence of IAA produced by bacteria [95]. *B. amyloliquefaciens* has the ability to produce gibberellin and its inoculation into seedlings can be beneficial to rice plants [96]. The

Introduction

inoculation with *B. amyloliquefaciens* promotes salt tolerance of maize by reducing the level of sodium in the rhizosphere; in response to the salinity stress, this bacterium produces the phytohormone abscisic acid which promotes the growth of maize plants [97].

Several strains belonging to the species of *B. amyloliquefaciens*, *B. subtilis*, and *B. pumilus* elicit significant reductions in the incidence rate or severity of various diseases caused by pathogens including *Fusarium*, *Rhizoctonia* and *Pythium* [98]. Furthermore, competition assays revealed antagonistic potential of *Paenibacillus pasadenensis* against *Botrytis cinerea* [99].

Bacillus and *Paenibacillus* ssp. participate in P solubilization processes in soil. The general P solubilization strategies of PGPR were described in detail in a previous chapter. However, here strategies mentioned here are typical for *Bacillus* and *Paenibaicillus* ssp. which are the main focus of this thesis. *In silico* analyses suggest that most *Paenibacillus* strains can solubilize phosphorus by the production of gluconate: a study of 35 strains comprising 18 strains belonging to *Paenibacillus* species revealed that the majority of them possess gene candidates encoding glucose dehydrogenase and gluconate dehydrogenase. The putative PSB included strains from the species *Paenibacillus azotofixans*, *Paenibacillus graminis*, *P. polymyxa*, *Paenibacillus sabinae*, *Paenibacillus sonchi*, *Paenibacillus vortex*, and *Paenibacillus zanthoxyli* [100].

1.2.3. Paenibacillus riograndensis SBR5: a promising candidate for crop inoculation

P. riograndensis SBR5 was isolated from wheat (*Triticum aestivum*) cultivated in fields in the south of Brazil [82]. It is a rod-shaped, facultatively anaerobic, endospore forming bacterium (Figure 3) and was proven to possess PGP activity. Specifically, this organism showed the ability to fix nitrogen and to produce siderophores and indole-3-acetic acid. The strain SBR5 is closely related to *P. graminis* RSA19^T, *P. odorifer* TOD45^T and *P. borealis* KK19^T with DNA-DNA hybridization values of 43, 35 and 28 %, respectively [101]. The inoculation with *P. riograndensis* SBR5 improves the growth of wheat in greenhouse conditions [102].

Introduction

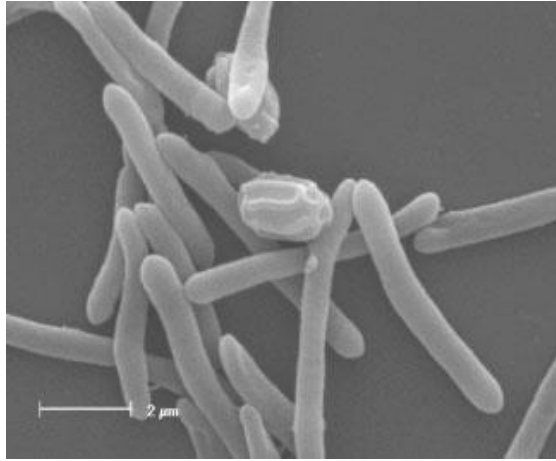


Figure 3. Scanning electron microscopy of vegetative cells of *P. riograndensis* SBR5 and spores showing a regular pattern of stripes (bar, 2 μm) [101].

The draft genome sequence of *P. riograndensis* SBR5 was generated and it revealed the presence of a single chromosome of 7,370,000 base pairs (bp) distributed in 2,276 contigs. This draft genome sequencing revealed 7,467 open reading frames, 16 tRNAs genes and a G+C content of 55.1% [103]. Twenty three genes involved in nitrogen fixation were found, as well as 6 genes encoding siderophore transport and uptake proteins [103]. Therefore, the nitrogen fixation and siderophore genetic basis and functionality in *P. riograndensis* SBR5 were further investigated. First, nitrogen fixation system in SBR5 was tested through differential RNA sequencing (RNAseq) and quantitative reverse transcription polymerase chain reaction (qRT-PCR) revealing three BNF-related gene clusters: one cluster comprising the genes *nifB1H1D1K1E1N1X1-orf1-hesA-V*; a second cluster containing *nif* genes *nifH2*, *B2*, *D2* and *K2*; and a third one containing alternative nitrogenase genes *anfHDGK* [104]. Moreover, the functionality of the alternative nitrogenase was confirmed by enzymatic assay [104]. Further, it was revealed that glutamine synthase senses the presence of nitrogen and transmits the nitrogen signal towards the transcriptional repressor GlnR, leading to the transcriptional repression of nitrogen fixation in SBR5 [105]. Secondly, differential RNAseq under iron depletion was performed [106]. In the event of iron deficiency, SBR5 expresses genes related to iron uptake and shows signs of stress resistance displayed by increased expression of genes involved in sporulation and DNA protection. Furthermore, although it was demonstrated that SBR5 can produce siderophores [101], genes putatively related to siderophore production were not expressed under iron starvation conditions. However, the *fecE* gene encoding Fe³⁺ siderophore transporter was upregulated [106]. Regarding the pathogen biocontrol, *P. riograndensis* SBR5 displays the antagonist activity against *Listeria monocytogenes* and *Pectobacterium carotovorum* [107].

Although a protocol for genetic transformation (based on electroporation) of *P. riograndensis* was developed [108], the tools for genetic manipulation thereof are very limited. The strain SBR5 was

Introduction

deposited as *P. riograndensis* SBR5^T (deposit number LFB-FIOCRUZ 1313). Despite the fact that *P. riograndensis* SBR5 was proposed as the type strain of the species [101], it is still not characterized in depth, e.g. only the draft genome sequence is available and some PGP activities of this organism remain elusive, e. g. the solubilization of soil phosphates. In the next chapters, I will present on how high-throughput sequencing technologies and genetic tools can be applied for elucidation of metabolism of PGPR.

1.3. Genome-based functional analysis of microorganisms

Due to environmental importance of PGPR, increasing numbers of genomic studies were performed on PGPR species, facilitating a holistic insight into their metabolism and the rapid identification of biosynthesis pathways of ecologically important metabolites. The whole genome sequencing data of an organism represents the big data that is interpreted with the help of bioinformatics tools in order to annotate genes and search for new relevant pathways. Since the beneficial properties of PGPR are mediated by enzymes and secondary metabolites, genome mining allows scrutinizing the whole genome of a PGPR strain for genes encoding enzymes that facilitate resource acquisition, as well as for biosynthetic gene clusters encoding PGPR-related active compounds. Since many genes are silent under standard laboratory conditions, due to the absence of appropriate natural triggers or stress signals, some functions of PGPR may be overlooked where only classical experimental methods are employed [109]. Based on that, genomes of a variety PGPR have been sequenced which contributed to identification of genes related to their PGP activities [110–114].

The complete genome sequences of *Paenibacillus* PGP members have been published recently [115,116]. Comparative genome analysis of different *Pseudomonas* species revealed important insights on the plant interaction process in this genus, showing strong genomic conservations on metabolism of plant-derived compounds, heavy metal resistance, and rhizosphere colonization [117]. Comparative genome analysis of the PGPR *Pseudomonas chlororaphis* helped to identify the regulation of genes related to the biosynthesis of the antimicrobial metabolite phenazine [118]. Genomic-based analysis was used to elucidate transcriptional regulation of nitrogen fixation in *P. riograndensis* SBR5 [105].

Over the past years, the understanding of bacterial transcription has advanced due to the combination of high-throughput technologies with classical genetics and biochemical assays. For instance, RNAseq has offered powerful tool for high-resolution transcriptome characterization, allowing both differential-expression analysis and identification of new transcripts not predicted by bioinformatics. The efforts in the transcriptome field have helped to elucidate the function of different genes in PGP processes. These efforts are mainly based on microarray or comparative RNAseq technologies. Microarray analysis was applied to demonstrate the gene expression profile of *B. subtilis* in the presence of rice seedlings, which led to the upregulation of the genes related to stress response and metabolism of carbohydrates and

Introduction

amino acids [119]. Transcriptomic response of *Herbaspirillum seropedicae* characterized by the means of RNAseq showed activation of nitrogen fixation, polyhydroxybutyrate metabolism, cell wall re-modeling and adhesion molecules such as adhesin, which suggests specific metabolic adaptations of the bacteria to the rhizospheric environment [120]. Differential gene expression analysis revealed genes involved in phosphate solubilization under P depletion in *Burkholderia multivorans*, confirming the role of organic acids production in this process [121]. Differential gene expression analysis also uncovered expression of the *nif* gene operon (*nifBHDKENXhesAnifV*) in *Paenibacillus* sp. under nitrogen fixation conditions [122].

For industrially relevant bacteria, like *Corynebacterium glutamicum* and *B. methanolicus*, the use of high-throughput RNAseq enabled genome-wide scale transcriptome analysis, uncovering transcriptional features of such organisms, for example promoter and ribosome binding site (RBS) motifs, operon structures and presence of novel transcripts [123,124]. This type of transcriptome analysis is a valuable basis for differential RNA sequencing analysis; however, so far they were not performed for PGPR. Draft genome and gene expression analysis of *P. riograndensis* have been published [103,104,106]. However, a complete genome sequence and genome-wide scale transcriptome analysis are still missing. One of the goals of this thesis was to address these shortcomings. The advance in genomic/transcriptomic studies on PGPR offers a high-throughput and valuable way of understanding bacterial metabolism and may contribute to increase the PGPR participation in fertilizer market. In next subchapters, I will present how the high-throughput technologies contributed to the improvement of understanding of biotin biosynthesis pathway and functioning of riboswitches in different bacterial species. Those processes served as an example in my thesis on how the genomic/transcriptomic data combined with functional analysis may contribute to uncovering physiology of bacterial species, here, particularly *P. riograndensis*.

1.3.1. Genome-based identification of biosynthesis pathways: biotin biosynthesis pathway in microorganisms

Biotin is part of a vitamin group B produced by PGPR that also include thiamine, niacin, pantothenic acid, and cobalamin, and may play a role in microbial competition for root colonization [125]. The biosynthesis of this component is well known in *Escherichia coli* and *B. subtilis*. The synthesis of biotin starts from pimeloyl-CoA (Figure 4). In *B. subtilis*, pimeloyl-CoA is obtained in a reaction catalyzed by enzyme coded by the genes *bioW* and *bioI*. BioI is an enzyme of the cytochrome P450 family that cleaves carbon bonds of fatty acids to generate pimeloyl-CoA while BioW is a 6-carboxyhexanoate-CoA ligase that catalyzes the conversion of the precursor pimelic acid into pimeloyl-CoA [126]. In *E. coli*, the synthesis of pimeloyl-CoA is mediated by BioC and BioH enzymes. BioC transfers a methyl group from S-adenosyl-L-methionine (SAM) to malonyl-CoA, to give malonyl-CoA methyl ester. BioH synthesizes pimeloyl-CoA by the hydrolysis of the ester bonds in the fatty acid synthetic pathway [127].

Introduction

Downstream of pimeloyl-CoA, the synthesis of biotin occurs in four steps mediated by BioF, BioA, BioD and BioB. BioF is a 7-keto-8-aminopelargonic acid (KAPA) synthase that catalyzes the decarboxylative condensation of pimeloyl-CoA and alanine to produce KAPA [128]. BioA is a 7,8-diaminopelargonic acid (DAPA) aminotransferase that uses S-adenosyl-L-methionine (SAM) as amino donor to KAPA to form DAPA [129]. BioD is a dethiobiotin synthase that forms dethiobiotin by the ATP-dependent insertion of CO₂ between the N7 and N8 nitrogen of DAPA [130]. BioB (biotin synthase) catalyzes the last step in this pathway, in which dethiobiotin is converted to biotin by the insertion of a sulfur atom into dethiobiotin by a radical mechanism [131].

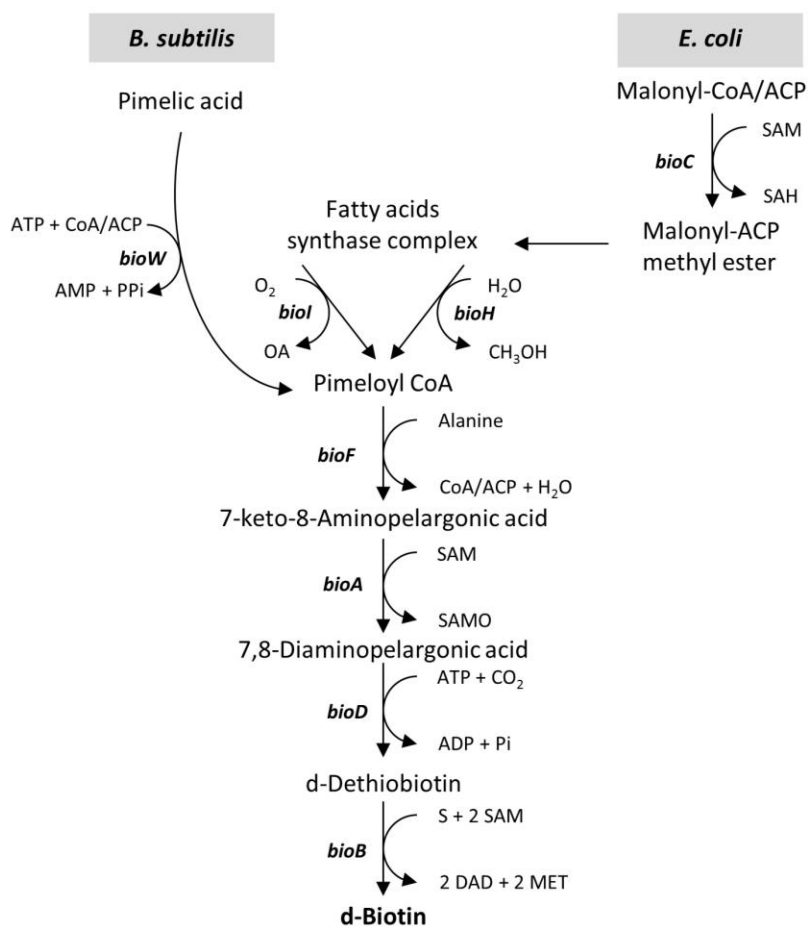


Figure 4. Scheme of biotin biosynthesis in the Gram-negative *E. coli* and the Gram-positive *B. subtilis* and the genes involved in this process. OA- octaonic acid; SAM- S-adenosyl-L-methionine; SAMO- S-adenosyl-4-methylthio-2-oxobutanoate; S- Sulphur.

Genomic findings associated with functional analysis could elucidate the genetic basics of biotin biosynthesis in *E. coli* and *B. subtilis*. In *E. coli* the genes encoding for biotin synthesis are organized in a bi-directional operon. On the right direction, the transcription unit includes the genes *bioB*, *bioF*, *bioC* and *bioD*, while on the left transcription unit includes the *bioA* gene and an additional open reading frame with unknown function named *orfX*. Located outside of this operon, a *bioH* gene is also required for biotin

Introduction

synthesis [132]. In *B. subtilis*, the *bio* genes are all co-transcribed in one single operon *bioWAFDBI* [133,134]. Although biotin is formed in bacteria by a well-defined pathway, much of the current knowledge on the molecular mechanisms has been derived from work in model organisms, as *E. coli* and *B. subtilis* [127]. Moreover, the biotin biosynthesis and its genetic basis in *P. riograndensis* are unknown and still needs further study.

1.3.2. Transcriptome-based identification of regulatory elements: gene regulation by riboswitches

Riboswitches are regulatory elements found in the 5'-untranslated regions (5'-UTR) of genes and they perform the regulatory control over the gene transcript by directly binding a small ligand molecule. Riboswitches often regulate expression of essential genes and as such they are interesting target structures for the development of novel compounds, e. g. antibiotics [135]. Most riboswitches are composed of two distinct functional domains: an aptamer domain that recognizes and binds to a small molecule (ligand) which leads to adopting a new conformation; and an expression platform, which contains a secondary structural switch that interfaces with the gene transcriptional or translational machinery (Figure 5). The aptamer must discriminate between chemically related metabolites with high selectivity to elicit the appropriate regulatory response. Regulation is achieved by action of a region of overlap between two domains of the riboswitch, whose pairing directs folding of the RNA into one of two mutually exclusive structures of the expression platform that represent the “on” and “off” states of the mRNA [136]. The most common mechanisms used by bacterial riboswitches in the presence of ligand to regulate gene expression are the transcription termination, the translation initiation and a dual effect of these mechanisms [137,138]. The transcription termination occurs through the aptamer control of the formation of the terminator stem usually by regulating the formation of a competing secondary structure called anti-terminator, which causes RNA polymerase to stall transcription. In case of regulation of translation initiation, an anti-sequestering stem is formed controlled by the aptamer and it results in the sequestration of the RBS sequence. Finally, a dual transcription and translation control occurs when the RBS is sequestered in a terminator stem (Figure 5).

Introduction

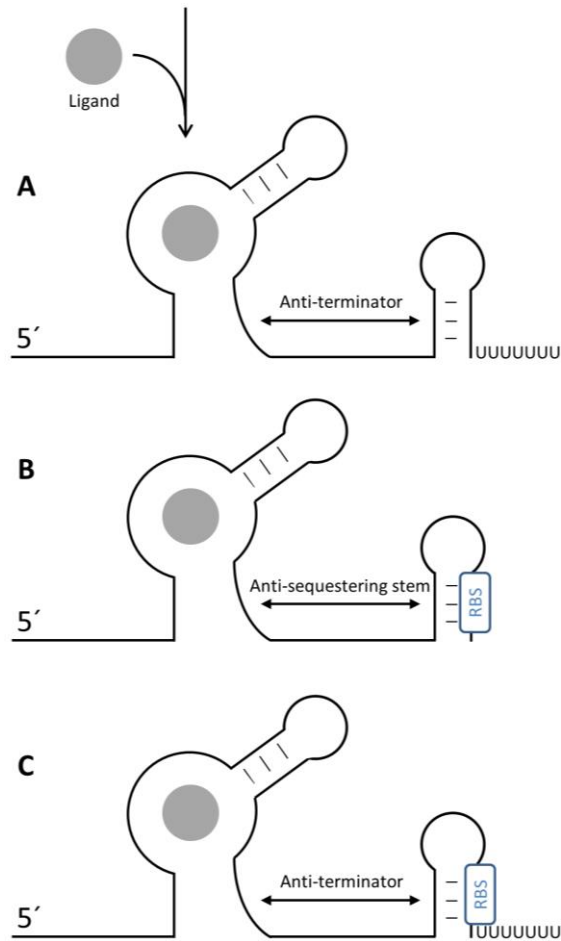


Figure 5. Riboswitch gene regulation mechanisms. The aptamer domain binds to a small molecule (ligand), adopting a new conformation that base pair with the RBS, blocking the translation; A- transcription termination; B- translation initiation control; and C- dual transcription and translation control.

Genome-wide searches have identified many conserved mRNA elements that could potentially function as riboswitches but were missing their validated ligands [139]. Furthermore, transcriptome analysis in bacteria could offer the prediction of riboswitches and their transcriptional organization [123,124]. The riboswitch mechanisms for regulation of gene expression has major impact on bacterial cell physiology, e. g. thiamine pyrophosphate (TPP)-responding riboswitches, which are involved in the regulation of thiamine metabolism in numerous bacteria, is well known for controlling the translation initiation in *E. coli* [140]. Hence, the search for riboswitches also allows the development of tools for manipulation of gene expression in a variety of biological systems. However, studies regarding gene regulation by riboswitches in PGPR are scarce.

As mentioned before, the putative riboswitches can be predicted solely on the basis of the genomic sequences e.g. by comparison to the sequences gather in RNA families databases such as Rfam

Introduction

[141]. The RNAseq analysis provides additional information on the transcriptional landscape which makes it useful tools in quest for putative riboswitches present in the transcriptome. However, the functionality of the putative riboswitch can only be confirmed by molecular studies, such as expression of a reporter gene under control of putative riboswitch. The detection and confirmation of functionality of putative riboswitches gives better insight into the regulation of different biosynthesis pathways. For example, transport and biosynthesis of TPP which is a cofactor in many metabolic reactions is feedback controlled by the TPP riboswitch in some bacterial species such as *B. subtilis* [142], *Bacillus anthracis* [143] and *E. coli* [144].

Thiamine is indispensable for the activity of the carbohydrate and branched-chain amino acid metabolic enzymes in its active form TPP [145]. As biotin, thiamine is part of the vitamin B group, which is suggested to improve the plant root colonization by PGPR [146]. Thiamine also acts as a cofactor of the principal enzyme (indolepyruvate decarboxylase) in synthesizing IAA in PGPR [147]. In *E. coli*, the precursors hydroxymethyl-pyrimidine diphosphate and hydroxyethyl-thiazole phosphate are utilized to synthesize TPP [148]. Thiamine biosynthesis protein ThiC converts aminoimidazole ribotide to hydroxymethyl-pyrimidine phosphate, which is subsequently phosphorylated by the bifunctional hydroxymethyl-pyrimidine phosphate P kinase ThiD to yield hydroxymethyl-pyrimidine pyrophosphate. On the other hand, the thiazole moiety of thiamine is derived from tyrosine, cysteine and 1-deoxy-D-xylulose phosphate. In a yet unresolved chain of reactions featuring *thiF*, *thiS*, *thiG*, *thiH*, *thiI* and *thiM* gene products, hydroxyethyl-thiazole phosphate is formed. Hydroxymethyl-pyrimidine pyrophosphate and hydroxyethyl-thiazole phosphate are joined by one enzymatic step mediated by the ThiE protein, followed by phosphorylation of the formed thiamine monophosphate by ThiL to create TPP (Figure 6) [144,148].

Introduction

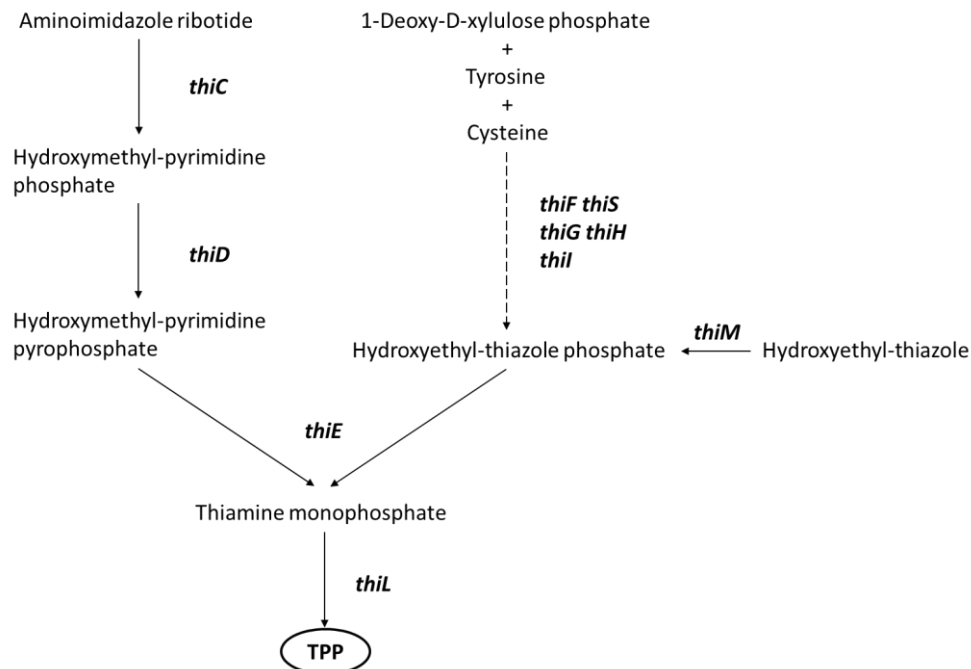


Figure 6. Scheme of TPP biosynthesis pathway in *E. coli* and the genes involved in this process.

In this light, the use of high-throughput sequencing technologies and molecular biology tools are important methods to elucidate a regulation of biosynthesis of compounds crucial for the metabolism of different bacterial species.

1.4. Molecular biology tools for functional study of PGPR features

Genetic manipulation is crucial for taking full advantage of the information generated by DNA sequences. The use of genetic manipulation has been applied to characterize different PGP features in bacteria. Molecular cloning was used to identify and characterize *rpoS* as non-siderophore production gene in *P. putida* [149]. An electroporation method was developed to transform *Azospirillum amazonense* with plasmid DNA, and further the vectors introduced into the cells were used for expression of heterologous fluorescent reporter gene [150]. The fluorescent reporter genes were applied in PGPR studies where *P. putida* and *Azotobacter chroococcum* were transformed with plasmid vector carrying gene coding for green fluorescence protein (*gfp*) to detect *gfp*-tagged bacterial cells colonizing sorghum tissues through microscopy [151]. The use of transposon mutagenesis and molecular cloning for the complementation of the mutants was used to characterize the production of a pathogen antagonist component phenazine by *Pseudomonas aereofaciens* [152]. A gene region that codes for pyrrolnitrin production enzyme was cloned in non-pyrrolnitrin-producing mutants of *P. fluorescens*, which led to restoration of pyrrolnitrin synthesis and suppression of *Rhizoctonia solani*-induced damping-off of cotton

Introduction

[153]. Furthermore, in *B. amyloliquefaciens*, the genes *patB* (encoding aminotransferase), *yclC* (encoding decarboxylase), and *dhaS* (encoding indole 3-acetaldehyde dehydrogenase), which were proposed to constitute the indole-3-pyruvic acid pathway for IAA biosynthesis, were expressed separately or co-expressed as an entire IAA synthesis pathway, which led to the increased IAA production by the recombinant *B. amyloliquefaciens* [154]. An electroporation method has been developed for *P. riograndensis*, resulting in recombinant cells with high transformation efficiency [108]. A genetic toolbox for *P.riograndensis* was missing, and it was one of the aims of this thesis to develop suitable molecular tools for this bacterium and apply them for the characterization of metabolism of this bacterium.

1.5. Objectives

P. riograndensis SBR5 is a plant growth promoting rhizobacterium, which is a promising candidate to serve as a crop inoculant. Despite its potential regarding environmental and economic benefits, the species *P. riograndensis* is poorly characterized and genetic tools are deficient. Based on that, the objective of this thesis is to improve the characterization of this organism, focusing on the following goals:

- To sequence, assemble and annotate the genome *P. riograndensis* SBR5 in order to determine its complete genome sequence.
- To perform a genome-wide scale transcriptome analysis of SBR5, providing the characterization of promoter and RBS motifs, operon structure, and transcriptional profile.
- To develop a molecular genetic toolbox for *P. riograndensis* SBR5.
- To investigate aspects of vitamin biosynthesis by SBR5 based on the genome/transcriptome data and utilizing the newly developed molecular genetic toolbox.
- To evaluate the transcriptional profiling of SBR5 in phosphate solubilization conditions using differential gene expression analysis based on the genome/transcriptome data.

1.6. References

1. FAO. Global agriculture towards 2050. High Level Expert Forum-How to feed the world 2050 [Internet]. 2009;1–4. Available from: http://www.fao.org/fileadmin/templates/wsfs/docs/Issues_papers/HLEF2050_Global_Agriculture.pdf
2. Vance CP, Uhde-stone C, Allan DL. Phosphorus acquisition and use: critical adaptations by plants for securing a nonrenewable resource. *New Phytol.* 2003;157:423–47.
3. FAOstat [Internet]. [cited 2017 May 15]. Available from: <http://www.fao.org/faostat/en/>

Introduction

4. Igbedioh S. Effects of agricultural pesticides on humans, animals, and higher plants in developing countries. *Arch. Environ. Health*. 1991;26:218–24.
5. Righi S, Lucialli P, Bruzzi L. Health and environmental impacts of a fertilizer plant - Part I: Assessment of radioactive pollution. *J. Environ. Radioact.* 2005;82:167–82.
6. Loganathan P, Hedley M, Grace N. Pasture soils contaminated with fertilizer-derived cadmium and fluorine: livestock effects. *Rev. Environ. Contam. Toxicol.* 2008;192:29–66.
7. Milton NM, Eiswerth BA, Ager CM. Effect of phosphorus deficiency on spectral reflectance and morphology of soybean plants. *Remote Sens. Environ.* 1991;36:121–7.
8. Shen J, Yuan L, Zhang J, Li H, Bai Z, Chen X. Phosphorus Dynamics: From Soil to Plant. *Plant Physiol.* 2011;156:997–1005.
9. Guidry MW, Mackenzie FT. Apatite weathering and the phanerozoic phosphorus cycle. *Geology*. 2000;28:631–4.
10. Ajmone-Marsan F, Côté D, Simard RR. Phosphorus transformations under reduction in long-term manured soils. *Plant Soil*. 2006;282:239–50.
11. Magette W, Carton O. *Agricultural Pollution. Environmental Engineering*. Maidenhead, UK: McGraw-Hill; 1996.
12. Mldgley AR. Phosphate fixation in soils-a critical review. *Soil Sci. Soc. Am. J.* 1941;5:24–30.
13. Johnston A. Nutrient removal as a soil fertility planning tool [Internet]. *Fertilization Facts*. 2002. Available from: <http://www.ppi-ppic.org>
14. Russell D. *Soil conditions and plant growth*. New York, NY, USA: Longman Group Ltd.; 1973.
15. Timmusk S, Behers L, Muthoni J, Muraya A, Aronsson A-C. Perspectives and challenges of microbial application for crop improvement. *Front. Plant Sci.* 2017;8:49.
16. Ahemad M, Khan MS. *Pseudomonas aeruginosa* strain PS1 enhances growth parameters of greengram [*Vignaradiata* (L.) Wilczek] in insecticide-stressed soils. *J. Pest. Sci.* 2011;84:123–31.
17. Whipps JM. *Carbon economy. The rhizosphere*. Chichester, UK: Wiley & Son; 1990. p. 59–87.
18. Dardanelli MS, Manyani H, González-Barroso S, Rodríguez-Carvajal MA, Gil-Serrano AM, Espuny MR, et al. Effect of the presence of the plant growth promoting rhizobacterium (PGPR) *Chryseobacterium balustinum* Aur9 and salt stress in the pattern of flavonoids exuded by soybean roots. *Plant Soil*. 2010;328:483–93.
19. Lynch JM, Whipps JM. Substrate flow in the rhizosphere. *Plant Soil*. 1990;129:1–10.
20. Degenhardt J, Gershenzon J, Baldwin IT, Kessler A. Attracting friends to feast on foes: engineering terpene emission to make crop plants more attractive to herbivore enemies. *Curr. Opin. Biotechnol.* 2003;14:169–76.
21. Dardanelli M, Angelini J, Fabra A. A calcium-dependent bacterial surface protein is involved in the attachment of rhizobia to peanut roots. *Can. J. Microbiol.* 2003;49:399–405.

Introduction

22. de Souza R, Ambrosini A, Passaglia LMP. Plant growth-promoting bacteria as inoculants in agricultural soils. *Genet. Mol. Res.* 2015;38:401–19.
23. Burgess BK, Lowe DJ. Mechanism of Molybdenum Nitrogenase. *Chem. Rev.* 1996;96:2983–3012.
24. Boddey RM, de Oliveira OC, Urquiaga S, Reis VM, de Olivares FL, Baldani VLD, et al. Biological nitrogen fixation associated with sugar cane and rice: Contributions and prospects for improvement. *Plant Soil.* 1995;174:195–209.
25. Martins MR, Jantalia CP, Reis VM, Döwich I, Polidoro JC, Alves BJR, et al. Impact of plant growth-promoting bacteria on grain yield, protein content, and urea-¹⁵N recovery by maize in a Cerrado Oxisol. *Plant Soil.* 2017;1–12.
26. Neilands JB. Siderophores: structure and function of microbial iron transport compounds. *J. Biol. Chem.* 1995;270:26723–6.
27. Radzki W, Man FJG, Algar E, Solano BR. Bacterial siderophores efficiently provide iron to iron-starved tomato plants in hydroponics culture. *Antonie Leeuwenhoek.* 2013;104:321–30.
28. Sharma A, Johri BN. Growth promoting influence of siderophore-producing *Pseudomonas* strains GRP3A and PRS 9 in maize (*Zea mays* L.) under iron limiting conditions. *Microbiol. Res.* 2003;158:243–8.
29. Krewulak KD, Vogel HJ. Structural biology of bacterial iron uptake. *Biochim. Biophys. Acta.* 2008;1778:1781–804.
30. Ross-Gillespie A, Dumas Z, Kümmerli R. Evolutionary dynamics of interlinked public goods traits: an experimental study of siderophore production in *Pseudomonas aeruginosa*. *J. Evol. Biol.* 2015;28:29–39.
31. Buckling A, Harrison F, Vos M, Brockhurst MA, Gardner A, West SA, et al. Siderophore-mediated cooperation and virulence in *Pseudomonas aeruginosa*. *FEMS Microbiol. Ecol.* 2007;62:135–41.
32. Loper JE, Henkels MD. Utilization of heterologous siderophores enhances levels of iron available to *Pseudomonas putida* in the rhizosphere. *Appl. Env. Microbiol.* 1999;65:5357–63.
33. Zaidi A, Khan M, Ahemad M, Oves M. Plant growth promotion by phosphate solubilizing bacteria. *Acta Microbiol. Immunol. Hung.* 2009;56:263–84.
34. Ahmad F, Ahmad I, Khan MS. Screening of free-living rhizospheric bacteria for their multiple plant growth promoting activities. *Microbiol. Res.* 2008;163:173–81.
35. Wani PA, Khan MS. *Bacillus* species enhance growth parameters of chickpea (*Cicer arietinum* L.) in chromium stressed soils. *Food. Chem. Toxicol. Elsevier Ltd;* 2010;48:3262–7.
36. Phi Q, Park Y, Seul K, Ryu C, Park S, Kim J, et al. Assessment of root-associated *Paenibacillus polymyxa* groups on growth promotion and induced systemic resistance in pepper. *J. Microbiol. Biotechnol.* 2010;20:1605–13.
37. Pieterse CMJ, Van der Does D, Zamioudis C, Leon-Reyes A, Van Wees SCM. Hormonal Modulation

Introduction

- of Plant Immunity. *Annu. Rev. Cell Dev. Biol.* 2012;28:489–521.
38. Kieffer M, Neve J, Kepinski S. Defining auxin response contexts in plant development. *Curr. Opin. Plant Biol.* 2010;13:12–20.
 39. Swarup R, Péret B. AUX/LAX family of auxin influx carriers—an overview. *Front. Plant Sci.* 2012;3:1–12.
 40. Amara U, Khalid R, Hayat R. Soil bacteria and phytohormones for sustainable crop production. *Bacterial Metabolites in Sustainable Agroecosystem.* Springer International Publishing; 2015. p. 87–103.
 41. Aeron A, Pandey P, Maheshwari DK. Differential response of sesame under influence of indigenous and non-indigenous rhizosphere competent fluorescent pseudomonads. *Curr. Sci.* 2010;99:166–8.
 42. Goswami D, Pithwa S, Dhandhukia P, Thakker JN. Delineating *Kocuria turfanaensis* 2M4 as a credible PGPR: a novel IAA-producing bacteria isolated from saline desert. *J. Plant Interact.* 2014;9:1–11.
 43. Raaijmakers JM, de Bruijn I, Nybroe O, Ongena M. Natural functions of lipopeptides from *Bacillus* and *Pseudomonas*: more than surfactants and antibiotics. *FEMS Microbiol. Rev.* 2010;34:1037–62.
 44. Meleigi MA El, Al-rogaibah AA, Ibrahim GH, Gamhan KA Al. Role of antibiosis and production of indole-3-acetic acid by bacilli strains in suppression of root pathogens and growth promotion of alfalfa seedlings. *Int. J. Curr. Microbiol. Appl. Sci.* 2014;3:685–96.
 45. Compant S, Duffy B, Nowak J, Cle C, Barka E a. Use of plant growth-promoting bacteria for Biocontrol of plant diseases: principles, mechanisms of action, and future prospects. *Appl. Env. Microbiol.* 2005;71:4951–9.
 46. Kim B, Moon SS, Hwang BK. Isolation, identification, and antifungal activity of a macrolide antibiotic, oligomycin A, produced by *Streptomyces libani*. *Can. J. Bot.* 1999;77:850–8.
 47. Srividya NAS. Potentiality of *Bacillus subtilis* as biocontrol agent for management of anthracnose disease of chilli caused by *Colletotrichum gloeosporioides* OGC1. *3 Biotech.* 2014;4:127–36.
 48. Andersen JB, Koch B, Nielsen TH, Sørensen D, Hansen M, Nybroe O, et al. Surface motility in *Pseudomonas* sp. DSS73 is required for efficient biological containment of the root-pathogenic microfungi *Rhizoctonia solani* and *Pythium ultimum*. *Microbiology.* 2017;149:37–46.
 49. Haas D, Défago G. Biological control of soil-borne pathogens by fluorescent pseudomonads. *Nat. Rev. Microbiol.* 2005;3:307–19.
 50. El-Tarabily K a. Rhizosphere-competent isolates of streptomycete and non-streptomycete actinomycetes capable of producing cell-wall-degrading enzymes to control *Pythium aphanidermatum* damping-off disease of cucumber. *Can. J. Bot.* 2006;84:211–22.
 51. Zebelo S, Song Y, Kloepper JW, Fadamiro H. Rhizobacteria activates (+)- δ -cadinene synthase genes and induces systemic resistance in cotton against beet armyworm (*Spodoptera exigua*). *Plant Cell*

Introduction

- Environ. 2016;39:935–43.
52. Rodríguez H, Fraga R. Phosphate solubilizing bacteria and their role in plant growth promotion. *Biotechnol. Adv.* 1999;17:319–39.
 53. Chen YP, Rekha PD, Arun AB, Shen FT, Lai W, Young CC. Phosphate solubilizing bacteria from subtropical soil and their tricalcium phosphate solubilizing abilities. *Appl. Soil Ecol.* 2006;34:33–41.
 54. Oteino N, Lally RD, Kiwanuka S, Lloyd A, Ryan D, Germaine KJ, et al. Plant growth promotion induced by phosphate solubilizing endophytic *Pseudomonas* isolates. *Front. Microbiol.* 2015;6:745.
 55. Jahanian A, Chaichi MR, Rezaei K, Rezayazdi K, Khavazi K. The effect of plant growth promoting rhizobacteria (PGPR) on germination and primary growth of artichoke (*Cynara scolymus*). *Intl. J. Agri. Crop Sci.* 2012;4:923–9.
 56. Afzal A, Bano A. Rhizobium and phosphate solubilizing bacteria improve the yield and phosphorus uptake in wheat (*Triticum aestivum*). *Int. J. Agri. Biol.* 2008;10:85–8.
 57. Mander C, Wakelin S, Young S, Condrón L, Callaghan MO. Incidence and diversity of phosphate-solubilising bacteria are linked to phosphorus status in grassland soils. *Soil Biol. Biochem.* 2012;44:93–101.
 58. Mikanová O, Nováková J. Evaluation of the P-solubilizing activity of soil microorganisms and its sensitivity to soluble phosphate. *Rost. Vyroba.* 2002;48:397–400.
 59. Wang X, Tang C, Guppy CN, Sale PWG. Phosphorus acquisition characteristics of cotton (*Gossypium hirsutum* L.), wheat (*Triticum aestivum* L.) and white lupin (*Lupinus albus* L.) under P deficient conditions. *Plant Soil.* 2008;312:117–28.
 60. Panhwar QA, Jusop S, Naher UA, Othman R, Razi MI. Application of potential phosphate-solubilizing bacteria and organic acids on phosphate solubilization from phosphate rock in aerobic rice. *Sci. World J.* 2013;2013:272409.
 61. Kucey R.M.N. JHH and LME. Microbially mediated increases in plant available phosphorus. *Adv. Agron.* 1989;42:199–221.
 62. Goldstein A. Involvement of the quinoprotein glucose dehydrogenase in the solubilization of exogenous phosphates by Gram-negative bacteria. *Phosphate in microorganisms: Cellular and molecular biology.* Washington (DC): ASM Press; 1994. p. 197–203.
 63. Patel DK, Archana G, Kumar G. Variation in the nature of organic acid secretion and mineral phosphate solubilization by *Citrobacter* sp. DHRSS in the presence of different sugars. *Curr. Microbiol.* 2008;56:168–74.
 64. Thomas L, Hodgson DA, Wentzel A, Nieselt K, Ellingsen TE, Moore J, et al. Metabolic switches and adaptations deduced from the proteomes of *Streptomyces coelicolor* wild type and *phoP* mutant

Introduction

- grown in batch culture. *Mol. Cell Proteomics*. 2012;11:M111.013797.
65. Zeng Q, Wu X, Wen X. Effects of soluble phosphate on phosphate-solubilizing characteristics and expression of *gcd* gene in *Pseudomonas frederiksbergensis* JW-SD2. *Curr. Microbiol. Springer US*; 2016;72:198–206.
 66. Chauhan A, Guleria S, Balgir PP, Walia A, Mahajan R, Mehta P, et al. Tricalcium phosphate solubilization and nitrogen fixation by newly isolated *Aneurinibacillus aneurinilyticus* CKMV1 from rhizosphere of *Valeriana jatamansi* and its growth promotional effect. *Braz. J. Microbiol.* 2016;48:294–304.
 67. Coleman JE. Structure and mechanism of alkaline phosphatase. *Annu. Rev. Biophys. Biomol. Struct.* 1992;21:441–83.
 68. Maseko ST, Dakora FD. Plant enzymes, root exudates, cluster roots and mycorrhizal symbiosis are the drivers of P nutrition in native legumes growing in P deficient soil of the Cape Fynbos in South Africa. *J. Agr. Sci. Tech.* 2013;3:331–40.
 69. Dick WA, Cheng L, Wang P. Soil acid and alkaline phosphatase activity as pH adjustment indicators. *Soil Biol. Biochem.* 2000;32:1915–9.
 70. Thaller MC, Berlutti F, Schippa S, Iori P, Passariello C, Rossolini GM. Heterogeneous patterns of acid phosphatases containing low-molecular-mass polypeptides in members of the family *Enterobacteriaceae*. *Int. J. Syst. Evol. Microbiol.* 1995;45:255–61.
 71. Gügi B, Orange N, Hellio F, Burini JF, Guillou C, Leriche F, et al. Effect of growth temperature on several exported enzyme activities in the psychrotrophic bacterium *Pseudomonas fluorescens*. *J. Bacteriol.* 1991;173:3814–20.
 72. Hsieh Y-J, Wanner BL. Global regulation by the seven-component Pi signaling system. *Curr. Opin. Microbiol.* 2010;13:198–203.
 73. Kertesz M, Elgorriaga A, Amrhein N. Evidence for two distinct phosphonate-degrading enzymes (C-P lyases) in *Arthrobacter* sp. GLP-1. *Biodegradation.* 1991;2:53–9.
 74. Seweryn P, Van LB, Kjeldgaard M, Russo CJ, Lori A, Hove-jensen B, et al. Structural insights into the bacterial carbon-phosphorus lyase machinery. *Nature.* 2016;525:68–72.
 75. Jog R, Pandya M, Nareshkumar G, Rajkumar S. Mechanism of phosphate solubilization and antifungal activity of *Streptomyces* spp . isolated from wheat roots and rhizosphere and their application in improving plant growth. *Microbiology.* 2017;778–88.
 76. Jorquera MA, Hernández MT, Rengel Z, Marschner P, De M, Mora L. Isolation of culturable phosphobacteria with both phytate-mineralization and phosphate-solubilization activity from the rhizosphere of plants grown in a volcanic soil. *Biol. Fertil. Soils.* 2008;44:1025–34.
 77. Korir H, Mungai NW, Thuita M, Hamba Y, Masso C. Co-inoculation effect of rhizobia and plant growth promoting rhizobacteria on common bean growth in a low phosphorus soil. *Front. Plant*

Introduction

Sci. 2017;08:141.

78. Govindasamy V, Senthilkumar M, Magheshwaran V, Kumar U, Bose P, Sharma V, et al. *Bacillus* and *Paenibacillus* spp.: potential PGPR for sustainable agriculture. *Plant Growth and Health Promoting Bacteria*. Springer; 2010. p. 333–64.
79. Ash C, Priest FG, Collins MD. Molecular identification of rRNA group 3 bacilli (Ash, Farrow, Wallbanks and Collins) using a PCR probe test. Proposal for the creation of a new genus *Paenibacillus*. *Antonie Leeuwenhoek*. 1993;64:253–60.
80. Seldin L, Rosado AS, William D, Cruz DA, Nobrega A, Elsas JANDVAN, et al. Comparison of *Paenibacillus azotofixans* strains isolated from rhizoplane, rhizosphere, and non-root-associated soil from maize planted in two different Brazilian soils. *Appl. Environ. Microbiol.* 1998;64:3860–8.
81. Rivas R, Gutiérrez C, Abril A, Mateos PF, Martínez-Molina E, Ventosa A, et al. *Paenibacillus rhizosphaerae* sp. nov., isolated from the rhizosphere of *Cicer arietinum*. *Int. J. Syst. Evol. Microbiol.* 2005;55:1305–9.
82. Beneduzi A, Peres D, Costa PB da, Zanettini MHB, Passaglia LMP. Genetic and phenotypic diversity of plant-growth-promoting bacilli isolated from wheat fields in southern Brazil. *Res. Microbiol.* 2008;159:244–50.
83. Ma YC, Chen SF. *Paenibacillus forsythiae* sp. nov., a nitrogen-fixing species isolated from rhizosphere soil of *Forsythia mira*. *Int. J. Syst. Evol. Microbiol.* 2008;58:319–23.
84. Ma Y, Zhang J, Chen S. *Paenibacillus zanthoxyli* sp. nov., a novel nitrogen-fixing species isolated from the rhizosphere of *Zanthoxylum simulans*. *Int. J. Syst. Evol. Microbiol.* 2007;57:873–7.
85. Wang L, Zhang L, Liu Z, Zhao D, Liu X, Zhang B, et al. A minimal nitrogen fixation gene cluster from *Paenibacillus* sp. WLY78 enables expression of active nitrogenase in *Escherichia coli*. *PLoS Genet.* 2013;9:10.
86. Xie J, Du Z, Bai L, Tian C, Zhang Y, Xie J, et al. Comparative genomic analysis of N₂-fixing and non-N₂-fixing *Paenibacillus* spp.: organization, evolution and expression of the nitrogen fixation genes. *PLoS Genet.* 2014;10:1371.
87. Grady EN, Macdonald J, Liu L, Richman A, Yuan ZC. Current knowledge and perspectives of *Paenibacillus*: a review. *Microb. Cell Fact. BioMed Central*; 2016;15:203.
88. Islam S, Akanda AM, Prova A, Islam MT, Hossain MM. Isolation and identification of plant growth promoting rhizobacteria from cucumber rhizosphere and their effect on plant growth promotion and disease suppression. *Front. Microbiol.* 2016;6:1360.
89. Kuan KB, Othman R, Rahim KA, Shamsuddin ZH. Plant growth-promoting rhizobacteria inoculation to enhance vegetative growth, nitrogen fixation and nitrogen remobilisation of maize under greenhouse conditions. *PLoS ONE.* 2016;11:e0152478.

Introduction

90. Figueiredo MVB, Martinez CR, Burity HA, Chanway CP. Plant growth-promoting rhizobacteria for improving nodulation and nitrogen fixation in the common bean (*Phaseolus vulgaris* L.). *World J. Microbiol. Biotechnol.* 2008;24:1187–93.
91. Park YG, Mun BG, Kang SM, Hussain A, Shahzad R, Seo CW, et al. *Bacillus aryabhattai* SRB02 tolerates oxidative and nitrosative stress and promotes the growth of soybean by modulating the production of phytohormones. *PLoS ONE.* 2017;12:1–28.
92. Abd El Daim IA, Häggblom P, Karlsson M, Stenström E, Timmusk S. *Paenibacillus polymyxa* A26 Sfp-type PPTase inactivation limits bacterial antagonism against *Fusarium graminearum* but not of *F. culmorum* in kernel assay. *Front. Plant Sci.* 2015;6:368.
93. Almaghrabi OA, Massoud SI, Abdelmoneim TS. Influence of inoculation with plant growth promoting rhizobacteria (PGPR) on tomato plant growth and nematode reproduction under greenhouse conditions. *Saudi J. Biol. Sci.* 2013;20:57–61.
94. Ambrosini A, Stefanski T, Lisboa BB, Beneduzi A, Vargas LK, Passaglia LMP. Diazotrophic bacilli isolated from the sunflower rhizosphere and the potential of *Bacillus mycoides* B38V as biofertiliser. *Ann. Appl. Biol.* 2016;168:93–110.
95. Bal HB, Nayak L. Isolation of ACC deaminase producing PGPR from rice rhizosphere and evaluating their plant growth promoting activity under salt stress. *Plant Soil.* 2013;366:93–105.
96. Shahzad R, Waqas M, Khan AL, Asaf S, Khan MA, Kang SM, et al. Seed-borne endophytic *Bacillus amyloliquefaciens* RWL-1 produces gibberellins and regulates endogenous phytohormones of *Oryza sativa*. *Plant Physiol. Biochem. Elsevier Ltd;* 2016;106:236–43.
97. Chen L, Liu Y, Wu G, Veronican Njeri K, Shen Q, Zhang N, et al. Induced maize salt tolerance by rhizosphere inoculation of *Bacillus amyloliquefaciens* SQR9. *Physiol. Plant.* 2016;158:34–44.
98. Choudhary DK, Johri BN. Interactions of *Bacillus* spp. and plants - with special reference to induced systemic resistance (ISR). *Microbiol. Res.* 2009;164:493–513.
99. Passera A, Venturini G, Battelli G, Casati P, Penaca F, Quaglino F, et al. Competition assays revealed *Paenibacillus pasadenensis* strain R16 as a novel antifungal agent. *Microbiol. Res. Elsevier GmbH;* 2017;198:16–26.
100. Xie J, Shi H, Du Z, Wang T, Liu X, Chen S. Comparative genomic and functional analysis reveal conservation of plant growth promoting traits in *Paenibacillus polymyxa* and its closely related species. *Sci. Rep.* 2016;6:21329.
101. Beneduzi A, Costa PB, Melo IS, Bodanese-zanettini MH, Passaglia LMP. *Paenibacillus riograndensis* sp. nov., a nitrogen-fixing species isolated from the rhizosphere of *Triticum aestivum*. *Int. J. Syst. Evol. Microbiol.* 2010;60:128–33.
102. Campos SB, Beneduzi A, Carvalho Fernandes G, Passaglia LMP. Genetic and functional characterization of *Paenibacillus riograndensis*: a novel plant growth-promoting bacterium

Introduction

- isolated from wheat. *Biological Nitrogen Fixation*. 2015. p. 941–8.
103. Beneduzi A, Campos S, Ambrosini A, de Souza R, Granada C, Costa P, et al. Genome Sequence of the Diazotrophic Gram-Positive Rhizobacterium *Paenibacillus riograndensis* SBR5^T. *J. Bacteriol.* 2011;193:6391–2.
 104. Fernandes GDC, Trarbach LJ, Campos SB De, Beneduzi A, Passaglia LMP. Alternative nitrogenase and pseudogenes: unique features of the *Paenibacillus riograndensis* nitrogen fixation system. *Res. Microbiol.* 2014;165:571–80.
 105. Fernandes G, Hauf K, Sant’Anna F, Forchhammer K, Passaglia L. Glutamine synthetase stabilizes the binding of GlnR to nitrogen fixation gene operators. *FEBS J.* 2017;284:903–18.
 106. Sperb ER, Tadra-sfeir MZ, Sperotto RA, Fernandes G de C, Pedrosa FO, de Souza EM, et al. Iron deficiency resistance mechanisms enlightened by gene expression analysis in *Paenibacillus riograndensis* SBR5. *Res. Microbiol.* 2016;167:501–9.
 107. Bach E, Seger GD dos S, Fernandes G de C, Lisboa BB, Passaglia LMP. Evaluation of biological control and rhizosphere competence of plant growth promoting bacteria. *Appl. Soil Ecol.* 2016;99:141–9.
 108. Bach E, Fernandes GDC, Maria L, Passaglia P. How to transform a recalcitrant *Paenibacillus* strain: From culture medium to restriction barrier. *J. Microbiol. Methods.* 2016;131:135–43.
 109. Paterson J, Jahanshah G, Li Y, Wang Q, Mehnaz S, Gross H. The contribution of genome mining strategies to the understanding of active principles of PGPR strains. *FEMS Microbiol. Ecol.* 2016;93:fiw249.
 110. Mathimaran N, Srivastava R, Wiemken A, Sharma A, Boller T. Genome sequences of two plant growth-promoting fluorescent *Pseudomonas* strains, R62 and R81. *J. Bacteriol.* 2012;194:3272–3.
 111. Song J, Kim H, Kim J, Kim S, Jeong H, Kang S, et al. Genome sequence of the plant growth-promoting rhizobacterium *Bacillus* sp. strain JS. *J. Bacteriol.* 2012;194:3760–1.
 112. Gamez R, Rodríguez F, Bernal JF, Richa A, Landsman D, Ramirez L. Genome sequence of the banana plant growth-promoting rhizobacterium *Bacillus amyloliquefaciens* BS006. *Genome Announc.* 2015;3:2013–4.
 113. Berendsen RL, Verk MC Van, Stringlis IA, Zamioudis C, Tommassen J, Pieterse CMJ, et al. Unearthing the genomes of plant-beneficial *Pseudomonas* model strains WCS358 , WCS374 and WCS417. *BMC Genomics.* 2015;16:539.
 114. Gupta A, Gopal M, Thomas G V, Manikandan V, Gajewski J, Thomas G, et al. Whole genome sequencing and analysis of plant growth promoting bacteria isolated from the rhizosphere of plantation crops coconut, cocoa and arecanut. *PLoS ONE.* 2014;9:e104259.
 115. Kim JF, Jeong H, Park S, Kim S, Park YK, Choi S, et al. Genome sequence of the polymyxin-producing plant-probiotic rhizobacterium *Paenibacillus polymyxa* E681. *J. Bacteriol.*

Introduction

- 2010;192:6103–4.
116. Kwak Y, Shin J. Complete genome sequence of *Paenibacillus beijingensis* 7188^T (=DSM 24997^T), a novel rhizobacterium from jujube garden soil. *J. Biotechnol.* 2015;206:75–6.
 117. Shen X, Hu H, Peng H, Wang W, Zhang X. Comparative genomic analysis of four representative plant growth-promoting rhizobacteria in *Pseudomonas*. *BMC Genomics.* 2013;14:271.
 118. Chen Y, Shen X, Peng H, Hu H, Wang W, Zhang X. Genomics data comparative genomic analysis and phenazine production of *Pseudomonas chlororaphis*, a plant growth-promoting rhizobacterium. *Genom. Data.* 2015;4:33–42.
 119. Xie S, Wu H, Chen L, Zang H, Xie Y, Gao X. Transcriptome profiling of *Bacillus subtilis* OKB105 in response to rice seedlings. *BMC Microbiol.* 2015;15:21.
 120. Pankiewicz V, Camilios-Neto D, Bonato P, Balsanelli E, Tadra-Sfeir M, Faoro H, et al. RNA-seq transcriptional profiling of *Herbaspirillum seropedicae* colonizing wheat (*Triticum aestivum*) roots. *Plant. Mol. Biol.* 2016;90:589–603.
 121. Zeng Q, Wu X, Wang J, Ding X. Phosphate solubilization and gene expression of phosphate-solubilizing bacterium *Burkholderia multivorans* WS-FJ9 under different levels of soluble phosphate. *J. Microbiol. Biotechnol.* 2017;27:844–55.
 122. Shi H, Wang L, Li X, Liu X, Hao T, He X, et al. Genome-wide transcriptome profiling of nitrogen fixation in *Paenibacillus* sp . WLY78. *BMC Microbiol.* 2016;16:25.
 123. Pfeifer-Sancar K, Mentz A, Rückert C, Kalinowski J. Comprehensive analysis of the *Corynebacterium glutamicum* transcriptome using an improved RNAseq technique. *BMC Genomics.* 2013;14:888.
 124. Irla M, Neshat A, Brautaset T, Rückert C, Kalinowski J, Wendisch VF. Transcriptome analysis of thermophilic methylotrophic *Bacillus methanolicus* MGA3 using RNA-sequencing provides detailed insights into its previously uncharted transcriptional landscape. *BMC Genomics.* 2015;16:73.
 125. Marek-Kozaczuk M, Skorupska A. Production of B-group vitamins by plant growth-promoting *Pseudomonas fluorescens* strain 267 and the importance of vitamins in the colonization and nodulation of red clover. *Biol. Fertil. Soils.* 2001;33:146–51.
 126. Streit W, Entcheva P. Biotin in microbes, the genes involved in its biosynthesis, its biochemical role and perspectives for biotechnological production. *Appl. Microbiol. Biotechnol.* 2003;61:21–31.
 127. Lin S, Cronan JE. Closing in on complete pathways of biotin biosynthesis. *Mol. BioSyst.* 2011;7:1811–21.
 128. Ploux O, Marquet A. Mechanistic studies on the 8-amino-7-oxopelargonate synthase, a pyridoxal-5'-phosphate-dependent enzyme involved in biotin biosynthesis. *Eur. J. Biochem.* 1996;236:301–8.
 129. Eisenberg M, Dtoner G. Biosynthesis of 7, 8-diaminopelargonic acid, a biotin intermediate, from 7-

Introduction

- Keto-8- aminopelargonic acid and S-adenosyl-L-methionine. *J. Bacteriol.* 1971;108:1135–40.
130. Alexeev D, Baxter RL, Smekal O, Sawyer L. Substrate binding and carboxylation by dethiobiotin synthetase - a kinetic and X-ray study. *Structure.* 1995;3:1207–15.
131. Lotierzo M, Bui BTS, Florentin D, Escalettes F, Marquet A. Biotin synthase mechanism: an overview. *Biochem. Soc. Trans.* 2005;33:820–3.
132. Otsuka AJ, Buoncristiani MR, Howard PK, Flamm J, Johnson C, Yamamoto R, et al. The *Escherichia coli* biotin biosynthetic enzyme sequences predicted from the nucleotide sequence of the *bio* operon. *J. Biol. Chem.* 1988;263:19577–85.
133. Pai C. Genetics of biotin biosynthesis in *Bacillus subtilis*. *J Bacteriol.* 1975;121:1–8.
134. Bower S, Perkins JB, Yocum RR, Howitt CL, Rahaim P, Pero J. Cloning, sequencing, and characterization of the *Bacillus subtilis* biotin biosynthetic operon. *J. Bacteriol.* 1996;178:4122–30.
135. Blount KF, Breaker RR. Riboswitches as antibacterial drug targets. *Nat. Biotechnol.* 2006;24:1558–64.
136. Garst AD, Edwards AL, Batey RT. Riboswitches: structures and mechanisms. *Cold Spring Harb. Perspect. Biol.* 2011;3:a003533.
137. Barrick JE, Breaker RR. The distributions, mechanisms, and structures of metabolite-binding riboswitches. *Genome Biol.* 2007;8:R239.
138. Breaker RR. Riboswitches and the RNA world. *Cold Spring Harb. Perspect. Biol.* 2012;4:a003566.
139. Weinberg Z, Wang JX, Bogue J, Yang J, Corbino K, Moy RH, et al. Comparative genomics reveals 104 candidate structured RNAs from bacteria, archaea, and their metagenomes. *Gen. Biol.* 2010;11:R31.
140. Chen L, Cressina E, Dixon N, Erixon K, Owusu K, Micklefield J, et al. Probing riboswitch-ligand interactions using thiamine pyrophosphate analogues. *Org. Biomol. Chem.* 2012;10:5924–31.
141. Gardner PP, Daub J, Tate JG, Nawrocki EP, Kolbe DL, Lindgreen S, et al. Rfam: updates to the RNA families database. *Nucleic Acids Res.* 2009;37:136–40.
142. Sudarsan N, Cohen-chalamish S, Nakamura S, Emilsson GM, Breaker RR. Thiamine pyrophosphate riboswitches are targets for the antimicrobial compound pyrithiamine. *Chem. Biol.* 2005;12:1325–35.
143. Welz R, Breaker RR. Ligand binding and gene control characteristics of tandem riboswitches in *Bacillus anthracis*. *RNA.* 2007;13:573–82.
144. Lünse CE, Scott FJ, Suckling CJ, Mayer G. Novel TPP-riboswitch activators bypass metabolic enzyme dependency. *Front. Chem.* 2014;2:53.
145. Pohl M, Sprenger GA, Müller M. A new perspective on thiamine catalysis. *Curr. Opin. Biotechnol.* 2004;15:335–42.

Introduction

146. Palacios OA, Bashan Y, De-Bashan LE. Proven and potential involvement of vitamins in interactions of plants with plant growth-promoting bacteria-an overview. *Biol. Fertil. Soils*. 2014;50:415–32.
147. Koga J, Adachi T, Hidaka H. Purification and characterization of indolepyruvate decarboxylase: a novel enzyme for indole-3-acetic acid biosynthesis in *Enterobacter cloacae*. *J. Biol. Chem.* 1992;267:15823–8.
148. Begley TP, Downs DM, Ealick SE, McLafferty FW, Van Loon AP, Taylor S, et al. Thiamin biosynthesis in prokaryotes. *Arch. Microbiol.* 1999;171:293–300.
149. Kojic M, Degrassi G, Venturi V. Cloning and characterisation of the *rpoS* gene from plant growth-promoting *Pseudomonas putida* WCS358 : RpoS is not involved in siderophore and homoserine lactone production. *BBA-Gene Struct. Expr.* 1999;1489:413–20.
150. Sant'Anna FH, Andrade DS, Trentini DB, Weber SS, Schrank IS. Tools for genetic manipulation of the plant growth-promoting bacterium *Azospirillum amazonense*. *BMC Microbiol.* 2011;11:107.
151. Sultana U, Desai S, Reddy G. Successful colonization of roots and plant growth promotion of sorghum (*Sorghum bicolor* L .) by seed treatment with *Pseudomonas putida* and *Azotobacter chroococcum*. *World J. Microbiol.* 2016;3:43–9.
152. Georgakopoulos DG, Hendson M, Panopoulos NJ, Schroth MN. Cloning of a phenazine biosynthetic locus of *Pseudomonas aureofaciens* PGS12 and analysis of its expression in vitro with the ice nucleation reporter gene. *Appl. Environ. Microbiol.* 1994;60:2931–8.
153. Hill DS, Stein JI, Torkewitz NR, Morse AM, Howell CR, Pachlatko JP, et al. Cloning of genes involved in the synthesis of pyrrolnitrin from *Pseudomonas fluorescens* and role of pyrrolnitrin synthesis in biological control of plant disease. *Appl. Env. Microbiol.* 1994;60:78–85.
154. Shao J, Li S, Zhang N, Cui X, Zhou X, Zhang G, et al. Analysis and cloning of the synthetic pathway of the phytohormone indole-3-acetic acid in the plant-beneficial *Bacillus amyloliquefaciens* SQR9. *Microb. Cell Fact.* 2015;14:130.

2. RESULTS

2.1. Complete genome sequence of Paenibacillus riograndensis SBR5^T, a Gram-positive diazotrophic rhizobacterium

Luciana Fernandes de Brito^{1,2}, Evelise Bach³, Jörn Kalinowski², Christian Rückert², Daniel Wibberg², Luciane M. Passaglia³, Volker F. Wendisch^{1,2}

¹Genetics of Prokaryotes, Faculty of Biology & ²Center for Biotechnology (CeBiTec), Bielefeld University, Universitätsstraße 25, 33615 Bielefeld, Germany

³Departamento de Genética, Instituto de Biociências, Universidade Federal do Rio Grande do Sul. Av. Bento Gonçalves, 9500, Caixa Postal 15.053, 91501-970 Porto Alegre, RS, Brazil

2.1.1. Abstract

Paenibacillus riograndensis is a Gram-positive rhizobacterium which exhibits plant growth promoting activities. It was isolated from the rhizosphere of wheat grown in the state of Rio Grande do Sul, Brazil. Here we announce the complete genome sequence of *P. riograndensis* strain SBR5^T. The genome of *P. riograndensis* SBR5^T consists of a circular chromosome of 7,893,056 bps. The genome was finished and fully annotated, containing 6,705 protein coding genes, 87 tRNAs and 27 rRNAs. The knowledge of the complete genome helped to explain why *P. riograndensis* SBR5^T can grow with the carbon sources arabinose and mannitol, but not *myo*-inositol, and to explain physiological features such as biotin auxotrophy and antibiotic resistances. The genome sequence will be valuable for functional genomics and ecological studies as well as for application of *P. riograndensis* SBR5^T as plant growth-promoting rhizobacterium.

2.1.2. Results and Discussion

Plant growth-promoting bacteria may be beneficial for crop production [1]. Bacterial communities can be characterized by metagenomics approaches as e.g. applied to monitor changes of root bacterial communities associated to two different development stages of canola (*Brassica napus* L. var *oleifera*) [2]. Studies focusing on isolation of plant growth-promoting

Results

bacteria are also often performed, e.g. for sugar cane [3], maize [4], rice [5], and wheat [6]. *Paenibacillus riograndensis* SBR5^T, a diazotrophic bacterium isolated from the rhizosphere of *Triticum aestivum* L. cultivated in Southern Brazil, has been described as a new species of the genus *Paenibacillus* [7]. The Gram-positive rod-shaped, facultative aerobic, motile, spore-forming *P. riograndensis* SBR5^T has been investigated for its plant growth promotion characteristics and its potential use as wheat inoculant [6]. The strain is available from the Brazilian type collection LFB-FIOCRUZ as CCGB1313 and from Spanish type collection CECT as CECT7330. The draft genome sequence has previously revealed the presence of *nif* genes as well as of genes related to the alternative nitrogen fixation system (*anf* genes) [8]. Since there are few studies about *anf* genes in Gram-positive diazotrophs, this species constitutes an interesting model for the study of the regulation of nitrogen fixation in this group of bacteria [9].

To perform the sequencing of *P. riograndensis* SBR5^T, two shotgun Paired-End and Mate-Pair libraries were generated. The libraries were prepared using Nextera DNA sample preparation kit and Nextera Mate-Pair sample preparation kit, respectively (Illumina, U.S.A.). The sequencing run was carried out using the Illumina MiSeq System. The genome sequencing resulted in 6,781,183 reads, assembled in 4 scaffolds and 198 contigs by the Newbler v.2.8 (Roche, Switzerland), with 198 fold average coverage. The largest scaffold had 7,885,596 bps and the largest contig had 437,460 bps. The average read lengths were 743 ± 249 bps for the Paired-End library and $9,692 \pm 2,423$ bps for the Mate-Pair library.

The genome finishing was performed using the CONSED Software package [10] to order and join the contigs, close gaps (repetitive sequences, which were confirmed by PCR) and resolve SNPs in repetitive regions. The whole genome of SBR5^T consists of a circular chromosome of 7,893,056 bps, with GC content of 50.97% (Table 1). The 523,056 bps absent from the draft genome sequence consisting of 2,276 contigs [8] were not clustered, but scattered over the whole genome. The finished sequence was submitted to GenDB Software [11] for automatic identification and annotation of the genes, resulting in 6,705 protein coding genes, 87 tRNAs and 27 rRNAs (Table 1). The rRNA genes (named Prio_6706 to Prio_6732) are organized in nine individual operons (*rrnA*, *rrnB*, *rrnC*, *rrnD*, *rrnE*, *rrnF*, *rrnG*, *rrnH* and *rrnI*) located in different regions of the genome. Each operon encodes the 5S, 16S, and 23S rRNAs in varied order except for operon *rrnG* which lacks a 5S rRNA gene while operon *rrnH* contains two 5S rRNA genes.

Results

Table 1. Genome features of *P. riograndensis* SBR5^T

Features	Chromosome
Length (bp)	7,893,056
G+C content (%)	50.97%
CDS	6,705
rRNA genes (operons)	27 (9)
tRNA genes	87

The genome of SBR5^T contains genes putatively involved in resistance to several antibiotics such as encoding the antibiotic efflux systems belonging to the RND (e.g. Prio_4911), ABC (e.g. Prio_6246), MFS (e.g. Prio_6658), and MATE (e.g. Prio_2495) protein families. Furthermore, genes that possibly confer specific antibiotic resistance including 10 *van* (e.g. Prio_6068) and 18 genes related to the general β -lactamase mediated resistance were found (e.g. Prio_6596). For example, the growth of SBR5^T on LB agar plates containing 200 $\mu\text{g ml}^{-1}$ erythromycin or 600 $\mu\text{g ml}^{-1}$ kanamycin (data not shown) may be explained by the gene encoding a multidrug exporter of the Emr protein family (Prio_3171), which confers erythromycin resistance in *Escherichia coli* [12], and the kanamycin nucleotidyltransferase gene (Prio_3529), respectively.

SBR5^T is not able to grow in minimal medium without biotin and this biotin auxotrophy is reflected by the absence of all biotin biosynthesis genes (*bioWAFDBI*), although the Prio_5347 encoded P450 enzyme shows similarity to BioI of *Bacillus subtilis*.

P. riograndensis SBR5^T is characterized by the ability to grow with the carbon sources arabinose and mannitol, but not *myo*-inositol [7]. A cluster of three adjacent genes (Prio_4651-4653) encoding uptake system AraE and the AraC-family two-component regulatory system and a cluster of four genes (Prio_6589-6592) encoding enzymes AraB, AraA and AraD as well as repressor AraR may explain uptake, utilization and regulation of arabinose. Mannitol uptake, phosphorylation and conversion to fructose-6-phosphate is commensurate with the presence of four adjacent genes (Prio_1805-1808) coding for mannitol specific PTS and mannitol-1-phosphate 5-dehydrogenase. *P. riograndensis* SBR5^T is unable to utilize *myo*-inositol which is reflected by the lack of the genes *iolB*, *iolD* and *iolJ*, although homologs of *idhA*, *iolE*, *iolC* and *iolA* are present (Prio_3014, Prio_4831, Prio_2204 and Prio_6323). Albeit SBR5^T was negative in a nitrate reduction assay [4], its genome encodes putative nitrate reductase NarGHJI (Prio_3572-3574), while there is no evidence for assimilatory nitrate reductase NasACKBDEF. The complete genome sequence will be valuable for future characterization of the physiology of

Results

the diazotroph *P. riograndensis* SBR5^T, functional genomics and its application in agrobiotechnology.

Sequence accession numbers

The complete genome sequence has been deposited in EMBL/GenBank with accession number LN831776.

2.2.3. References

1. Da Costa PB, Granada CE, Ambrosini A, Moreira F, De Souza R, Dos Passos JFM, et al. A model to explain plant growth promotion traits: a multivariate analysis of 2,211 bacterial isolates. PLoS ONE. 2014;9:1–25.
2. de Campos SB, Youn J-W, Farina R, Jaenicke S, Jünemann S, Szczepanowski R, et al. Changes in root bacterial communities associated to two different development stages of canola (*Brassica napus* L. var *oleifera*) evaluated through next-generation sequencing technology. Microb. Ecol. 2013;65:593–601.
3. Beneduzi A, Moreira F, Costa PB, Vargas LK, Lisboa BB, Favreto R, et al. Diversity and plant growth promoting evaluation abilities of bacteria isolated from sugarcane cultivated in the South of Brazil. Appl. Soil Ecol. 2013;63:94–104.
4. Arruda L, Beneduzi A, Martins A, Lisboa B, Lopes C, Bertolo F, et al. Screening of rhizobacteria isolated from maize (*Zea mays* L.) in Rio Grande do Sul State (South Brazil) and analysis of their potential to improve plant growth. Appl. Soil Ecol. 2013;63:15–22.
5. de Souza R, Beneduzi A, Ambrosini A, da Costa PB, Meyer J, Vargas LK, et al. The effect of plant growth-promoting rhizobacteria on the growth of rice (*Oryza sativa* L.) cropped in southern Brazilian fields. Plant Soil. 2013;366:585–603.
6. Beneduzi A, Peres D, da Costa PB, Bodanese-zanettini MH, Passaglia LMP. Genetic and phenotypic diversity of plant-growth-promoting bacilli isolated from wheat fields in southern Brazil. Res. Microbiol. 2008;159:244–50.
7. Beneduzi A, Costa PB, Melo IS, Bodanese-zanettini MH, Passaglia LMP. *Paenibacillus riograndensis* sp. nov., a nitrogen-fixing species isolated from the rhizosphere of *Triticum aestivum*. Int. J. Syst. Evol. Microbiol. 2010;60:128–33.

Results

8. Beneduzi A, Campos S, Ambrosini A, de Souza R, Granada C, Costa P, et al. Genome sequence of the diazotrophic Gram-positive rhizobacterium *Paenibacillus riograndensis* SBR5^T. *J. Bacteriol.* 2011;193:6391–2.
9. Fernandes GDC, Trarbach LJ, Campos SBD, Beneduzi A, Passaglia LMP. Alternative nitrogenase and pseudogenes : unique features of the *Paenibacillus riograndensis* nitrogen fixation system. *Res. Microbiol.* 2014;165:571–80.
10. Gordon D. Viewing and editing assembled sequences using Consed. *Curr. Protoc. Bioinforma.* Ed. Board Andreas Baxevanis AI. 2003;Chapter 11:Unit11.2.
11. Meyer F, Goesmann A, McHardy AC, Bartels D, Bekel T, Clausen J, et al. GenDB - An open source genome annotation system for prokaryote genomes. *Nucleic Acids Res.* 2003;31:2187–2195.
12. Nishino K, Yamaguchi A. Analysis of a complete library of putative drug transporter genes in *Escherichia coli*. *J. Bacteriol.* 2001;183:5803–12.

2.2. Detailed transcriptome analysis of the plant growth promoting *Paenibacillus riograndensis* SBR5 using RNAseq technology

Luciana Fernandes de Brito^{1,2}, Marta Irla^{1,2,3}, Jörn Kalinowski² and Volker F. Wendisch^{1,2}

¹Genetics of Prokaryotes, Faculty of Biology & ²Center for Biotechnology (CeBiTec), Bielefeld University, Universitätsstraße 25, 33615 Bielefeld, Germany

³Department of Biotechnology and Food Science, Norwegian University of Science and Technology, Trondheim, Norway

2.2.1. Abstract

Background: The plant growth promoting rhizobacterium *Paenibacillus riograndensis* SBR5 is a promising candidate to serve as crop inoculant. Despite its potential regarding environmental and economic benefits, the species *P. riograndensis* is poorly characterized. Here, we performed for the first time a detailed transcriptome analysis of *P. riograndensis* SBR5 using RNAseq technology.

Results: *P. riograndensis* SBR5 was cultivated under 16 different growth conditions and RNA was isolated from samples collected during growth experiment and combined together in order to analyze an RNA pool representing a large set of expressed genes. The resultant total RNA was used to generate two different libraries, one enriched in 5'-ends of the primary transcripts and the other representing the whole transcriptome. Both libraries were sequenced and analyzed to identify the conserved sequences of ribosome binding sites and translation start motifs, and to elucidate operon structures present in the transcriptome of *P. riograndensis*. Sequence analysis of the library enriched in 5'-ends of the primary transcripts was used to identify 1,082 TSS belonging to novel transcripts and allowed us to determine a promoter consensus sequence and regulatory sequences in 5' untranslated regions including riboswitches. A putative thiamine pyrophosphate dependent riboswitch upstream of the thiamine biosynthesis gene *thiC* was characterized by translational fusion to a fluorescent reporter gene and shown to function in *P. riograndensis* SBR5.

Results

Conclusions: Our RNAseq analysis provides insight into the *P. riograndensis* SBR5 transcriptome at the systems level and will be a valuable basis for differential RNAseq analysis of this bacterium.

2.2.2. Background

Members of *Paenibacillus* genus are Gram-positive, spore-forming, motile and facultatively anaerobic bacteria [1]. This group is biochemically and morphologically diverse and is found in various environments, such as soil [2], rhizosphere [3], insect larvae [4], and clinical samples [5]. Originally, *Paenibacillus* belonged to the genus *Bacillus*; however, in 1993 it was reclassified as a separate genus [6]. The important plant growth promoting (PGP) species *Paenibacillus polymyxa*, *Paenibacillus macerans* and *Paenibacillus azotofixans* were included in the new genus when it was proposed [6]. The genus *Paenibacillus* currently comprises more than 150 named species; approximately 6% of these are able to fix nitrogen and possess some other plant growth promotion abilities [7].

Paenibacillus riograndensis SBR5 is the type strain of this species and was isolated from rhizosphere of wheat (*Triticum aestivum*) fields in the south of Brazil (Rio Grande do Sul) [8]. It was shown that *P. riograndensis* SBR5 is a promising candidate for crop inoculation because of its nitrogen fixation ability and other plant growth promotion characteristics such as production of phytohormones and antimicrobial substances [9,10].

A phylogenetic analysis of SBR5 based on the 16S rRNA gene sequence has showed that it is most closely related to *Paenibacillus graminis* RSA19^T (98.1 % similarity) [9]. The genome of SBR5 was completely sequenced and annotated; its circular chromosome consists of 7,893,056 bps, with GC content of 50.97% [11]. The annotation of the finished genome sequence showed the presence of 6,705 protein coding genes, 87 tRNAs and 27 rRNAs genes [11].

Recent research efforts on transcriptome characterization in paenibacilli focused on comparative transcriptomic analysis under different plant-related conditions [12,13]. Contrary to these differential transcriptomic analyses, comprehensive transcriptome analysis allows to chart the RNA landscape of a particular organism for improvement of the genome annotation, detection of novel transcripts and conserved sequence motifs such as transcription start sites (TSS), promoters and ribosomal binding sites [14,15]. These comprehensive analyses have been performed for bacteria of industrial or public health relevance such as *Corynebacterium*

Results

glutamicum [14] and *Salmonella* [16], respectively. Although complete genome sequences of several *Paenibacillus* PGP members have been published [11,17–19], a whole transcriptome analysis for a member of this genus is still missing.

In this study, we describe genome-wide TSS mapping and whole transcriptome analysis of *P. riograndensis* SBR5 cultivated under 16 conditions. Conserved sequence motifs for promoters, ribosome binding sites, riboswitches and other RNA families were determined, and the function of a TPP (thiamine pyrophosphate) riboswitch confirmed by translational fusion with a green fluorescence protein (GfpUV) reporter gene.

2.2.3. Materials and Methods

Cultivation of P. riograndensis SBR5 in different conditions

P. riograndensis SBR5, the bacterial strain used in this study, was obtained from the strain collection of the Department of Genetics at Universidade Federal do Rio Grande do Sul. Here, we performed different cultivations in order to expose SBR5 to varied growth conditions. In all experiments, the bacterial cells were grown in 500 mL shaking flasks containing 50 mL of medium shaking at 120 rpm and at temperature of 30°C, if not stated otherwise. For each condition tested, four biological replicates were used: one for harvesting of bacterial cells and total RNA isolation, and three for further determination of growth characteristics. The optical density at 600 nm ($OD_{600\text{ nm}}$) of the cultivated cells was measured throughout growth. The initial $OD_{600\text{ nm}}$ in all cultivations was approximately 0.05.

The first experiment was performed with lysogeny broth (LB) as growth medium; the cells were grown under three different temperatures: 20°C, 30°C or 37°C. Cells were also cultivated at 30°C for further application of 5 minute-cold shock (from 30°C to 4°C) or heat shock (from 30°C to 50°C) when the middle of the exponential phase was reached. The PbMM (*P. riograndensis* minimal medium: MVcMY without vitamin complex and yeast extract) [20] with 20 mM glucose as carbon source was used for application of the remaining stress conditions. The growth of SBR5 was carried with addition of 100 mM KCl or NaCl or addition of 2 g L⁻¹ of ethanol or methanol to the medium. Moreover, growth in PbMM with addition of three different carbon sources of was compared: 20 mM of glucose, 40 mM of glycerol or 10 mM of sucrose. Finally, the cells were cultivated in three different pHs: 5, 7 or 8, buffered with 50 mM of 2-(N-

Results

morpholino)ethanesulfonic acid (MES), 3-morpholinopropane-1-sulfonic acid (MOPS) and 3-[[1,3-dihydroxy-2-(hydroxymethyl)propan-2-yl]amino]propane-1-sulfonic acid (TAPS), respectively. The bacterial cells were harvested in the middle of the exponential phase and the harvesting procedure was done according to Irla et al. [15].

For the cultivation of the *P. riograndensis* transformants harboring plasmid DNA with *gfpUV* reporter gene under control of the pyruvate kinase promoter (Ppyk) with either native 5' UTR (pP2pyk-*gfpUV*) or 5' UTR of the gene *P.riograndensis_final_150* (pP2pyk_TPP-*gfpUV*), the cells were routinely grown at 30°C, shaking at 120 rpm, in medium DSMZ 220 [21] with addition of 5.5 µg mL⁻¹ of chloramphenicol. *Escherichia coli* strains were routinely cultivated at 37 °C in LB supplied with 15 µg mL⁻¹ of chloramphenicol when needed. To assay the effect of thiamine on *gfpUV* expression by the two *P. riograndensis* strains, bacterial cells were transferred from DSMZ 220 medium to glucose minimal medium PbMM [21] with 0, 5, 10, 15, 20 or 25 µM of thiamine for SBR5(pP2pyk_TPP-*gfpUV*) and 0 or 25 µM of thiamine for SBR5(pP2pyk-*gfpUV*). After overnight growth, cells in minimal medium were used to inoculate fresh PbMM medium containing its respective thiamine concentration.

RNA isolation and preparation of cDNA libraries for sequencing

In order to isolate total RNA from SBR5 cells, bacterial cell pellets previously harvested and kept at -80°C were thawed in ice and RNA was extracted individually for each cultivation condition using NucleoSpin RNA isolation kit (Macherey-Nagel, Düren, Germany). Polymerase Chain Reactions (PCRs) with two pairs of primers amplifying two different genome regions was performed to detect the presence of remaining genomic DNA in the samples (primer sequences in Additional file 2: Table 2). RNA samples with genomic DNA contamination were treated with the RNase-free DNase set (Qiagen, Hilden, Germany). The concentration of isolated RNA was determined by DropSense™ 16 (Trinean, Ghent, Belgium; software version 2.1.0.18). To verify the quality of RNA samples, we performed capillary gel electrophoresis (Agilent Bioanalyzer 2100 system using the Agilent RNA 6000 Pico kit; Agilent Technologies, Böblingen, Germany). All procedures to obtain high quality RNA were done according to manufacturer's recommendations. The extracted RNA samples were pooled in equal parts and the pool of total RNA was subsequently used for the preparation of two different cDNA libraries.

Results

The cDNA libraries of SBR5 were prepared according to two different protocols. One library followed the protocol for the enrichment of 5'-ends of primary transcripts, while the other method allowed the analysis of the whole transcriptome [14,15]. The libraries were prepared and sequenced according to Irla et al. [15].

Mapping sequenced reads onto the genome of P. riograndensis SBR5

Before mapping to the reference genome, the reads obtained during sequencing of the whole transcriptome and 5'-end enriched library were trimmed to a minimal length of 20 base pairs with the Trimmomatic ver. 0.33 [22]. The reads of 5'-end enriched library were trimmed in the single end mode, whereas those of whole transcriptome library in paired end mode. Trimmed reads were mapped to the reference genome of *P. riograndensis* SBR5 (accession number LN831776.1) using the software for short read alignment Bowtie [23].

Determination of transcription start sites (TSS) based on 5'-end enriched library

To determine and classify the TSS based on mapped 5'-end enriched library, we used the software for visualization of mapped sequences ReadXplorer [24]. This determination was done in two steps, one automatic TSS determination and one manual data set curing. First, the TSS were automatically detected by ReadXplorer Transcription Analysis Parameter Wizard, following two different selected sets of criteria described in Table 1. In the generated data, to each TSS detected, several characteristics were reported; including: 70 base pairs sequence upstream the TSS, the assigned gene name and product, the DNA strand to which the assigned gene belongs, the assigned gene start and end position, the distance between the given TSS and its assigned TLS and its classification regarding a TSS assigned to t/mRNA or a novel transcript. As second step, the data generated through the two parameter sets were combined and manually cross-checked to classify the novel transcripts as antisense, intergenic or intragenic, and also to eliminate false positives, as previously described by Irla et al. [15].

Results

Table 1. Parameter sets selected for transcription analysis of *P. riograndensis* SBR5.

Transcription start site detection parameters	1	2
Minimum number of read starts	5	3
Minimum percent of coverage increase	48	48
Maximum low coverage read start count	0	20
Minimum low coverage read starts	0	3
Minimum transcript extension coverage	20	5
Maximum distance to feature of leaderless transcripts	300	5,500
Associate neighboring TSS in a base pair window of	3	3

Determination of 5' UTR length and identification of cis-regulatory elements in 5' UTRs of P. riograndensis SBR5 genes

A genome-wide analysis was performed in order to identify putative RNA motifs in the genome of SBR5. To this end, we used the Infernal tool [25]. The RNAs were annotated to the genome of SBR5 in conjunction with the Rfam library [26]. Furthermore, based on the difference between the position of the analyzed TSS and its assigned TLS, we could determine the 5' UTR length of each TSS belonging to an annotated gene. The 5' UTRs which were longer than 100 base pairs were used as candidates to evaluate whether they contain *cis*-regulatory elements. In total, 209 5' UTRs were analyzed by comparison to Rfam database [27]. One of the detected riboswitches was selected for further analysis; a 313 base pairs sequence of the TPP riboswitch present in the 5' UTR of the *thiC* gene was analyzed in the ARNold tool for identification of transcriptional terminators [28] and in the RNAfold tool for determination of its secondary structure [29].

Detection of conserved ribosomal binding site (RBS) and promoter motifs sequences

To identify the conserved promoter motifs, 70 base pairs sequences upstream the TSS assigned to annotated genes were analyzed. All the genes with identified TSS were considered in the analysis of translation start sites (TLS) and RBS motifs, for this analysis 50 bp upstream of TLS were considered. The Improbizer [30] program was used to find the motifs and the tool WebLogo [31] was used to generate the visualization charts. In both programs, the default settings were applied for the analysis. In the final charts, the conserved motifs are represented in

Results

upper or lower case depending on its conservation, as follows: nucleotides in upper case letters represent more than 80% of occurrence among all analyzed sequences, nucleotides in lower case letters represent occurrence of more than 40%, but less than 80% of all cases. If a base occurs less often than 40%, the letter “n” in lower case appears.

Determination of most abundant genes transcribed in P. riograndensis SBR5

In order to determine the most abundant genes transcribed in the applied cultivation conditions in SBR5, the whole transcriptome library data set was used. The data was normalized by calculation of Reads Per Kilobase per Million mapped reads (RPKM) [32]. The calculation of abundances was automatically generated by the ReadXplorer software [24] as described in Irla et al. [15]. When the transcripts of proteins of unknown function were automatically defined as the most abundant, the gene sequences were submitted to BLASTx analysis to identify the family to which the protein in question belongs [33].

Identification of operon structures in P. riograndensis SBR5

The operon structures present in this transcription analysis were automatically detected in the ReadXplorer software [24]. The same approach was previously shown in Irla et al. [15]. Based on the whole transcriptome library data set, the operon was identified if the intergenic space of two genes positioned in same orientation linked those genes by a bridge of at least two paired mappings. The operons and suboperons were classified separately: a primary operon was considered when a TSS was assigned to the first gene of the operon; and a suboperon was detected when a TSS was assigned within primary operons. Furthermore, the automatically generated operon set was manually cross-checked with the complete whole transcriptome RNAseq data. Finally, the difference between the position in the genome of the first nucleotide and the last nucleotide of the suboperons/operons was calculated to determine the approximated suboperons/operons length distribution. This calculation does not take the lengths of 5' UTRs and 3' UTRs into account.

Results

Strains, plasmid construction and primers

P. riograndensis SBR5 was used as host for heterologous expression of *gfpUV*. Information about the plasmids constructed in this work and primer sequences is available in Additional file 2: Table S2. Molecular cloning was performed as described by Sambrook [34]. Chemically competent cells of *E. coli* DH5 α were prepared for cloning [35]. Genomic DNA of *P. riograndensis* SBR5 was isolated as described by Eikmanns et al. [36]. The NucleoSpin® Gel and PCR Clean-up kit (Machery-Nagel, Düren, Germany) was used for PCR clean-up and plasmids were isolated using the GeneJET Plasmid Miniprep Kit (Thermo Fisher Scientific, Waltham, USA). Plasmid pNW33Nkan backbone was cut with restriction enzyme *Bam*HI (Thermo Fisher Scientific, Waltham, USA) and inserts were amplified using Allin HiFi DNA polymerase (HighQu, Kraichtal, Germany) and the overlapping regions joined by Gibson assembly [37]. For colony PCR the Taq polymerase (New England Biolabs) was used. The correctness of insert sequences was confirmed by sequencing. The constructed plasmids were named pP2pyk-*gfpUV* or pP2pyk_TPP-*gfpUV* and transformed to *P. riograndensis* SBR5 via magnesium-aminoclay method as described by Brito et al. (2016).

Fluorescence-activated cell scanning analysis

To quantify the fluorescence intensities, SBR5 cells were analyzed by means of flow cytometry. Routinely, the SBR5 transformants were grown until reaching the middle of the logarithmic phase and centrifuged for 15 minutes at 4,000 rpm. The pellets were washed three times in NaCl 0.9 % solution and the OD_{600nm} was adjusted to 0.3. The fluorescence of the cell suspension was measured using flow cytometer (Beckman Coulter, Brea, US) and the data analyzed in the Beckman Coulter Kaluza Flow Analysis Software. The settings for the emission signal and filters within the flow cytometer for detection of GfpUV were 550 short pass and 525 band pass in FL9 filter.

Results

2.2.4. Results

Cultivation of P. riograndensis SBR5 under various growth conditions

Apart from a core subset of constitutively expressed genes, most genes are transcribed only under certain conditions. In order to obtain a broad representation of the whole transcriptome, we performed several shaking flasks cultivations of SBR5 under different conditions for subsequent RNA extraction. *P. riograndensis* SBR5 was cultivated in lysogeny broth (LB) at three different temperatures (20°C, 30°C and 37°C) and was also submitted to five minutes of cold (4°C) and heat (50°C) shock during growth at 30°C. As standard growth condition in a mineral salts medium, SBR5 was cultivated in *Paenibacillus* minimal medium (PbMM) at 30°C and pH 7 with 20 mM glucose as sole carbon source. In addition, the medium pH was adjusted to pH 5 or pH 8 for growth in moderately acidic or alkaline conditions, respectively. As stress conditions, 100 mM of KCl or NaCl, or 2 g L⁻¹ of ethanol or methanol was added to the minimal medium PbMM. Glycerol or sucrose was used as alternative carbon source. Compared to standard conditions, growth of SBR5 under stress conditions was in general slower (Additional file 1: Table S1). Hyperosmotic stress, low or high pH and low temperature (20°C) affected growth of SBR5 to the largest extent (Additional file 1: Table S1). Under all conditions, exponentially growing cells were harvested for RNA isolation.

Preparation and mapping of DNA sequence reads onto P. riograndensis SBR5 genome

After confirmation of RNA integrity and absence of DNA contamination, the prepared RNA samples were pooled. Two cDNA libraries were prepared for sequencing: a 5'-end enriched library and a whole transcriptome library. The generated whole transcriptome and 5'-end enriched cDNA libraries were sequenced on a single flow cell of a MiSeq Desktop Sequencer system. The total number of reads generated from whole transcriptome and 5'-end enriched libraries were 11.57 million and 1.40 million, respectively (Table 2). Trimming of the reads with a length threshold of 20 bp resulted in 5.87 million (51% of the total reads) remaining reads for the whole transcriptome library and 827,376 (59% of total reads) for the 5'-end enriched library (data not shown). The trimmed reads were mapped to the genome of *P. riograndensis* SBR5, and 1.22 million whole transcriptome library reads and 345,313 reads of the 5'-end enriched library

Results

were uniquely aligned to the genome of SBR5 while 122,980 and 31,899 reads were aligned to multiple genome regions, respectively (Table 2).

Table 2. Sequencing and mapping features of cDNA libraries of *P. riograndensis* SBR5.

	Whole transcriptome	5' enriched ends
Total reads	11,577,588	1,401,776
Mapped reads	5,876,240	345,313
Mapped at single position	1,228,354	313,414
Mapped at multiple position	122,980	31,899

Identification of transcription start sites (TSS) based on the mapped 5'-end enriched data

In order to detect putative TSS in the mapped 5'-end enriched data; two TSS analysis parameter sets were chosen (Table 1). The use of the parameter set 1 led to the automatic detection of 849 TSS and by using parameter set 2 1,951 TSS were detected (Table 1). Subsequently, these results were merged. Figure 1 shows the scheme of the manual review of the automatically detected TSS which led to the identification of 86 TSS belonging to rRNA or tRNA genes. Moreover, 363 elements were considered not to be TSS or to be false positives. The 2,651 remaining TSS were classified as either belonging to 5' UTRs of annotated genes or of novel transcripts. Out of the 6,705 genes annotated in the genome of SBR5 (Brito et al., 2015), 1,173 were found to possess TSS. The detected TSS were classified as single (1,102) or multiple (166). The remaining 1,082 TSS were classified as belonging to novel transcripts, divided into the groups of antisense (170), intergenic (77) or intragenic (835) transcripts (Figure 1).

Results

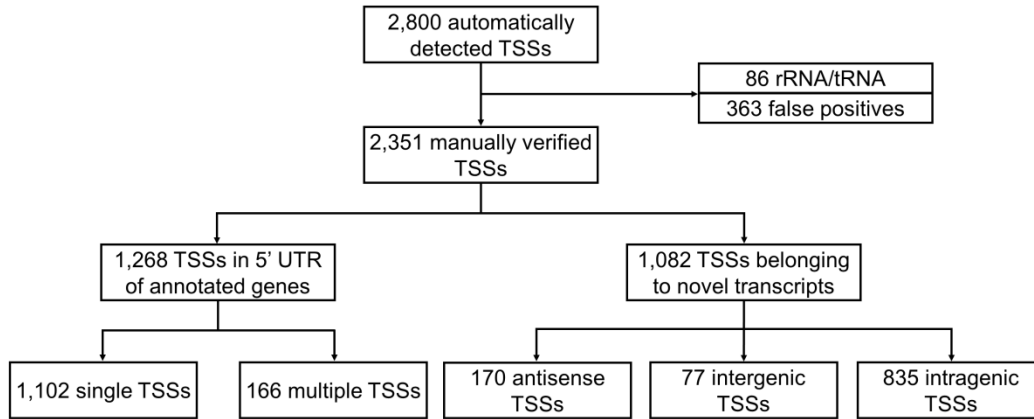


Figure 1. Classification of TSS identified with RNAseq. Schematic view of the TSS analysis flow: TSS automatic identification by ReadXplorer [24], filtering of false positives and rRNA/tRNA, manual verification and classification of TSS between TSS belonging to 5' UTR of annotated genes or to novel transcripts.

Distribution of 5' UTR length in P. riograndensis SBR5

The sequences located between TSS and the gene start codons were used for the analysis of 5' UTR lengths. For this purpose, only the 5' UTRs assigned to annotated genes were considered. The length of 5' UTRs in *P. riograndensis* varied from 0 to 799 base pairs. Only two of the genes with annotated TSS were considered leaderless (no 5' UTR present): *P.riograndensis_final_2873* and *P.riograndensis_final_5691* (Additional file 3: Table S3). Moreover, 9 of the analyzed 5' UTRs were found to be shorter than 10 base pairs (Additional file 3: Table S3). Figure 2 shows the distribution of the 5' UTR lengths indicating that the majority of 5' UTRs is 25 to 50 base pairs long. Among the 1,269 analyzed 5' UTRs, 209 (16.4%) were longer than 100 base pairs (Figure 2). Those 5' UTRs were further used in a screen for *cis*-regulatory RNA elements.

Results

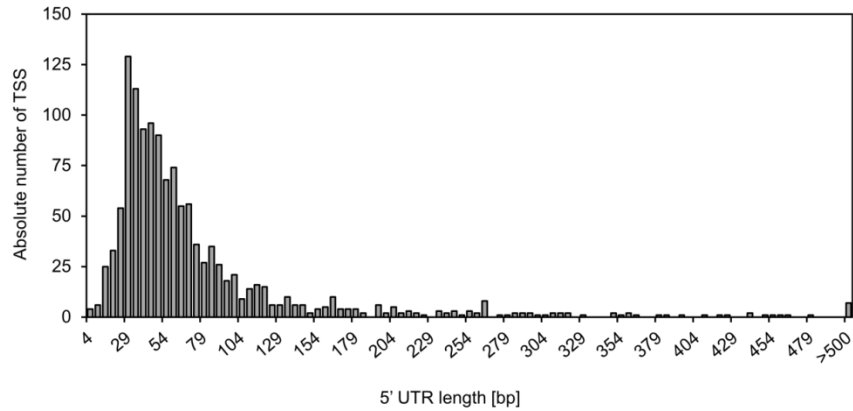


Figure 2. Distribution of 5' UTR lengths of mRNAs assigned to genes in *P. riograndensis* SBR5. The 5' UTR length was the distance between the identified TSS and its assigned TLS. The lengths of the 1,268 5' UTRs of annotated genes were grouped in a crescent interval of 5 base pairs or longer than 500 base pairs.

Identification of consensus promoter motif sequences in P. riograndensis SBR5

The 1,269 TSS identified as belonging to annotated genes were used in a search for the conserved promoter motifs (Figure 1). The software Improbizer was applied to predict the motifs in a DNA region 70 base pairs upstream of each of those TSS (Ao et al., 2004). Conserved -35 and -10 promoter sequence motifs were found in 1,220 (96.1%) and 1,217 (95.9%) of the analyzed sequences, respectively (Figure 3). Figure 3 shows the -10 and -35 motif sequence logos generated by WebLogo software [31], which were ttgaca for -35 hexamer motif and TATAaT for the -10 hexamer motif. The mean spacer lengths between the -35 and -10 motifs and -10 motifs and TSS were 17.6 base pairs and 4.1 base pairs, respectively (Figure 3).

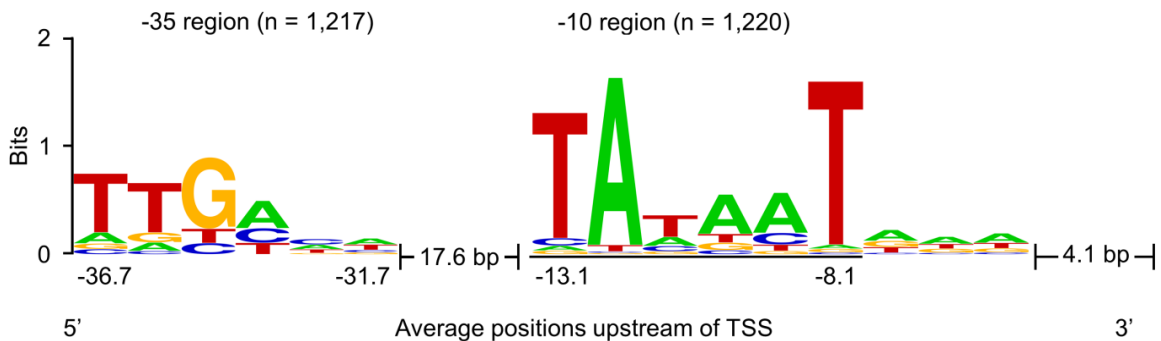


Figure 3. Analysis of promoter motifs in *P. riograndensis* SBR5. The nucleotide distribution in the promoter motifs of *P. riograndensis* SBR5 were determined by using the Improbizer tool [30]. WebLogo tool [31] was used to determine the

Results

conservation of the nucleotides which was measured in bits and represented in the plot by the size of the nucleotide. Nucleotides in upper case letters represent more than 80% of occurrence among all analyzed sequences, nucleotides in lower case letters represent occurrence of more than 40%, but less than 80% of all cases. If a base occurs less often than 40%, the letter “n” in lower case appears.

Identification of RBS (ribosome binding site) and TLS (translation start site) consensus sequences in P. riograndensis SBR5

Similarly to the analysis of the promoter motifs, the Improbizer software was used to determine the consensus sequence of RBS and TLS in the sequence 50 base pairs upstream of the translation start codon of genes associated to the 1,269 previously identified TSS (Figure 1). Some genes were characterized as associated to multiple TSS (Figure 1), therefore the upstream sequence of these genes was only included once in the analysis. Hence, the 1,173 remaining sequences were extracted from the genome of SBR5 and submitted to Improbizer and WebLogo for the identification of the conserved motifs of RBS and TLS (Figure 4). RBS motifs were identified in 98% (1,155) of analyzed sequences. The determined RBS motif of *P. riograndensis* SBR5 consists of three conserved guanines (aGGaGg, in capital letters) in approximately 90% of the analyzed sequences (Figure 4). Translational start codons were identified in all the analyzed sequences (Figure 4). The TLS found in the analyzed sequences were ATG (924; 79%), GTG (138; 12%) and TTG (111; 9%). The lengths of the spacer sequence between RBS and TLS varies between 5 and 13 base pairs, with an average of 7.8 ± 2.0 base pairs (Figure 4).

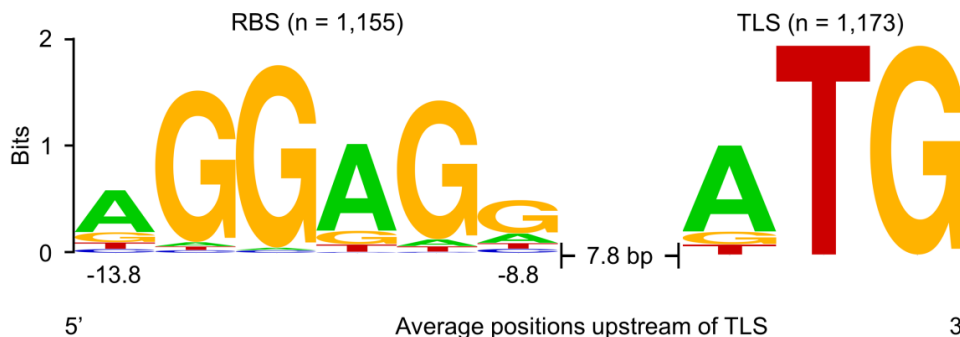


Figure 4. Ribosome binding site and translation start site analysis in *P. riograndensis* SBR5. The nucleotide distribution in ribosome binding sites and translation start sites were determined by using the Improbizer tool [30]. WebLogo tool [31] was used to determine the conservation of the nucleotides which was measured in bits and represented in the plot by the size of the

Results

nucleotide. Nucleotides in upper case letters represent more than 80% of occurrence among all analyzed sequences, nucleotides in lower case letters represent occurrence of more than 40%, but less than 80% of all cases. If a base occurs less often than 40%, the letter “n” in lower case appears.

Identification of cis-regulatory elements in 5' UTRs of P. riograndensis SBR5 genes

In order to identify putative RNA motifs in the genome sequence of *P. riograndensis* SBR5, we used the Infernal tool [25] and the Rfam database, which contains hundreds of RNA families [26]. This approach revealed 327 RNA motifs that subsequently were manually cross checked. Matches to tRNAs, ribosomal RNAs and RNA motifs from Eukaryotes or different bacterial groups were not considered. As result, 98 RNA motifs among 31 Rfam families were identified (Additional file 7: Table S7).

In an alternative approach based on the RNAseq data, we analyzed 209 5' UTRs longer than 100 base pairs (Figure 2) for the presence of *cis*-regulatory elements by comparison to the Rfam database. This analysis revealed 10 putative *cis*-regulatory elements grouped in 8 types of riboswitch families (Table 3). Thus, 10 of 98 putative 5' UTR RNA motifs upstream of annotated genes are found in the RNAseq analysis of pooled RNA from 16 conditions. A TPP (thiamine pyrophosphate) sensitive riboswitch was predicted to be present in the 5' UTR of the gene *P.riograndensis_final_150* (*thiC*) encoding phosphomethylpyrimidine synthase, which is putatively involved in thiamine biosynthesis, and in the 5' UTR belonging to the operon *P.riograndensis_final_504-502*. Although *P.riograndensis_final_503* gene is automatically annotated as a hypothetical protein, BLASTx analysis revealed that it belongs to the thiamine-binding protein superfamily. More vitamin and amino acid related riboswitches were found: a pantothenate related *pam* riboswitch in the 5' UTR of putative pantothenate synthesis operon and a riboswitch recognizing S-adenosylmethionine (SAM) in the 5' UTR of an operon encoding homoserine O-succinyltransferase and cystathionine gamma-lyase proteins. The T-box regulatory elements were found in 5' UTR of the genes coding for D-3-phosphoglycerate dehydrogenase (*serA*) and valine tRNA ligase (*valS*). Furthermore, the protein dependent L20 leader and L21 leader riboswitches, the metabolite dependent *ydaO-yuaA* riboswitch and the *pfl* riboswitch were identified in this work (Table 3).

Results

Table 3. Riboswitches detected in the transcriptome of *P. riograndensis* SBR5 and their transcriptional organization.

Accession	Riboswitch and its transcriptional organization	Related function	Locus tag
RF00379	(ydaO-yuaA)- P.riograndensis_final_93	Cell wall-associated hydrolase (invasion- associated protein)	P.riograndensis_final_93
RF00059	(TPP)- <i>thiC</i> (TPP)- P.riograndensis_final_504-	Phosphomethylpyrimidine synthase Conserved hypothetical protein-	P.riograndensis_final_150 P.riograndensis_final_504-
RF00059	P.riograndensis_final_503- P.riograndensis_final_502 (L20 leader)- <i>infC</i> -	Hypothetical protein- Biding protein dependent transport system inner membrane component Translation initiation factor IF-3-	P.riograndensis_final_503- P.riograndensis_final_502
RF00558	P.riograndensis_final_1528- P.riograndensis_final_1529	Conserved hypothetical protein- Ribosomal protein L20	P.riograndensis_final_1527- P.riograndensis_final_1528- P.riograndensis_final_1529
RF00162	(SAM)- <i>metaA</i> - P.riograndensis_final_2059	Homoserine O-succinyltransferase- Cystathionine gamma-lyase	P.riograndensis_final_2058- P.riograndensis_final_2059
RF01749	(pan)- <i>panB</i> - <i>panC</i> - P.riograndensis_final_4379	3-Methyl-2- oxobutanoatehydroxymethyltransferase- Pantothenate synthetase-	P.riograndensis_final_4381- P.riograndensis_final_4380- P.riograndensis_final_4379
RF00230	(T-box)- <i>serA</i> (L21 leader)- <i>rplU</i> -	Aspartate 1-decarboxylase alpha D-3-phosphoglycerate dehydrogenase	P.riograndensis_final_4453 P.riograndensis_final_5298-
RF00559	P.riograndensis_final_5299- P.riograndensis_final_5300	Conserved hypothetical protein- 50S ribosomal protein L27	P.riograndensis_final_5299- P.riograndensis_final_5300
RF00230	(T-box)- <i>valS</i> (pfl)-	Valine tRNA ligase	P.riograndensis_final_5318
RF01750	P.riograndensis_final_6217	Hypothetical protein	P.riograndensis_final_6217

A TPP riboswitch influences gfpUV expression in P. riograndensis SBR5

The prediction of the secondary structure of the TPP riboswitch (in the 5' UTR of *thiC* gene with 313 base pairs sequence) showed that it contains no terminator sequence, but a 5'-GAUAA-3' sequence and its complementary 5'-UUAUC-3' is present in many predicted stems, including the stems of the aptamer region. This indicates the existence of anti-sequestering stems in this molecule, as showed schematically in Figure 5A. SBR5 cells were transformed with the plasmid pP2pyk_TPP-*gfpUV* which carries the constitutive promoter Ppyk with the 5' UTR replaced by the 5' UTR of the P. riograndensis_final_150 gene driving the expression of the reporter gene *gfpUV* (Additional file 2: Table S2). The 5' UTR of the P. riograndensis_final_150 gene contains the sequence of a TPP riboswitch (Table 3). Our aim was to detect the influence of the *P. riograndensis* TPP riboswitch on gene expression in the presence of different concentrations of its ligand thiamine. The cells were grown in glucose minimal medium PbMM supplied with 0, 5, 10, 15, 20 or 25 μ M of thiamine and the GfpUV fluorescence was measured by the means of flow cytometry. As control for this assay, the plasmid pP2pyk-*gfpUV*, containing

Results

Ppyk native 5' UTR was used to transform SBR5 cells and the resultant strain was also cultivated in glucose PbMM, but supplied with 0 or 25 μM of thiamine. The median fluorescence intensity (MFI) of the control strain SBR5(pP2pyk-*gfpUV*) remained the same when the cells were in absence or in presence of 25 μM of thiamine (Figure 5B). In contrast, when in presence of gradually increasing concentrations of thiamine, the GfpUV MFI of the TPP riboswitch-containing strain SBR5(pP2pyk_TPP-*gfpUV*) decreased drastically (Figure 5B). The GfpUV MFI of SBR5(pP2pyk_TPP-*gfpUV*) was similar to the control strain when no thiamine was added to the growth medium. The addition of 5 μM of thiamine readily reduced the expression of *gfpUV* about three times (Figure 5B). Furthermore, there was no difference in GfpUV MFI of SBR5(pP2pyk_TPP-*gfpUV*) when 5, 10, 15, 20 or 25 μM of thiamine were added to the medium (Figure 5B).

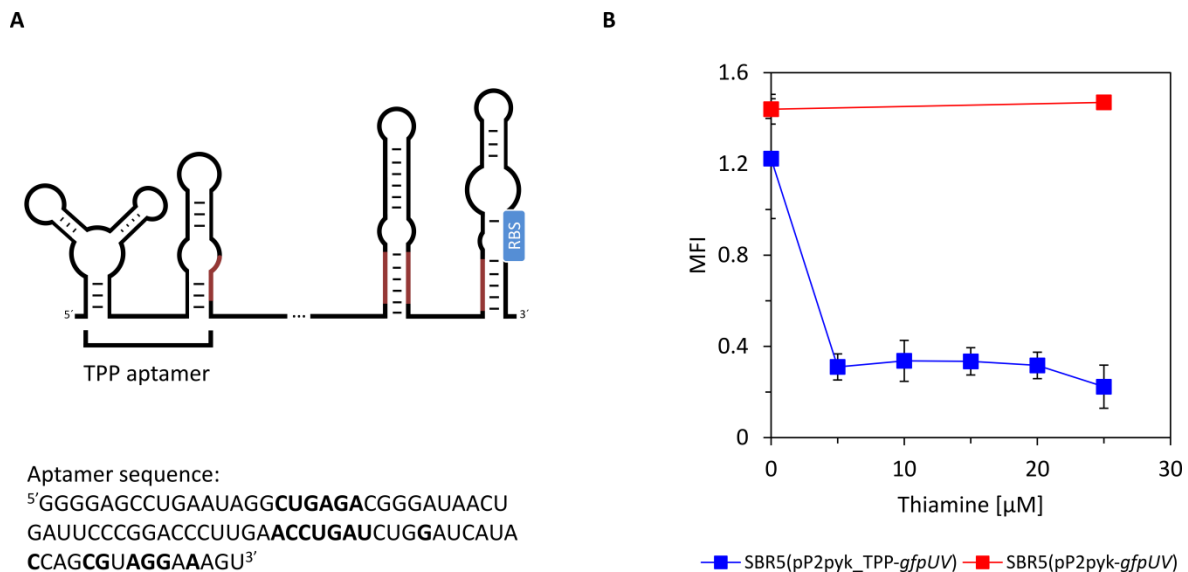


Figure 5. TPP riboswitch influence on the reporter *gfpUV* gene expression of *P. riograndensis* SBR5. A. Schematic representation of the TPP riboswitch and TPP aptamer sequence predicted using RNAfold tool [29]; regions of riboswitch scheme in red represents possible anti-sequestering stems present in the riboswitch sequence; regions of aptamer sequence in bold are identical to the TPP riboswitch consensus sequence of *B. subtilis*. B. GfpUV median fluorescence intensity (MFI) in SBR5 under six gradually increasing concentrations of thiamine; *gfpUV* expression was driven either by the *pyk* promoter with 5' UTR exchanged by the *thiC* gene 5' UTR or *pyk* promoter carrying native 5' UTR. Means and standard deviation of biological triplicates were measured by flow cytometry of 20,000 cells.

Results

Identification and characterization of novel transcripts

Here, we performed the characterization of *P. riograndensis* novel transcripts based on the 5'-end enriched data set. Among the 2,351 manually verified TSS, 1,082 were classified as belonging to novel transcripts. Depending on their position in genes or untranslated regions, these TSS belonged to antisense transcripts (170), transcripts intragenic (835) to annotated genes or their 5'/3' UTRs, or intergenic (77) transcripts (Figure 1). Additional file 5: Table S5 shows the intragenic transcripts which were organized according to their position and associated gene. As intergenic novel transcripts could not be assigned to annotated genes, they were manually annotated as unknown transcripts. The length of those features was determined on the basis of the whole transcriptome data (Additional file 6: Table S6). BLAST analysis of the intergenic novel transcripts resulted in discovery of 34 small proteins and 27 small RNAs. Small RNAs were analyzed in the Rfam database and three of them were annotated as Small SRP (*P.riograndensis_final_s0002*), BsrC sRNA (*P.riograndensis_final_s0008*) and RNase P (*P.riograndensis_final_s0013*)(Table 5).

Table 5. Novel transcripts with known function in *P. riograndensis* SBR5.

Feature	Class	Locus tag	Feature start	Feature stop	Length	Strand
Small SRP	Small RNA	<i>P.riograndensis_final_s0002</i>	130367	130639	272	+
BsrC sRNA	Small RNA	<i>P.riograndensis_final_s0008</i>	688067	687745	322	-
RNase P	Small protein	<i>P.riograndensis_final_s0039</i>	6002090	6001625	465	-

Gene expression ranked according to transcript abundances

The abundance of transcripts in the analyzed RNA samples was quantified on the basis of the whole transcriptome dataset using RPKM values. 6,367 transcripts were detected during the analysis, corresponding to 94% of the total number of genes annotated in the genome of *P. riograndensis*. Transcript abundance varied over six orders of magnitude with RPKM values ranging from 0.11 to 71,849.57 and was categorized arbitrarily as follows. Transcript abundance was considered low for 70% of transcripts (with RPKM values < 100), intermediate (RPKM between 100 and 1,000) for 11% of the detected transcripts and high for 261 transcripts (RPKM

Results

between 1,000 and 10,000). Twenty one transcripts showed RPKM values exceeding 10,000 and these were considered as transcripts with very high transcript abundance and are listed in Table 4.

Table 4. Most abundant transcripts of *P. riograndensis* SBR5 under the chosen cultivation conditions.

Gene	Product	RPKM Value
<i>rpsH</i>	30S ribosomal protein S8	71,849.57
P.riograndensis_final_4321	<i>N-acetyltransferase superfamily</i>	70,789.99
P.riograndensis_final_30	<i>Veg protein; sporulation, Stimulates biofilm formation via transcriptional activation of extracellular matrix genes</i>	53,361.67
P.riograndensis_final_5486	Hypothetical protein	39,913.22
P.riograndensis_final_2764	Hypothetical membrane protein	28,462.66
P.riograndensis_final_2316	<i>Small, acid-soluble spore protein superfamily</i>	24,204.00
P.riograndensis_final_1999	<i>PTS maltose transporter subunit IIBC</i>	21,134.31
P.riograndensis_final_6014	50S ribosomal protein L24	20,187.98
P.riograndensis_final_4594	Hypothetical protein	18,591.09
P.riograndensis_final_2529	Hypothetical protein	17,946.18
P.riograndensis_final_956	<i>Recombinase RecA</i>	17,771.90
P.riograndensis_final_5132	<i>Ribosomal S21 superfamily</i>	17,463.97
P.riograndensis_final_5601	<i>Small, acid-soluble spore protein superfamily</i>	16,757.65
P.riograndensis_final_1944	<i>Protein of unknown function DUF1292 superfamily</i>	15,456.74
<i>ftsH</i>	ATP-dependent zinc metalloprotease FtsH	15,355.15
<i>rpsS</i>	30S ribosomal protein S19	15,060.69
P.riograndensis_final_6183	Conserved hypothetical protein	14,247.19
P.riograndensis_final_6034	<i>50S ribosomal protein L7A</i>	14,218.27
P.riograndensis_final_1943	<i>Crossover junction endodeoxyribonuclease RuvA</i>	11,659.67
P.riograndensis_final_1181	Transcriptional regulator, TetR family	11,466.86
P.riograndensis_final_6018	50S ribosomal protein L16	10,826.18

Gene products in italics were predicted with BLASTx analysis.

BLASTx analysis of the 14 genes which were automatically annotated to code for hypothetical proteins or proteins with unknown function was performed to predict their functions. However, for 5 genes with very highly abundant transcripts a function could not be predicted (Table 4). Part of the very highly abundant transcripts code for ribosomal proteins (6 genes). Remarkably, three genes related to bacterial sporulation had very highly abundant transcripts (Table 4). Noteworthy, the transcripts of a gene coding for putative phosphocarrier HPr protein which belongs to the phosphoenolpyruvate-dependent sugar phosphotransferase system (PTS) were also very highly abundant. This may likely reflect that glucose, a PTS substrate in *Paenibacilli*, was used as carbon source under most growth conditions.

Results

Identification of operon structures in P. riograndensis SBR5

Here, we identified operon structures in *P. riograndensis* SBR5. Based on the mapped reads generated from whole transcriptome library, we assigned genes either to monocistronic transcripts, primary operons or suboperons. Operon structures were automatically detected when two or more combined reads connected neighboring genes. Suboperons were found manually, when the TSS were located within operon structures. Genes with annotated TSS that were not automatically detected as primary operons were classified as monocistronic transcripts. In total, 919 monocistronic transcripts were detected, and 1,776 genes were assigned to 622 operons and 248 suboperons (Figure 6B; Additional file 8: Table S8). The length distribution of the operons and sub-operons was estimated and shown to peak between 1,000 and 3,000 base pairs for operons, while the majority of the suboperons were shorter than 2,000 base pairs (Figure 6A). In general, the number of operons decreases with the number of genes in those operons and most operon structures (71%) are composed of 2 genes while only 5 operons contained more than 7 genes (Figure 6B). Notably, riboswitches were found in the 5' UTRs of 5 operons *P.riograndensis_final_502-504*, *infC-P.riograndensis_final_1528-1529*, *metA-P.riograndensis_final_2059*, *panB-panC-P.riograndensis_final_4379* and *rplU-P.riograndensis_final_5299-5300* (Table 3).

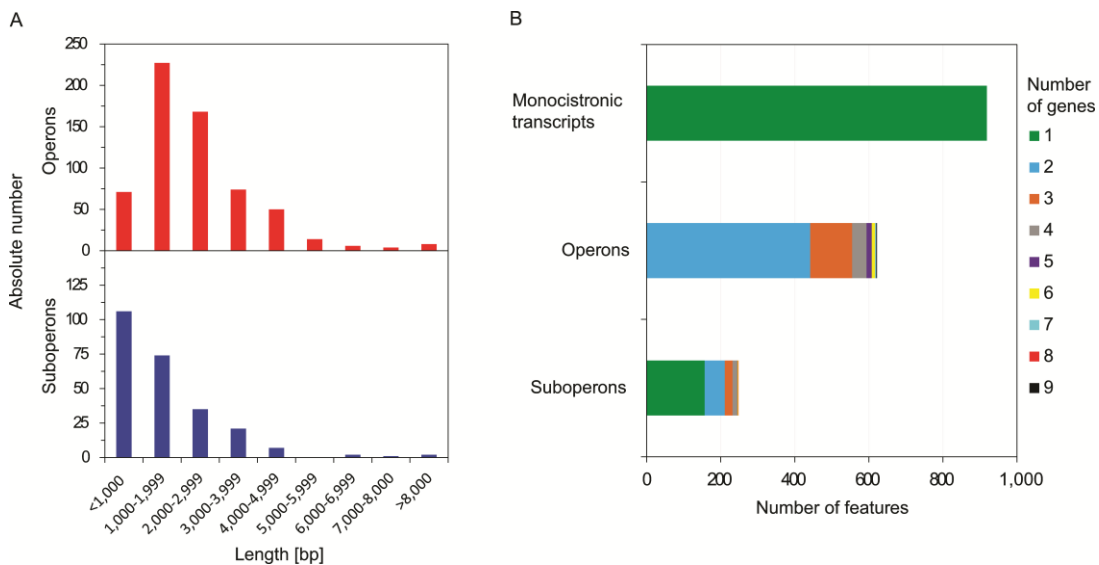


Figure 6. Operon analysis in *P. riograndensis* SBR5. A. Length distribution (in base pairs) of detected operons and suboperons; B. Analysis of feature number in monocistronic transcripts, operons and suboperons in *P. riograndensis* SBR5.

Results

2.2.5 Discussion

The complete genome sequence of the plant growth promoter *P. riograndensis* SBR5 has been determined previously and shown to code for 6,705 proteins [11]. In the present study, we performed a detailed transcriptome analysis of this bacterium. The TSS, promoter motifs, operon structures, RBS motifs, translation starts and transcriptional organization were characterized. This work lays a foundation for understanding of gene expression in this bacterium and complements differential gene expression analysis. Recently, the transcriptional profile of nitrogen fixation by *P. riograndensis* SBR5 was assayed, where the nitrogen fixation genes grouped in three genome clusters were characterized by transcript analysis by the means of quantitative real time-qPCR [10]. Among the three clusters of nitrogen fixation genes present in the genome sequence of SBR5 [10,38] three operons were found: *nifB1H1D1K1E1N1X1-orf1-hesA-V*, *nifE2N2X2* and *anfHDGK* [10]. In the present study, these operons were not found to be expressed under the chosen growth conditions, whereas a different gene related to nitrogen fixation encoding putative nitrogenase (flavodoxin; P.riograndensis_final_4327; Additional file 8: Table S8) was found to be expressed. The lack of expression of the nitrogen fixation genes in the transcriptome analysis presented in this study may be explained by the fact that all growth conditions were characterized by sufficient nitrogen concentrations (in LB medium or minimal media with 16 mM ammonium sulfate) while it is known that nitrogen fixation genes are generally transcribed under poor nitrogen supply conditions [13,39,40]. In a different study, 150 genes were shown to be differentially expressed under iron-replete in comparison to iron-limiting conditions [41]. Surprisingly, a high expression level of the Fe³⁺ siderophore transporter gene *fecE* was observed suggesting that *P. riograndensis* SBR5 can uptake Fe³⁺ siderophore from the environment although is not able to produce those siderophores itself [41]. Here, we could identify two operon structures putatively involved in Fe³⁺ siderophore uptake and transport: the operon *fhuB* - P. riograndensis_final_3660 which encodes a putative Fe³⁺ hydroxamate import system permease and a component of an ABC type Fe³⁺ siderophore transport system, respectively, and the operon P. riograndensis_final_5688 - P. riograndensis_final_5687 which comprises a gene encoding the Fe³⁺ siderophore ABC transporter permease (Additional file 8: Table S8).

In the transcriptome of *P. riograndensis* SBR5, the abundantly transcribed genes could be grouped by their presumed functions: ribosomal proteins, sporulation related proteins, proteins related to carbon metabolism and others. Many abundantly transcribed genes encode proteins of

Results

unknown function (Table 4). Among the highly expressed genes, we have detected one gene coding for a subunit of a carbohydrate phosphotransferase system (Table 4), which may be due to the fact that we mostly used sucrose and glucose as carbon sources (give gene IDs of the glucose PTS and sucrose PTS). A transcriptome analysis of carbon source utilization (β -glucan, starch, cellobiose, maltose, glucose, xylose and arabinose) by *Paenibacillus* sp. JDR-2 revealed a regulatory connection for the utilization of the polysaccharides β -glucan, starch and xylans, while transcription of genes coding for proteins involved in monosaccharide (e.g. arabinose and glucose) utilization was less apparent [12]. BLASTx analysis revealed three sporulation-related genes (*P.riograndensis_final_4321*, *P.riograndensis_final_2316* and *P.riograndensis_final_5601*) among the most abundantly expressed genes (Table 4). This result might be due to the fact that different stress conditions were applied during cultivations of SBR5, which included five minutes of cold and heat shock but also exposure to salinity, solvent, low temperature and low pH along the bacterial growth. The exposure to stress conditions affected growth rates in comparison to the optimal growth conditions, and might have also induced expression of sporulation related genes (Additional file 1: Table S1). Very recently, sporulation genes *spoVT* and *spoIIIAH* were shown to be transcribed by *P. riograndensis* SBR5 under iron-limiting conditions [41]. Moreover, the related *P. polymyxa* SC2 expressed sporulation genes (*spo0A*, *spoIIE*, *spoIIAA*, *spoIIAB*, *sigE* and *sigF*) when cultivated under sporulation conditions (cultivation in LB for one day) [42].

The transcriptional organization of 1,776 genes of *P. riograndensis* SBR5 in 622 operons including 248 suboperons and 919 monocistronically transcribed genes (Figure 6B; Additional file 8: Table S8) was comparable to that found in *B. methanolicus*, in which 1,164 genes were assigned to 381 operons and 94 suboperons, and also ~ 900 monocistronic transcripts were detected [15]. Similarly, in *B. subtilis* 736 regulated operons were found [43] and 1,013 genes were organized in 616 operons (including 565 suboperons) for the actinobacterium *C. glutamicum* [14]. Most operons detected here were composed of only two genes and were between 1,000 and 3,000 base pairs in length (Figure 6). Accordingly, most suboperons comprised only one gene and were smaller than 2,000 base pairs (Figure 6). The length distribution of suboperons/operons and the number of genes constituting these are commensurate with the average length of the genes in *P. riograndensis* SBR5 genome of 1,008 base pairs (data not shown).

Surprisingly, the absolute number of TSS (present in 5' UTR of annotated genes together with TSS belonging to novel transcripts) in the present work were comparable to those detected

Results

for *B. methanolicus* MGA3 [15]; they were 2,350 and 2,167 respectively, although the genome of *P. riograndensis* SBR5 is about ~4.5 Mbp larger than the genome of *B. methanolicus* MGA3 [15]. This observation may reflect the fact that RNA was pooled from cell cultivated under various growth and stress conditions that were chosen with a similar rationale both for *B. methanolicus* MGA3 and *P. riograndensis* SBR5. Under similar cultivation conditions 2,591 TSS were also detected in the transcriptome of *C. glutamicum* [14], despite the difference in genome size of ~4.6Mbp [44]. This may indicate that a similar set of genes is transcribed in these three species under a comparable set of stress/cultivation conditions. It is also evident that expression of a larger part of the *P. riograndensis* genes could be not be detected under the chosen cultivation conditions and they may only be expressed under yet to be defined growth/stress conditions.

Our RNAseq analysis allowed us to identify 1,082 novel transcripts in *P. riograndensis* SBR5 that were classified as antisense (16%), intragenic (77%) or intergenic (7%) transcripts (Figure 1). Antisense transcripts were found to be abundant in *P. riograndensis* SBR5. The number of reported antisense RNAs varies between bacteria and the biological advantages of such overlapping transcription remains unclear, but antisense RNAs may play important roles in regulation e.g. by transcription interference [45]. Commensurate with this notion, we could identify that transcription of three antisense RNAs initiates in the 5' UTRs of the genes on the complementary strand and, thus, antisense transcription may interfere or attenuate with their transcription (P.riograndensis_final_5580, P.riograndensis_final_6016 and P.riograndensis_final_6182; Additional file 3: Table S3). Novel transcripts were also identified in the intergenic regions between previously known genes. Of these, 34 were predicted to encode small proteins, for example, small signal recognition particle (or small SRP; P.riograndensis_final_s0002), which is known to be involved in protein targeting in other bacteria [46]. Twenty seven small RNA genes were found (Table 5), e.g. the small RNA *bsrC* (P.riograndensis_final_s0008), which is present also in *B. subtilis* [47] and RNase P (P.riograndensis_final_s0013), the ubiquitous endonuclease that catalyzes the maturation of the 5' end of the tRNAs [48].

The sequence motifs for initiation of transcription and translation (-10 and -35 promoter, RBS and TLS sequence motifs) identified for the *P. riograndensis* SBR5 transcripts expressed under the chosen growth conditions are similar to microbial consensus sequences. For example, the -10 box consensus sequence in SBR5 (TAtaaT) was conserved in this bacterium, *E. coli*,

Results

B. subtilis and *B. methanolicus* [15,49,50]. The conserved -35 region in SBR5 was similar to the -35 box described for other bacilli [15,51] as were the spacings between -10 and -35 boxes (17.6 base pairs) and between -10 box and TSS (4.1 base pairs) (Figure 3). The RBS consensus sequence in *P. riograndensis* SBR5 was aGGaGg (Figure 4); this sequence corresponds to the RBS consensus sequence historically assigned for bacteria [52]. Moreover, the distance between RBS sequence and translation starts is 7.8 base pairs in average (Figure 4) which is in the range of the spacing optima determined for *B. subtilis* and *E. coli* [53]. As expected, the majority of the translation start sequences found in this study was ATG (79% of the analyzed sequences) and the TLS GTG and TTG were present in 12% and 9% of the analyzed sequences, respectively (Figure 4). This frequency is typical for bacterial genomes [54].

In silico analysis, performed by Zheng et al. [55] showed that 207 among 953 analyzed bacterial genomes possess leaderless genes including species of the *Firmicutes* and *Actinobacteria* phyla. RNAseq analysis revealed six leaderless transcripts in the transcriptome of *B. methanolicus* [15]. In the present study, two transcripts (*P.riograndensis_final_2873* and *P.riograndensis_final_5691*) were found to be leaderless in *P. riograndensis* SBR5 (Additional file 3: Table S3). The scarcity of leaderless transcripts in the transcriptomes of the low-GC Gram-positives *B. methanolicus* and *P. riograndensis* contrasts with a large proportion of leaderless transcripts (33%) in the high-GC Gram-positive actinobacteria: *Actinoplanes sp.* (20%) [56] and *C. glutamicum* (33%) [14]. On the other hand, the overall 5' UTR length distribution peaking around 30 base pairs is comparable in *P. riograndensis* SBR5 (Figure 2), *Actinoplanes sp.*, *C. glutamicum* and *B. methanolicus* [14,15,56].

Riboswitch-mediated control of expression of a variety of genes in bacteria could have practical implications, such as development of new antibacterial drugs [57], or more generally contribute to improvement of the understanding of bacterial metabolism. The genome-based riboswitch analysis revealed 98 putative RNA motifs, 10 of which were also detected in the sequenced RNAs (Additional file 7: Table S7). Ten different 5' UTRs represented in the transcriptome analysis of *P. riograndensis* SBR5 under the chosen growth conditions were found to contain 8 classes of riboswitches (Table 3). The groups of riboswitches identified in the transcriptome of SBR5 were: a pantothenate related *pam* riboswitch; a riboswitch recognizing S-adenosylmethionine; T-box regulatory elements; protein dependent L20 leader and L21 leader riboswitches; a metabolite dependent *ydaO-yuaA* riboswitch; a *pfl* riboswitch; and TPP sensitive riboswitches (Table 3). In *Firmicutes*, the SAM riboswitch is part of the S-box group of

Results

riboswitches which are involved in regulation of SAM, cysteine and methionine biosynthesis, and sulfur metabolism [58,59]. This type of riboswitch has been well characterized in bacilli, for example in *B. subtilis*, which has at least 11 operons and 26 genes under control of S-box RNA [60]. S-box RNA from *B. subtilis* directly senses the level of SAM and functions as SAM dependent riboswitch [61]. However, the most frequent mechanism of riboswitch regulation of amino acid operons expression in the *Firmicutes* is the T-box regulatory system [62,63]. In *B. subtilis* and other *Firmicutes*, the T-box can regulate infinity of genes encoding amino acid biosynthetic enzymes and transporters [64]. The *ydaO-yuaA* riboswitches occur upstream of these two genes in *B. subtilis* and operate as a genetic “off” switch [65]. Furthermore, recognition of the cyclic di-AMP by *ydaO-yuaA* was characterized and also shown to exist in *B. subtilis* [66,67]. The riboswitches in *P. riograndensis* SBR5 identified in the present study need to be investigated to some detail to unravel their regulatory function

In order to analyze the function of one exemplary riboswitch found in the transcriptome of *P. riograndensis* SBR5, we selected the TPP dependent riboswitch present upstream of the *thiC* gene (Table 3) and we tested its effect on the expression of the reporter gene *gfpUV*. The gene *thiC* encodes a phosphomethylpyrimidine synthase involved in TPP biosynthesis [68]. To drive the expression of *gfpUV*, the 5' UTR of the *thiC* gene was placed downstream of the Ppyk promoter, which was previously shown to be a strong promoter of *P. riograndensis* SBR5 [21]. TPP riboswitches typically bind TPP and regulate expression of genes that are involved in biosynthesis and transport of thiamine in eukaryotes and bacteria making them interesting targets for the study of antibacterial compounds [57]. Our data could show that a TPP riboswitch predicted on the basis of the RNAseq data was functional in *P. riograndensis* SBR5.

The *E. coli thiC* riboswitch controls translation initiation and in the presence of TPP *thiC* product is not translated [69,70]. The thiamine analog triazoletiamine showed a concentration dependent reporter gene repression by the TPP riboswitch in the 5' UTR of the thiamine kinase *thiK* in a concentration dependent manner [69]. In the present study, thiamine was added to the growth medium and already 5 μ M thiamine fully reduced *gfpUV* expression (Figure 5B). *P. riograndensis* SBR5 is a thiamine prototroph capable of growing in minimal medium without added thiamine (data not shown). Without thiamine added to the growth medium *gfpUV* expression remained high (Figure 5B) suggesting that the amount of thiamine synthesized by SBR5 did not activate the TPP riboswitch.

Results

Riboswitch aptamers remain highly conserved through evolution because each one must preserve a selective binding pocket for its target metabolite. Hence, the conserved TPP riboswitch consensus regions of *B. subtilis* were also present in the TPP riboswitch aptamer sequence targeted in this study (Figure 5A) [57]. The secondary structure analysis showed that, in contrast to the *tenA* TPP riboswitch in *B. subtilis* [57], the SBR5 *thiC* TPP riboswitch does not possess a transcriptional terminator sequence. This led us to investigate the presence of sequestering/anti-sequestering stems that could participate in the “on/off” state of the *P. riograndensis* SBR5 *thiC* TPP riboswitch. The schematic representation of the *thiC* TPP riboswitch secondary structure shows that the RBS is sequestered within a stem-loop structure predicted to inhibit translation initiation (Figure 5A). We could detect the sequence 5'-GATAA-3' and its complementary region 5'-UUAUC-3' inserted in the TPP aptamer sequence, in the stem-loop containing the *thiC* RBS and also in the sequence of one stem-loop located before RBS containing stem (Figure 5A). Comparable secondary structures and gene expression control has very recently been described for the *E. coli thiC* TPP riboswitch [70]. *P. riograndensis* possesses three further putative TPP riboswitches, one of which was expressed under the growth conditions of the RNAseq analysis presented here (Table 3; Additional File 7: Table S7). Although they share conserved sequences and secondary structure predictions (data not shown) it remains to be studied if these putative TPP riboswitches are indeed responsive to TPP and if they operate as transcriptional or translational riboswitches.

2.2.6. Conclusions

The examination of the whole transcriptome of *P. riograndensis* SBR5 gives valuable contribution to the transcriptome studies on SBR5. Moreover, our data validated the uncovering of novel transcripts and the presence of hundreds of operons and revealed a functional TPP riboswitch in gene regulation of SBR5. Finally, the data generated in this study should be valuable for future development of genetic tools for this poorly characterized species as much as for the genus *Paenibacillus*. Finally, our RNAseq analysis could provide new insight into the *P. riograndensis* SBR5 transcriptome at the systems level and will be a valuable basis for differential RNAseq analysis of this bacterium.

Results

Availability data and material

The data sets supporting the results of this article are available in the NCBI Gene Expression Omnibus database; under the accession number GSE98766.

2.2.7. References

1. Govindasamy V, Senthilkumar M, Magheshwaran V, Kumar U, Bose P, Sharma V, et al. *Bacillus* and *Paenibacillus* spp.: potential PGPR for sustainable agriculture. *Plant Growth and Health Promoting Bacteria*. Springer; 2010. p. 333–64.
2. Andreeva I, Morozov I, Pechurkina N, Morozova O, Ryabchikova E, Saranina I, et al. Isolation of bacteria of the genus *Paenibacillus* from soil and springs of the Valley of Geysers (Kamchatka). *Microbiology*. 2010;79:705–13.
3. Beneduzi A, Moreira F, Costa PB, Vargas LK, Lisboa BB, Favreto R, et al. Diversity and plant growth promoting evaluation abilities of bacteria isolated from sugarcane cultivated in the South of Brazil. *Appl. Soil Ecol*. 2013;63:94–104.
4. Genersch E, Forsgren E, Pentika J, Ashiralieva A, Rauch S, Kilwinski J, et al. Reclassification of *Paenibacillus larvae* subsp . *pulvifaciens* and *Paenibacillus larvae* subsp . *larvae* as *Paenibacillus larvae* without subspecies differentiation. *Microbiology*. 2016;501–11.
5. Drancourt M, Berger P, Raoult D. Systematic 16S rRNA gene sequencing of atypical clinical isolates identified 27 new bacterial species associated with humans. *J. Clin. Microbiol*. 2004;42:2197–202.
6. Ash C, Priest FG, Collins MD. Molecular identification of rRNA group 3 bacilli (Ash, Farrow, Wallbanks and Collins) using a PCR probe test. Proposal for the creation of a new genus *Paenibacillus*. *Antonie Leeuwenhoek*. 1993;64:253–60.
7. Xie J, Shi H, Du Z, Wang T, Liu X, Chen S. Comparative genomic and functional analysis reveal conservation of plant growth promoting traits in *Paenibacillus polymyxa* and its closely related species. *Sci. Rep*. 2016;1–12.
8. Beneduzi A, Peres D, Costa PB da, Zanettini MHB, Passaglia LMP. Genetic and phenotypic diversity of plant-growth-promoting bacilli isolated from wheat fields in southern Brazil. *Res. Microbiol*. 2008;159:244–50.
9. Beneduzi A, Costa PB, Melo IS, Bodanese-zanettini MH, Passaglia LMP. *Paenibacillus*

Results

- riograndensis* sp. nov., a nitrogen-fixing species isolated from the rhizosphere of *Triticum aestivum*. Int. J. Syst. Evol. Microbiol. 2010;60:128–33.
10. Fernandes GDC, Trarbach LJ, Campos SB De, Beneduzi A, Passaglia LMP. Alternative nitrogenase and pseudogenes: unique features of the *Paenibacillus riograndensis* nitrogen fixation system. Res. Microbiol. 2014;165:571–80.
 11. Brito LF, Bach E, Kalinowski J, Rückert C, Wibberg D, Passaglia LMP, et al. Complete genome sequence of *Paenibacillus riograndensis* SBR5, a Gram-positive diazotrophic rhizobacterium. J. Biotechnol. 2015;207:30–1.
 12. Sawhney N, Crooks C, Chow V, Preston JF, John FJS. Genomic and transcriptomic analysis of carbohydrate utilization by *Paenibacillus* sp. JDR-2: systems for bioprocessing plant polysaccharides. BMC Genomics. 2016;17:131.
 13. Shi H, Wang L, Li X, Liu X, Hao T, He X, et al. Genome-wide transcriptome profiling of nitrogen fixation in *Paenibacillus* sp. WLY78. BMC Microbiol. 2016;16:25.
 14. Pfeifer-Sancar K, Mentz A, Rückert C, Kalinowski J. Comprehensive analysis of the *Corynebacterium glutamicum* transcriptome using an improved RNAseq technique. BMC genomics. 2013;14:888.
 15. Irla M, Neshat A, Brautaset T, Rückert C, Kalinowski J, Wendisch VF. Transcriptome analysis of thermophilic methylotrophic *Bacillus methanolicus* MGA3 using RNA-sequencing provides detailed insights into its previously uncharted transcriptional landscape. BMC Genomics. 2015;16:73.
 16. Perkins TT, Kingsley RA, Fookes MC, Gardner PP, James KD, Yu L, et al. A strand-specific RNA-seq analysis of the transcriptome of the typhoid bacillus *Salmonella typhi*. PLoS Genet. 2009;5:e1000569.
 17. Kim JF, Jeong H, Park S, Kim S, Park YK, Choi S, et al. Genome sequence of the polymyxin-producing plant-probiotic rhizobacterium *Paenibacillus polymyxa* E681. J. Bacteriol. 2010;192:6103–4.
 18. Mingchao M, Wang C, Ding Y, Li L, Shen D, Jiang X, et al. Complete genome sequence of *Paenibacillus polymyxa* SC2, a strain of plant growth-promoting rhizobacterium with broad-spectrum antimicrobial activity. J. Bacteriol. 2011;193:311–2.
 19. Kwak Y, Shin J. Complete genome sequence of *Paenibacillus beijingensis* 7188^T (=DSM 24997^T), a novel rhizobacterium from jujube garden soil. J. Biotechnol. 2015;206:75–6.
 20. Jakobsen OM, Brautaset T, Degnes KF, Heggeset TMB, Balzer S, Flickinger MC, et al.

Results

- Overexpression of wild-type aspartokinase increases L-lysine production in the thermotolerant methylotrophic bacterium *Bacillus methanolicus*. *Appl. Environ. Microbiol.* 2009;75:652–61.
21. Brito LF, Irla M, Walter T, Wendisch VF. Magnesium aminoclay-based transformation of *Paenibacillus riograndensis* and *Paenibacillus polymyxa* and development of tools for gene expression. *Appl. Microbiol. Biotechnol.* 2017;101:735–47.
 22. Bolger AM, Lohse M, Usadel B. Trimmomatic: a flexible trimmer for Illumina sequence data. *Bioinformatics.* 2014;30:2114–20.
 23. Langmead B, Trapnell C, Pop M, Salzberg SL. Ultrafast and memory-efficient alignment of short DNA sequences to the human genome. *Genome Biol.* 2009;10:R25.
 24. Hilker R, Stadermann KB, Doppmeier D, Kalinowski J, Stoye J, Straube J, et al. ReadXplorer—visualization and analysis of mapped sequences. *Bioinformatics.* 2014;30:2247–54.
 25. Nawrocki EP, Eddy SR. Infernal 1.1: 100-fold faster RNA homology searches. *Bioinformatics.* 2013;29:2933–5.
 26. Gardner PP, Daub J, Tate JG, Nawrocki EP, Kolbe DL, Lindgreen S, et al. Rfam: updates to the RNA families database. *Nucleic Acids Res.* 2009;37:136–40.
 27. Griffiths-jones S, Bateman A, Marshall M, Khanna A, Eddy SR. Rfam: an RNA family database. *Nucleic Acids Res.* 2003;31:439–41.
 28. Naville M, Ghuillot-Gaudeffroy A, Marchais A, Gautheret D. ARNold: a web tool for the prediction of Rho-independent transcription terminators. *RNA Biol.* 2011;8:11–3.
 29. Lorenz R, Bernhart SH, Siederdisen CH zu, Tafer H, Flamm C, Stadler PF, et al. ViennaRNA Package 2.0. *Algorithms Mol. Biol.* 2011;6:26.
 30. Ao W, Gaudet J, Kent WJ, Muttumu S, Mango SE. Environmentally induced foregut remodeling by PHA-4/FoxA and DAF-12/NHR. *Science.* 2004;305:1743–6.
 31. Crooks G, Hon G, Chandonia J, Brenner S. WebLogo: a sequence logo generator. *Genome Res.* 2004;14:1188–90.
 32. Mortazavi A, Williams BA, McCue K, Schaeffer L, Wold B. Mapping and quantifying mammalian transcriptomes by RNA-Seq. *Nat. Methods.* 2008;5:621–8.
 33. Altschup SF, Gish W, Miller W, Myers E, Lipman D. Basic local alignment search tool. *J. Mol. Biol.* 1990;215:403–10.
 34. Sambrook J. *Molecular cloning: a laboratory manual*. New York: Cold Spring Harbor; 2001.

Results

35. Hanahan D. Studies on transformation of *Escherichia coli* with plasmids. *J. Mol. Biol.* 1983;166:557–80.
36. Eikmanns BJ, Thum-schmitz N, Eggeling L, Ludtke K, Sahm H. Nucleotide sequence, expression and transcriptional analysis of the *Corynebacterium glutamicum* *gltA* gene encoding citrate synthase. *Microbiology.* 1994;140:1817–28.
37. Gibson DG. Programming biological operating systems : genome design , assembly and activation. *Nat. Methods.* 2014;11:521–6.
38. Beneduzi A, Campos S, Ambrosini A, de Souza R, Granada C, Costa P, et al. Genome Sequence of the Diazotrophic Gram-Positive Rhizobacterium *Paenibacillus riograndensis* SBR5^T. *J. Bacteriol.* 2011;193:6391–2.
39. Poza-carrión C, Jiménez-vicente E, Navarro-rodríguez M, Echavarri-erasun C, Rubio LM. Kinetics of *nif* Gene Expression in a Nitrogen-Fixing Bacterium. *J. Bacteriol.* 2014;196:595–603.
40. Wealand JAYL, Myers JA, Hirschberg R. Changes in gene expression during nitrogen starvation in *Anabaena variabilis* ATCC 29413. *J. Bacteriol.* 1989;171:1309–13.
41. Sperb ER, Tadra-sfeir MZ, Sperotto RA, Fernandes G de C, Pedrosa FO, de Souza EM, et al. Iron deficiency resistance mechanisms enlightened by gene expression analysis in *Paenibacillus riograndensis* SBR5. *Res. Microbiol.* 2016;167:501–9.
42. Hou X, Yu X, Du B, Liu K, Yao L, Zhang S, et al. A single amino acid mutation in Spo0A results in sporulation deficiency of *Paenibacillus polymyxa* SC2. *Res. Microbiol.* 2016;167:472–9.
43. Sierra N, Makita Y, Hoon M De, Nakai K. DBTBS : a database of transcriptional regulation in *Bacillus subtilis* containing upstream intergenic conservation information. *Nucleic Acids Res.* 2008;36:93–6.
44. Kalinowski J, Bathe B, Bartels D, Bischoff N, Bott M, Burkovski A, et al. The complete *Corynebacterium glutamicum* ATCC 13032 genome sequence and its impact on the production of L-aspartate-derived amino acids and vitamins. *J. Biotechnol.* 2003;104:5–25.
45. Thomason MK, Storz G. Bacterial antisense RNAs: How many are there and what are they doing? *Annu. Rev. Genet.* 2011;44:167–88.
46. Zwieb C, Nues RW V, Rosenblad MALM, Brown JD, Samuelsson T. A nomenclature for all signal recognition particle RNAs. *RNA.* 2005;48:7–13.

Results

47. Saito S, Kakeshita H, Nakamura K. Novel small RNA-encoding genes in the intergenic regions of *Bacillus subtilis*. *Gene*. 2009;428:2–8.
48. Kazantsev A V, Pace NR. Bacterial RNase P: a new view of an ancient enzyme. *Nat. Rev. Microbiol.* 2006;4:729–40.
49. Hawley DK, McClure WR. Compilation and analysis of *Escherichia coli* promoter DNA sequences. *Nucleic Acids Res.* 1983;11:2237–55.
50. Camacho A, Salas M. Effect of mutations in the “extended -10” motif of three *Bacillus subtilis* α^A -RNA polymerase-dependent promoters. *J. Mol. Biol.* 1999;286:683–93.
51. Helmann JD. Compilation and analysis of *Bacillus subtilis* α^A -dependent promoter sequences: evidence for extended contact between RNA polymerase and upstream promoter DNA. *Nucleic Acids Res.* 1995;23:2351–60.
52. Shine J, Dalgarno L. The 3'-terminal sequence of *Escherichia coli* 16S ribosomal RNA: complementarity to nonsense triplets and ribosome binding sites. *Proc. Natl. Acad. Sci. USA.* 1974;71:1342–6.
53. Vellanoweth RL, Rabinowitz JC. The influence of ribosome-binding-site elements on translational efficiency in *Bacillus subtilis* and *Escherichia coli* in vivo. *Mol. Microbiol.* 1992;6:1105–14.
54. Villegas A, Kropinski AM. An analysis of initiation codon utilization in the Domain Bacteria - concerns about the quality of bacterial genome annotation. *Microbiology.* 2017;154:2559–61.
55. Zheng X, Hu G, She Z, Zhu H. Leaderless genes in bacteria: clue to the evolution of translation initiation mechanisms in prokaryotes. *BMC Genomics.* 2011;12:361.
56. Schwientek P, Neshat A, Kalinowski J, Klein A, Rückert C, Schneiker-bekel S, et al. Improving the genome annotation of the acarbose producer *Actinoplanes* sp. SE50/110 by sequencing enriched 5'-ends of primary transcripts. *J. Biotechnol.* 2014;190:85–95.
57. Sudarsan N, Cohen-chalamish S, Nakamura S, Emilsson GM, Breaker RR. Thiamine pyrophosphate riboswitches are targets for the antimicrobial compound pyrithiamine. *Chem. Biol.* 2005;12:1325–35.
58. Nudler E, Mironov AS. The riboswitch control of bacterial metabolism. *Trends Biochem. Sci.* 2004;29:11–7.
59. Vitreschak AG, Rodionov DA, Mironov AA, Gelfand MS. Riboswitches: the oldest mechanism for the regulation of gene expression? *Trends Genet.* 2004;20:44–50.

Results

60. Grundy FJ, Henkin TM. The S box regulon: a new global transcription termination control system for methionine and cysteine biosynthesis genes in Gram-positive bacteria. *Mol. Microbiol.* 1998;30:737–49.
61. McDaniel BAM, Grundy FJ, Artsimovitch I, Henkin TM. Transcription termination control of the S box system: direct measurement of S-adenosylmethionine by the leader RNA. *Proc. Natl. Acad. Sci USA.* 2003;100:3083–8.
62. Grundy FJ, Henkin TM. The T box and S box transcription termination control systems. *Front. Biosci.* 2003;8:20–31.
63. Merino E, Yanofsky C. Transcription attenuation: a highly conserved regulatory strategy used by bacteria. *Trends Genet.* 2005;21:260–4.
64. Vitreschak AG, Mironov AA, Lyubetsky VA, Gelfand MS. Comparative genomic analysis of T-box regulatory systems in bacteria. *RNA.* 2008;14:717–35.
65. Barrick JE, Corbino KA, Winkler WC, Nahvi A, Mandal M, Collins J, et al. New RNA motifs suggest an expanded scope for riboswitches in bacterial genetic control. *Proc. Natl. Acad. Sci. USA.* 2004;101:6421–6.
66. Sudarsan N, Lee ER, Weinberg Z, Moy RH, Kim JN, Link KH, et al. Riboswitches in eubacteria sense the second messenger cyclic di-GMP. *Science.* 2008;321:411–3.
67. Gao A, Serganov A. Structural insights into recognition of c-di-AMP by the *ydaO* riboswitch. *Nat. Chem. Biol.* 2014;10:787–92.
68. Begley TP, Downs DM, Ealick SE, McLafferty FW, Van Loon AP, Taylor S, et al. Thiamin biosynthesis in prokaryotes. *Arch. Microbiol.* 1999;171:293–300.
69. Lünse CE, Scott FJ, Suckling CJ, Mayer G. Novel TPP-riboswitch activators bypass metabolic enzyme dependency. *Front. Chem.* 2014;2:53.
70. Chauvier A, Picard-Jean F, Berger-Dancause J-C, Bastet L, Naghdi MR, Dubé A, et al. Transcriptional pausing at the translation start site operates as a critical checkpoint for riboswitch regulation. *Nat. Commun.* 2016;8:13892.

2.3. Magnesium aminoclay-based transformation of *Paenibacillus riograndensis* and *Paenibacillus polymyxa* and development of tools for gene expression

Luciana Fernandes Brito, Marta Irla, Tatjana Walter, Volker F. Wendisch

Genetics of Prokaryotes, Faculty of Biology & Center for Biotechnology (CeBiTec), Bielefeld University, Universitätsstraße 25, 33615 Bielefeld, Germany

2.3.1. Abstract

Members of the genus *Paenibacillus* are widespread facultative anaerobic, endospore-forming bacteria. Some species such as *P. riograndensis* or *P. polymyxa* fix nitrogen and may play an important role in agriculture to reduce mineral nitrogen fertilization in particular for non-legume plants. The genetic manipulation of *Paenibacillus* is an imperative for the functional characterization e.g. of its plant growth promoting activities and metabolism. This study showed that *P. riograndensis* and *P. polymyxa* can be readily transformed using physical permeation by magnesium aminoclays. By the means of the fluorescent reporter genes *gfpUV*, *mcherry* and *crimson*, a two-plasmid system consisting of a theta-replicating plasmid and a rolling circle-replicating plasmid was shown to operate in both species. Xylose-inducible and mannitol-inducible fluorescent reporter gene expression was demonstrated in the compatible two-plasmid system by fluorescence activated cell scanning. As a metabolic engineering application, the biotin requiring *P. riograndensis* was converted to a biotin prototrophic strain based on mannitol-inducible expression of the biotin biosynthesis operon *bioWAFDBI* from *Bacillus subtilis*.

2.3.2. Introduction

The genus *Paenibacillus* includes several diazotrophic species broadly distributed in the environment, for example in different types of soil, the rhizosphere and plant tissues [1] They may play an important role in the agriculture since the use of diazotrophic bacteria inoculants can reduce the mineral nitrogen fertilization that represents a significant cost in non-legume cultures. The diazotroph *Paenibacillus riograndensis* SBR5 is a Gram-positive, rod-shaped, endospore forming rhizobacterium that was isolated from the rhizosphere of *Triticum aestivum* in

Results

southern Brazil (Rio Grande do Sul) [2]. The genome of *P. riograndensis* SBR5 was sequenced and fully annotated, and consists of a single chromosome of 7,893,056 base pairs containing 6,705 protein coding, 87 tRNA and 27 rRNA genes [3]. Simple mineral salts media support the growth of SBR5. Since SBR5 is auxotrophic for biotin, it is necessary to add this vitamin to the minimal medium [3]. Previous studies have shown that this bacterium exhibits nitrogen fixation activity [4] and other plant growth promoting characteristics such as indol-3-acetic acid and siderophore production have been described [2,5].

Despite its potential as a plant growth promoting rhizobacterium (PGPR), some of the PGPR and metabolic activities of *P. riograndensis* SBR5 still remain to be studied (e.g. its function in the soil phosphorus cycle). Since the genetic tools are not well developed for this species, functional genomics analyses are very difficult to perform. For this reason an efficient method for transformation of *P. riograndensis* SBR5 would be beneficial to further study its PGPR activities and metabolism.

Some transformation methods for related *Paenibacillus* species have been reported previously, most of them based on electroporation. For example, a transformation efficiency of 1.9×10^5 transformants per μg of plasmid DNA have been achieved for *P. larvae* [6]. An electroporation method was shown to function efficiently for the plant growth promoting *P. polymyxa*, but much less efficiently for the related *P. azotofixans* [7]. For *P. larvae*, a polyethylene glycol-based protoplast transformation method was also reported [8].

A simple, inexpensive and efficient bacterial transformation method based on physical permeation using magnesium aminoclays was recently shown to be functional for both the Gram-positive *Streptococcus mutans* and the Gram-negative *Escherichia coli* [9] as well as for the microalga *Chlamydomonas reinhardtii* [10]. Unlike chemical transformation, electrotransformation, biolistic transformation or sonic transformation, this method is based on the Yoshida effect [11]. Sliding friction applied to a colloidal solution with a nanosized acicular material and bacterial cells increases the frictional coefficient rapidly, and the resulting complex increases in size and penetrates the bacterial cells, which results in the uptake of exogenous DNA [12]. Transformation of *Paenibacillus* based on physical permeation using magnesium aminoclays has not yet been reported. In the present work, the magnesium aminoclay-based transformation method was adapted to *P. riograndensis*. The heterologous *gfpUV*, *mcherry* and *crimson* reporter genes were functionally expressed in *P. riograndensis* SBR5 under the control of constitutive or inducible promoters from either theta-replicating or rolling circle-replicating

Results

plasmids. As an example of a biotechnological application, *P. riograndensis* was rendered biotin prototrophic by inducible expression of the *bioWAFDBI* operon from *B. subtilis*. Moreover, the transformation method and the plasmids developed for *P. riograndensis* were shown to be transferable to *P. polymyxa* DSM-365.

2.3.3. Materials and Methods

Strains, plasmid DNA and primers

P. riograndensis SBR5, *P. polymyxa* DSM-365 and *Bacillus methanolicus* MGA3 were used as hosts for heterologous fluorescence genes expression. SBR5 was kindly provided by the strain collection of the Genetics Department in Universidade Federal do Rio Grande do Sul (UFRGS, Brazil), DSM-365 purchased from DSMZ and *B. methanolicus* MGA3 obtained from SINTEF in Trondheim, Norway (Table 1). Information about the plasmids used as empty vectors in this work is available in Table 1, they were: two rolling circle-replicating plasmids conferring chloramphenicol resistance and containing a methanol inducible promoter from *B. methanolicus*, named pNW33Nmp and pTH1mp (pRE); and third theta-replicating plasmid pHCMC04 here named pTE containing the xylose inducible promoter PxylA and the gene encoding the xylose regulator XylR amplified from the genome of *Bacillus megaterium* [13]. All the empty vectors were obtained from SINTEF, Trondheim. Sequences for origin of replication of *E. coli* and *B. subtilis* are present in all the shuttle vectors. The primers used for strain construction are presented in Table S1.

Table1. Bacterial strains and plasmids used in this study.

Bacteria	Characteristics	Reference or source
<i>B. methanolicus</i>	MGA3	SINTEF
<i>P. polymyxa</i>	DSM-365	DSMZ
<i>B. subtilis</i>	168	BGSC
<i>E. coli</i>	DH5 α	[14]
<i>P. riograndensis</i>	SBR5; biotin auxotrophic	UFRGS
Plasmid	Characteristics	Reference or source
pRE	Cm ^R ; pTH1mp: rolling circle-replicating vector with methanol inducible promoter of methanol dehydrogenase (Pmdh) derived from <i>Bacillus methanolicus</i> ; contains origin of replication (ORI) sequences from <i>Bacillus subtilis</i> and <i>E. coli</i>	[15]
pR- <i>gfpUV</i>	Cm ^R ; pRE with <i>gfpUV</i> cloned downstream the Pmdh	[15]
pTE	Cm ^R , Amp ^R ; pHCMC04: theta-replicating vector	[16]

Results

pNW33Nmp	with xylose inducible promoter from <i>B. megaterium</i> ; contains ORI sequences from <i>Bacillus subtilis</i> and <i>E. coli</i> Cm ^R , Km ^R ; pNW33N derivative in which the Pmdh was inserted	[15]
pR _{fc} -crimson	Cm ^R ; protein fusion of Crimson and the Cm ^R from pRE: amplification of pRE back bone excluding the TAA sequence of cm ^R including <i>crimson</i> sequence instead	This work
pR _{fc} -mCherry	Cm ^R ; protein fusion of mCherry and the Cm ^R from pRE: amplification of pRE back bone excluding the TAA sequence of cm ^R including mCherry sequence instead	This work
pR _{fc} -gfpUV	Cm ^R ; protein fusion of GfpUV and the Cm ^R from pRE: amplification of pRE back bone excluding the TAA sequence of cm ^R including <i>gfpUV</i> sequence instead	This work
pPpyk-gfpUV	Cm ^R ; pRE with Pmdh replaced by pyruvate kinase promoter (amplified from SBR5 genome) upstream <i>gfpUV</i>	This work
pPtuf-gfpUV	Cm ^R ; pRE with Pmdh replaced by the elongation factor Tuf promoter (amplified from SBR5 genome) upstream <i>gfpUV</i>	This work
pPgap-gfpUV	Cm ^R ; pRE with Pmdh replaced by glyceraldehyde-3-phosphate dehydrogenase promoter (amplified from SBR5 genome) upstream <i>gfpUV</i>	This work
pRM1-gfpUV	Cm ^R ; pRE- <i>gfpUV</i> with Pmdh replaced by <i>mtlA</i> mannitol inducible promoter amplified from SBR5 genome	This work
pRM2-gfpUV	Cm ^R ; pRE- <i>gfpUV</i> with Pmdh replaced by <i>mtlR</i> mannitol inducible promoter amplified from MGA3 genome	[15]
pRM3-gfpUV	Cm ^R ; pRE- <i>gfpUV</i> with Pmdh replaced by <i>mtlA</i> mannitol inducible promoter amplified from 168 genome	This work
pRX-gfpUV	Cm ^R ; pRE derivative for <i>gfpUV</i> expression under control of the xylose inducible promoter from <i>B. megaterium</i>	[15]
pTX-crimson	Cm ^R , Amp ^R ; pTE derivative with <i>crimson</i> sequence inserted in <i>EcoRV</i> GAT [^] ATC site	This work
pTX-mCherry	Cm ^R , Amp ^R ; pTE derivative with <i>mCherry</i> sequence inserted in <i>EcoRV</i> GAT [^] ATC site	This work
pEKEx3-bioWAFDBI	Spec ^R ; C. glutamicum/ <i>E. coli</i> shuttle vector for IPTG inducible expression of <i>bioWAFDBI</i> from <i>B. subtilis</i>	[17]
pRM2-bioWAFDBI	Cm ^R ; pRM2- <i>gfpUV</i> in which <i>gfpUV</i> was replaced by <i>bioWAFDBI</i> amplified from pEKEx3- <i>bioWAFDBI</i>	This work

Medium and growth conditions

For the cultivation of *Paenibacillus* transformants, the cells were routinely grown at 30 °C and 120 rpm, in medium Caso broth (medium 220 from DSMZ) containing: peptone from casein (15 g L⁻¹), peptone from soymeal (5 g L⁻¹), yeast extract (3 g L⁻¹) and NaCl (5 g L⁻¹) with pH adjusted to 7.15 with NaOH. Antibiotics were added accordingly to the antibiotic resistance of the plasmid in use, 5.5 µg mL⁻¹ of chloramphenicol and 10 µg mL⁻¹ of ampicillin. *E. coli* strains were routinely cultivated at 37 °C in lysogeny broth supplied with 10 µg mL⁻¹ of

Results

chloramphenicol and $100 \mu\text{g mL}^{-1}$ of ampicillin when necessary. The strains of *B. methanolicus* were grown as described before [15].

To test the inducible systems, the transformant cells of SBR5 with reporter gene under control of mannitol inducible system were grown in Caso broth supplemented with gradually increasing concentrations of mannitol (0, 20, 40, 80 and 160 mM). The transformant cells of SBR5 with reporter gene under control of the xylose inducible system were grown in Caso broth supplemented with 0, 25, 50, 100, 200 or 400 mM of xylose, and DSM-365 transformants were grown in Caso broth supplemented with 0, 25, 50, or 100 mM xylose. In co-transformation with two inducible plasmids, the transformant cells of SBR5 and DSM-365 were grown in Caso broth with addition of both mannitol and xylose in concentration of 0, 25 or 50 mM. In the biomass formation assay of the *P. riograndensis* SBR5(pRM2-*bioWAFDBI*), the recombinant cells were grown over night in Caso broth and centrifuged for 15 minutes at 4,000 rpm. After washing the pellet for three times with NaCl 0.89% solution, the cells were transferred to the PbMM *P. riograndensis* minimal medium (MVcMY without vitamin complex and yeast extract) [18] using 50 mM xylose as carbon source, supplemented or not with 0.1 mg L^{-1} biotin and 160 mM inducer (mannitol).

Plasmids construction and preparation of recombinant strains

Molecular cloning was performed as described by Sambrook [19]. Chemically competent cells of *E. coli* DH5 α were prepared for cloning [14]. All the information about the polymerase chain reactions (PCRs) for plasmid construction in this work is present in Table 1 and the oligonucleotide sequences described in Table S1. Genomic DNA of *P. riograndensis* was isolated as described by Eikmanns et al. [20]. *B. methanolicus* DNA isolation procedure, competent cells preparation and transformation method are described in Irla et al. [15]. The NucleoSpin® Gel and PCR Clean-up kit (Machery-Nagel, Düren, Germany) was used for PCR clean-up and plasmids were isolated using the GeneJET Plasmid Miniprep Kit (Thermo Fisher Scientific, Waltham, USA). Plasmid backbones and inserts were amplified using Phusion® DNA polymerase (New England Biolabs, Ipswich, England) and the overlapping regions joined by Gibson assembly [21]. For colony PCR the Taq polymerase (New England Biolabs) was used.

Results

Preparation of the magnesium aminoclays

The preparation of the magnesium aminoclays was done according to [22]. An ethanolic solution of 200 mM MgCl₂ 6H₂O was stirred for 20 minutes and 13 mL of 3-aminopropyl triethoxysilane (Carl Roth, Karlsruhe, Germany) was added dropwise. The bulk solution was stirred at room temperature for 18 hours. After stirring, the milky solution was centrifuged for 10 minutes at 4,000 rpm and the white pellet washed with ethanol. The pellet was dried at 50 °C for 24 hours and the white product was grinded and autoclaved inside falcon tubes.

Magnesium aminoclays-based transformation method assay

The bacterial transformation method using magnesium aminoclays was developed and optimized by Choi et al. [9]. Here, we performed similar experiments by varying the parameters for adaptation of this method for *P. riograndensis* SBR5. The magnesium aminoclay solution was prepared by mixing 10 mg of magnesium aminoclays with 1 mL of deionized sterile water one day before the transformation for total dissolution. The plasmid DNA, in amounts of 0.05, 0.1, 0.3, 0.5 or 1 µg was mixed with 0.05 mL of the aminoclay solution and the volume was completed to 0.5 mL with deionized sterile water. The bacterial cells were grown in Caso broth medium until reaching the logarithmic phase, when they were centrifuged at 4,000 rpm for 10 minutes. The pellet was resuspended in pure sterile water (OD_{600nm} adjusted to 1) and 0.5 mL of cell suspension was mixed to the aminoclay-plasmid solution. For mixing we fixed the amount of plasmid DNA of 0.1 µg and two treatments were applied: vortexing the mixture for 10, 30, 60, 120 or 180 seconds or short time ultrasonication, using amplitude of 40 % for 5, 10, 20 or 30 seconds. To test the friction force, Caso broth agar plates were prepared with 1.5 or 3 % of agar, and the remaining parameters were: 0.1 µg of DNA and 60 seconds of vortexing. The spreading time of the 1.5 % agar varied being 30, 60, 120 or 180 seconds and on the plates with 3% agar the spreading time (of 60 seconds) was not varied. After 48 hours incubation at 30 °C, the colony forming units were counted.

Results

Recombinant P. riograndensis plasmid isolation and retransformation to E. coli

The plasmid isolation procedure used in this work was performed as following: an overnight culture (30 mL) of *P. riograndensis* SBR5 transformed with the plasmid pNW33mp was centrifuged for 15 minutes at 4,000 rpm and the pellet was washed and resuspended in 40 μ L of the TE buffer (0.05 M Tris, pH 8.0, 0.01 M EDTA). The cell suspension was added to 600 μ L freshly prepared lysis buffer (TE buffer with 4%SDS, pH adjusted to 12.45) filled into an Eppendorf tube and the lysis was completed by the incubation of the mixture at 37°C for 60 minutes. The lysate was neutralized by the addition of 30 μ L of 2 M Tris, pH 7.0. For precipitation of the chromosomal DNA and proteins, 240 μ L of 5 M NaCl was added to the lysate and the mixture was incubated in ice for 6 hours. After the incubation, the lysate was centrifuged for 10 min at 11,000 rpm the supernatant was transferred to a new tube. For DNA recovery, 10 % (v/v) of 3 M sodium acetate, pH 5.2 was added to the aqueous plasmid DNA solution and plasmid DNA was precipitated by addition of -20 °C cooled ethanol absolute. After 45 minutes centrifugation at 11,000 rpm the DNA pellet was washed twice with ethanol 70 % solution and air dried for 10 minutes before resuspension in deionized water.

E. coli DH5 α was transformed with the isolated plasmid DNA via heat shock and the resulting transformants were used for a plasmid mini preparation kit (Macherey-Nagel) according to the manufacture specifications. The plasmid DNA isolated from SBR5 and the plasmid isolated from the *E. coli* transformed with plasmid DNA isolated from SBR5 were digested with the restriction enzyme *AcuI* (Thermo Fisher Scientific) according to the manufacturer specifications and the presence of digested plasmid DNA was confirmed by agarose gel electrophoresis.

Fluorescence measurement by fluorescence activated cell scanning

To quantify the fluorescence intensities, transformants of *P. riograndensis* SBR5, *P. polymyxa* DSM-365 and *B. methanolicus* MGA3 were analysed by flow cytometry. Routinely, the *P. riograndensis* SBR5, and *P. polymyxa* DSM-365 cells were grown until reaching the logarithmic phase and centrifuged for 10 minutes at 4,000 rpm. The pellets were washed two times in NaCl 0.89 % solution and the OD_{600nm} was adjusted to 0.5. The *B. methanolicus* cells were prepared as described before [15]. The fluorescence of the cell suspension was measured

Results

using flow cytometer (Beckman Coulter, Brea, US) and the data analyzed in the Beckman Coulter Kaluza® Flow Analysis Software. The settings for the emission signal and filters within the flow cytometer for detection of GfpUV, Crimson and mCherry fluorescence were 550/525 bandpass FL9 filter, 710/660 bandpass FL6 filter and 655/620 bandpass FL3 filter, respectively.

2.3.4. Results

Transformation of Paenibacillus using physical permeation by magnesium aminoclays

In order to be able to study the function of the genes with respect to their physiological roles in *P. riograndensis*, a method for transformation of this bacterium using plasmid DNA has to be developed. In addition to transformation methods commonly used in bacteria such as heat-shock or electroporation, a simple and efficient procedure for plasmid transformation by physical permeation using magnesium aminoclays has been recently developed [9,12]. In this method, a plasmid DNA and magnesium aminoclay supercomplex is formed and used to physically permeate the bacterial cell wall using sonication and/or spreading of the cell suspension on agar plates. Here, it was assessed whether this method, originally developed for *E. coli* and *Streptococcus mutans* [9], can be adapted for transformation of *Paenibacillus*. Two different plasmid backbones (pNW33Nmp and pTE) were tested. Transformation efficiency using physical permeation by magnesium aminoclays may depend on the concentration of plasmid DNA and physical parameters such as sonication, spreading time and the agar concentration. To this end, these parameters were varied for transformation of *P. riograndensis* SBR5. The cell forming units (CFU) in the selective agar plates were counted. For both plasmids the highest transformation efficiencies (about $1.1 \cdot 10^3$ CFU per μg pNW33Nmp DNA and about $1.8 \cdot 10^3$ CFU per μg pTE DNA) were observed when 0.1 μg of plasmid DNA was added to the aminoclay solution, vortexed for one minute with the cell suspension and spread for one minute on a 1.5 % agar plate (Figure S1). Extended duration of vortexing or spreading did not improve transformation efficiency. The use of short ultrasonification treatment to better mix the cell suspension with the plasmid-aminoclay solution did not result in higher transformation efficiency compared to the treatment using vortexing (Figure S1).

To verify transformation, plasmid DNA from *P. riograndensis* transformed with pNW33Nmp was isolated using a classical plasmid DNA isolation method and subsequently used

Results

to transform *E. coli* via heat shock. The plasmid DNA isolated from the transformed *E. coli* cells was compared to that of transformed *P. riograndensis* cells by restriction enzyme digestion with the restriction enzyme *AcuI*. The agarose gel electrophoresis of cut plasmid DNA revealed the expected two identical DNA patterns (1530 and 3776 base pairs), thus, indicating that intact DNA of plasmid pNW33Nmp could be isolated from *P. riograndensis* transformants and used for transformation into *E. coli* (Figure S2).

Next, we tested if heterologous fluorescent reporter proteins can be produced in *P. riograndensis* transformants. For this reason genes coding for fusion proteins were constructed by removing the stop codon of the chloramphenicol resistance cassette (Cm^{R}) from vector pRE and introduction of the genes coding for fluorescent reporter proteins (GfpUV, mCherry or Crimson) downstream and in frame of this sequence. The resulting vectors were named pR_{fc}-*gfpUV*, pR_{fc}-*mCherry* and pR_{fc}-*crimson* and used to transform *P. riograndensis* SBR5. The fluorescence of the transformants was quantified by flow cytometry analysis of populations with 20,000 transformed cells (Figure 1). The chloramphenicol resistant *P. riograndensis* transformants expressed the reporter gene fusions since increased fluorescence was observed for Crimson (8.5 times higher than the empty vector carrying control), mCherry (5 times higher) and for GfpUV (5 times higher; Figure 1). Thus, *P. riograndensis* could successfully be transformed by physical permeation using the magnesium aminoclay method and genes for fusion proteins of the chloramphenicol resistance marker protein with the fluorescent proteins Crimson, GfpUV and mCherry, respectively, could be functionally expressed.

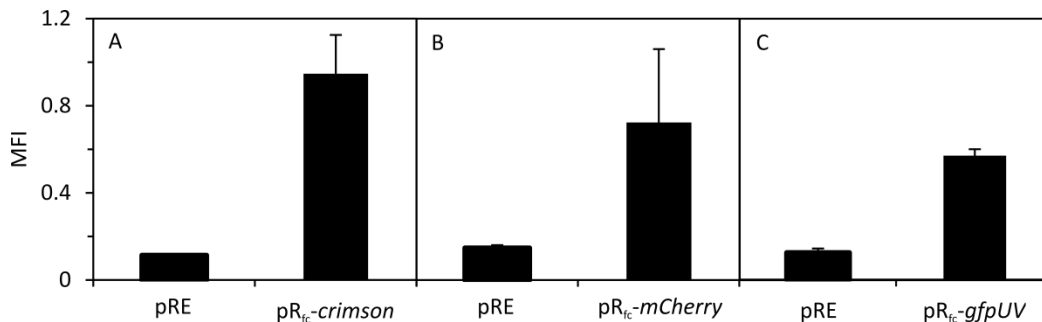


Figure 1. Fluorescence analysis of *P. riograndensis* SBR5 cells carrying plasmids encoding protein fusions of the chloramphenicol resistance protein and either Crimson (A), mCherry (B) or GfpUV (C). Mean fluorescence intensities of populations of 20,000 cells analysed by flow cytometer are shown as means and standard deviation of biological triplicates. Transformants carrying the empty vector pRE were analysed for comparison.

Results

A rolling circle-replicating plasmid for constitutive expression at different levels

In order to develop plasmids for constitutive gene expression of different promoter strengths, three different promoters were cloned upstream of the promoterless gene *gfpUV* on the rolling circle-replicating plasmid pRE: Ptuf, Pgap and Ppyk. Since the orthologous promoters were characterized as strong in *Corynebacterium glutamicum* [23,24], the respective open reading frames from *C. glutamicum* were used as queries for nucleotide BLAST search [25] against the genome sequence of *P. riograndensis* SBR5. The thus identified *P. riograndensis* SBR5 genes PRIO_0184, PRIO_2339 and PRIO_6140 are annotated to encode glyceraldehyde-3-phosphate dehydrogenase, pyruvate kinase and elongation factor G, respectively. The Bacterial Promoter Prediction (BPROM) tool on the SoftBerry platform [26] detected -10 and -35 hexamer regions in the 300 base pairs sequence upstream of the start codons of these genes (Table 2).

Table 2. Sequences and positions of the -10 and -35 regions within the 300 base pairs sequences upstream the several *P. riograndensis* SBR5 genes. The promoters were predicted bioinformatically using the Bacterial Promoter Prediction (BPROM) tool on SoftBerry platform [26].

Promoter Name	Gene ID	...	-35 box	...	-10 box	...	Start Codon
PgapA	PRIO_0184	N ₂₃₈	TTGACA	N ₁₃	GTCTTGAAT	N ₃₁	ATG
Ppyk	PRIO_2339	N ₁₉	CTCAAT	N ₁₂	CAGTATACT	N ₂₅₄	ATG
Ptuf	PRIO_6140	N ₁₆₆	TCTC CA	N ₃₀	TAACTT	N ₉₂	ATG

The plasmids containing Ptuf, Pgap and Ppyk upstream of the promoterless gene *gfpUV* were named pPgap-*gfpUV*, pPpyk-*gfpUV* and pPtuf-*gfpUV* (Table 1) and used to transform *P. riograndensis*. GfpUV fluorescence was measured after growth in Caso broth for 6 hours. *P. riograndensis* transformed with the empty vector showed a background median fluorescence intensity (MFI) of approximately 0.1, whereas GfpUV fluorescence of *P. riograndensis* transformed with pPgap-*gfpUV*, pPpyk-*gfpUV* or pPtuf-*gfpUV* was significantly higher (Figure 2). Promoter strengths differed and the fluorescence intensity of the analyzed strains increased in the following pattern: pPgapA-*gfpUV* (11 fold higher than the empty vector carrying control strain), pPtuf-*gfpUV* (6 fold) and pPpyk-*gfpUV* (2.9 fold; Figure 2). Thus, three different endogenous promoters are available to drive expression of heterologous genes with strengths at different levels.

Results

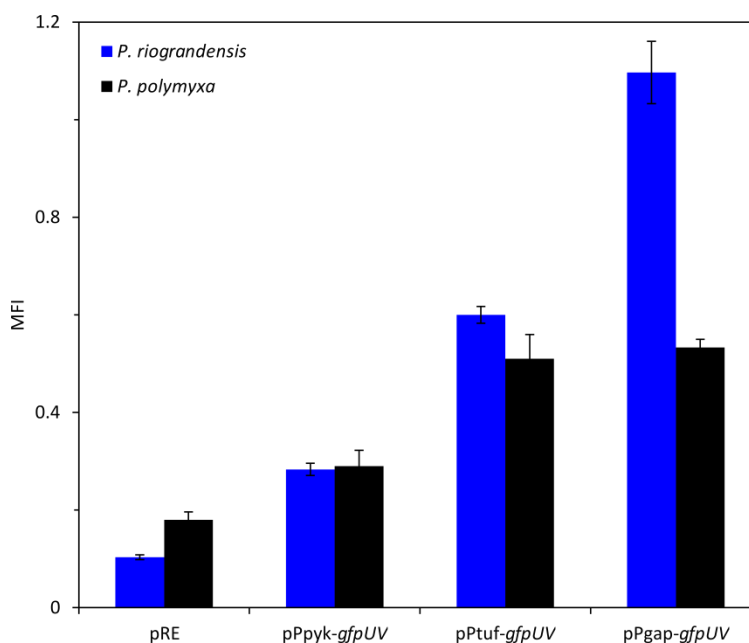


Figure 2. Reporter gene expression analysis of vectors with different constitutive promoters. GfpUV fluorescence of *P. riograndensis* SBR5 (blue) and *P. polymyxa* DM36 (black) cells carrying plasmids with *gfpUV* gene under control of three different constitutive promoters (Ppyk, Pgap and Ptuf), or the empty vector plasmid pRE are given as means and standard deviation of biological triplicates measured by flow cytometer of 20,000 cells.

Inducible and gradable expression system using the heterologous XylR system from Bacillus megaterium

In order to develop a gene expression system that is inducible and gradable by an external trigger, the xylose inducible XylR system from *B. megaterium* was tested in *P. riograndensis*. To this end, the pRE-based vector pRX-*gfpUV* was used [15]. The transformants were cultivated in Caso broth supplemented with 0, 24, 50, 100 or 200 mM of xylose. GfpUV fluorescence of *P. riograndensis* SBR5(pRX-*gfpUV*) cells increased with increasing concentrations of the inducer xylose (Figure 3A). Induction was about 6 fold higher when 24 mM xylose was added compared to the non-induced control and reached close to maximal values (about 12 fold higher in comparison to non-induced conditions) in the presence of 50 mM xylose.

Results

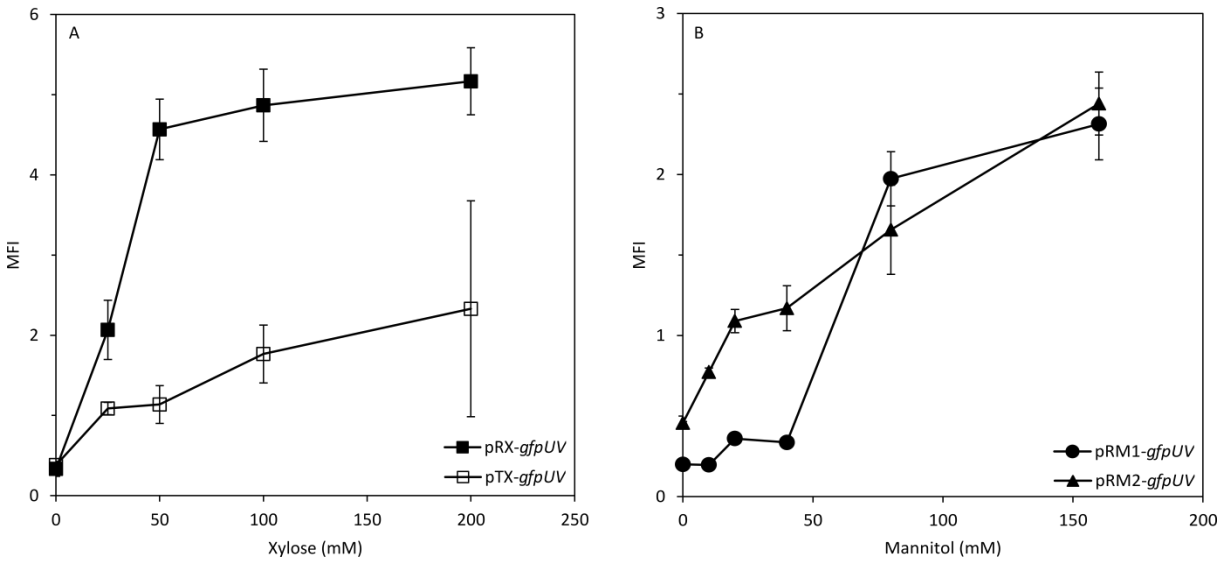


Figure 3. Reporter gene expression analysis of plasmids with xylose inducible (A) or mannitol inducible (B) promoters. GfpUV fluorescence of *P. riograndensis* SBR5 cells carrying (A) rolling circle-replicating, xylose inducible plasmid pRX-*gfpUV* gene or theta-replicating, xylose inducible plasmid pTX or (B) carrying plasmids with the *gfpUV* gene under control of mannitol inducible promoter from *P. riograndensis* SBR5 (pRM1-*gfpUV*) or *B. methanolicus* MGA3 (pRM2-*gfpUV*) was analysed by flow cytometry of populations of 20.000 cells. Gene expression was induced by 0, 25, 50, 100 and 200 mM xylose or addition of 0, 10, 20, 40, 80 and 160 mM mannitol added to the growth medium at inoculation. Means and standard deviations of biological triplicates are depicted.

To test the xylose-inducible expression system in a theta-replicating vector, *gfpUV* was cloned into the multiple cloning site of the vector pTE, which also contains the xylose repressor gene *xyIR* and xylose inducible promoter. The resulting plasmid was named pTX-*gfpUV* and used to transform *P. riograndensis* SBR5. The transformants were cultivated in the presence of 0, 24, 50, 100 or 200 mM xylose. GfpUV fluorescence increased with increasing xylose concentrations (Figure 3A). The GfpUV fluorescence levels were lower for the theta-replicating vector pTX-*gfpUV* than for rolling circle-replicating vector pRX-*gfpUV* (Figure 3A). Taken together, theta-replicating and rolling circle replication plasmids for gradable, xylose inducible gene expression were developed and shown to function in *P. riograndensis*.

Results

Mannitol inducible and gradable expression based on endogenous or heterologous promoter and activator genes

Genes of mannitol catabolism are typically regulated by the availability of the carbon source mannitol as for example shown for *Bacillus methanolicus* [18] and *B. subtilis* subsp. *subtilis* str. 168 [27]. Based on microarray and RNAseq [28,29] analysis of mannitol inducible genes in this bacterium, a mannitol inducible gene expression system employing the promoter of the *mtlR* gene of *B. methanolicus* was developed [15]. To identify potentially mannitol inducible promoters, a BLAST analysis of the genome of *P. riograndensis* SBR5 using the upstream region of -35 sequence of *mtlR* gene of *B. methanolicus* as query was performed and revealed similarity to the upstream region of -35 sequences of *mtlA* from *P. riograndensis* SBR5. As a first test of this promoter, its expression was analysed heterologously in *B. methanolicus* using plasmid pRM1-*gfpUV* and compared to the mannitol inducible *mtlR* promoter from *B. methanolicus* (pRM2-*gfpUV*) and the mannitol inducible *mtlA* promoter from *B. subtilis* subsp. *subtilis* str. 168 (pRM3-*gfpUV*). GfpUV fluorescence under non-inducing and inducing conditions was determined by flow cytometry. As shown in Table 3, the promoters from *B. methanolicus* and *P. riograndensis* were active and mannitol inducible in *B. methanolicus*, whereas the *mtlA* promoter from *B. subtilis* was not (Table 3). Thus, the *mtlA* promoter from *P. riograndensis* SBR5 allowed for mannitol inducible gene expression in the heterologous *B. methanolicus*.

Table 3. GfpUV fluorescence of *B. methanolicus* MGA3 strains carrying plasmids with *gfpUV* gene under control of different mannitol inducible promoters. The promoterless *gfpUV* gene was fused to putative mannitol inducible promoters from *P. riograndensis* (pRM1-*gfpUV*), *B. methanolicus* (pRM2-*gfpUV*) or *B. subtilis* (pRM3-*gfpUV*). Gene expression was induced by addition of 50 mM mannitol to the growth medium. The table shows means and standard deviations of technical triplicates.

Construct	Mean GfpUV fluorescence intensity		
	pRM1- <i>gfpUV</i>	pRM2- <i>gfpUV</i>	pRM3- <i>gfpUV</i>
0 mM mannitol	0.1 ± 0.0	0.2 ± 0.0	0.2 ± 0.0
50 mM mannitol	0.8 ± 0.1	1.1 ± 0.1	0.2 ± 0.0

To test if the *mtlA* promoter from *P. riograndensis* SBR5 is mannitol inducible in the native host, pRM1-*gfpUV* was used to transform *P. riograndensis* SBR5. As control *P. riograndensis* SBR5(pRM2-*gfpUV*) with the mannitol inducible promoter from *B. methanolicus* MGA3 was constructed. Both strains were analyzed by flow cytometry analysis

Results

after cultivation in Caso broth in the presence of 0, 20, 40, 80 or 160 mM of mannitol. This dose response analysis revealed increasing GfpUV fluorescence with increasing mannitol concentrations and comparable maxima for both, SBR5(pRM1-*gfpUV*) and SBR5(pRM2-*gfpUV*) (Figure 3B). Thus, the *mtlA* promoter from *P. riograndensis* SBR5 was shown to be mannitol inducible in the native host. An almost linear correlation between the inducer concentration and the mean GfpUV fluorescence intensity was only found for SBR5(pRM2-*gfpUV*) in the concentration range of 40 to 160 mM (Figure 3B). Taken together, mannitol inducible expression vectors carrying either an endogenous promoter or a heterologous promoter from *B. methanolicus* can be used for controlled gene expression in *P. riograndensis*. Mannitol induction of these promoters in *B. methanolicus* as well as in *P. riograndensis* relies on hitherto unknown trans-regulatory factors, likely activators, since these are not encoded on the gene expression vectors used.

Inducible gene expression using a two vector system

In order to test if the compatible expression vectors pTX (based on theta-replicating plasmid pTE, carrying xylose inducible gene expression system) and pRM2 (based on rolling circle-replicating plasmid pRE, carrying mannitol inducible promoter) allow for independently controllable gene expression in a single cell, *P. riograndensis* SBR5 was transformed with the following pairs of expression vectors: pRE and pTE, pRM2-*gfpUV* and pTE, pTX-*crimson* and pRE or pRM2-*gfpUV* and pTX-*crimson*. The double transformants were cultivated under noninducing conditions (in the absence of inducers) and under inducing conditions (in the presence of 50 mM xylose and 50 mM mannitol). The double transformants carrying the empty vectors showed background GfpUV and Crimson fluorescence of about 0.2 to 0.4 irrespective of the presence or absence of the inducers (Figure 4; Table S2). Transformants carrying pTX-*crimson* showed increased mean Crimson fluorescence intensities of 1.2 to 2.1 under inducing conditions and transformants carrying pRX-*gfpUV* showed increased mean GfpUV fluorescence intensities of about 1.6 to 2.2 when induced (Figure 4; Table S2). Double fluorescent cells (increased mean Crimson and GfpUV fluorescence intensities) were observed for transformants carrying pTX-*crimson* and pRX-*gfpUV* (Figure 4; Table S2).

Results

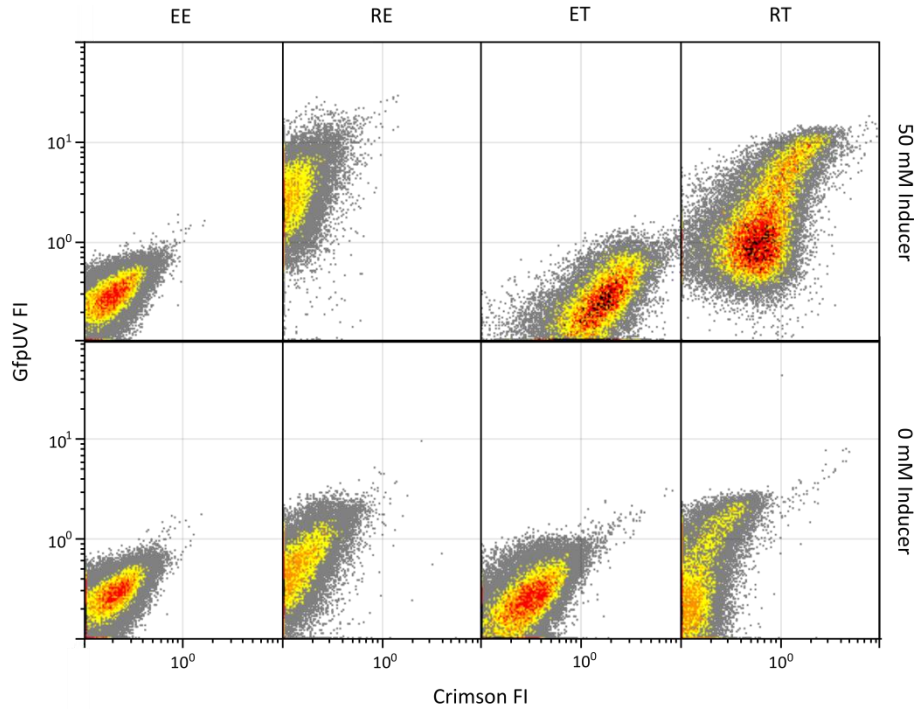


Figure 4. Reporter gene expression analysis of cells carrying two compatible expression vectors. GfpUV and Crimson fluorescence was analysed by flow cytometry of populations of 20,000 *P. riograndensis* cells carrying the two compatible plasmids pRE and pTE (EE), pRM2-*gfpUV* and pTE (RE), pTX-*crimson* and pRE (ET) or pRM2-*gfpUV* and pTX-*crimson* (RT), respectively. Cells were cultivated in the absence of inducers or in the presence of a mixture of 50 mM xylose and 50 mM mannitol.

To test if mannitol and xylose inducible gene expression can be controlled independently, *P. riograndensis* SBR5(pRX-*gfpUV*)(pTX-*crimson*) was cultivated either without inducers, with 50 mM xylose and 50 mannitol, with 50 mM xylose alone, as well as with 50 mM mannitol alone. As expected, GfpUV fluorescence-positive, but Crimson fluorescence-negative cells were observed with mannitol alone, GfpUV-negative, but Crimson-positive cells with xylose alone, and GfpUV and Crimson double-positive cells were only observed in the presence of both inducers (Figure S3).

Controlled expression of heterologous bioWAFDBI genes rendered P. riograndensis SBR5 biotin-prototrophic

P. riograndensis lacks genes coding for biotin biosynthesis enzymes, thus, it requires biotin as supplement when grown in minimal media [3]. The plasmid pEKEx3-*bioWAFDBI* [17]

Results

was used to subclone the *bioWAFDBI* operon from *B. subtilis* 168 into the expression vector pRM2. The resulting vector pRM2-*bioWAFDBI* was used to transform *P. riograndensis* SBR5. After pre-growth in the biotin-containing medium PbMM, *P. riograndensis* strains SBR5(pRE) and SBR5(pRM2-*bioWAFDBI*) were transferred repeatedly either to biotin-free or to biotin-containing medium in the absence of mannitol as inducer (Figure 5). In addition, SBR5(pRM2-*bioWAFDBI*) was tested in the presence of 160 mM mannitol as inducer (Figure 5). In biotin-containing minimal medium, both SBR5(pRE) and SBR5(pRM2-*bioWAFDBI*) grew to comparable biomass concentrations (given as $\Delta OD_{600\text{ nm}}$) for 7 serial transfers (Figure 5B). As expected, *P. riograndensis* SBR5(pRE) failed to grow in biotin-free medium after the third transfer (Figure 5A). By contrast, SBR5(pRM2-*bioWAFDBI*) grew for seven serial transfers to biotin-free medium when gene expression was induced by mannitol (Figure 5A). Thus, induced pRM2-based expression of *bioWAFDBI* was sufficient to render *P. riograndensis* biotin prototrophic. It has to be noted that some growth of SBR5(pRM2-*bioWAFDBI*) was observed in the absence of the inducer mannitol upon repeated transfer to biotin-free medium ($\Delta OD_{600\text{ nm}}$ of 0.3 without induction as compared to $\Delta OD_{600\text{ nm}}$ of 1.0 when induced) indicating possible promoter leakage.

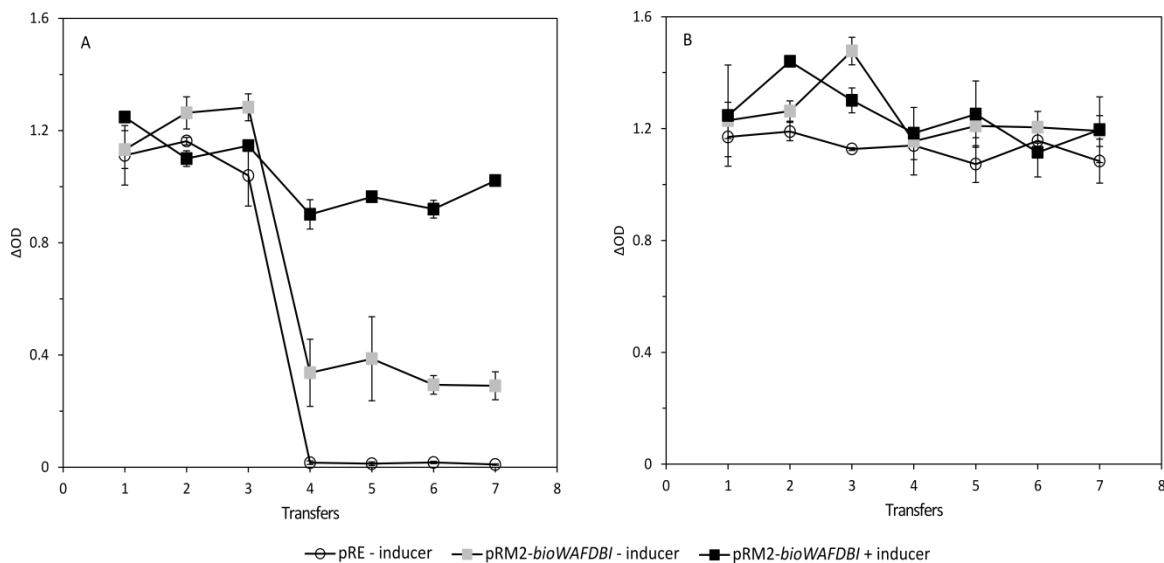


Figure 5. Growth of *P. riograndensis* SBR5(pRE) and SBR5(pRM2-*bioWAFDBI*) in PbMM minimal medium lacking biotin (A) or containing 0.1 mg L^{-1} biotin (B). SBR5(pRM2-*bioWAFDBI*) was cultivated without (grey squares) or with induction with 160 mM mannitol (black squares). The biomass formed ($\Delta OD_{600\text{ nm}}$) after growth for at least 24h is shown for repeated transfers to

Results

fresh, biotin-free PbMM (A) or fresh biotin-containing PbMM (B). Means and standard deviations of biological triplicates are shown.

Transfer of the transformation protocol and gene expression vector systems to P. polymyxa DSM-365

In order to test if the magnesium aminoclay-based transformation protocol and the constructed inducible expression vectors can be applied to another species of the genus *Paenibacillus*, *P. polymyxa* DSM-365 was transformed with the plasmids pNW33mp and pTE, respectively, using the conditions optimized for *P. riograndensis*. Transformation of both plasmids was successful; however, the transformation efficiency of approximately $1.0 \cdot 10^2$ transformants per μg of DNA was about 10 fold lower than in *P. riograndensis*.

The constitutive expression plasmids pPpyk-*gfpUV*, pPtuf-*gfpUV* and pPgap-*gfpUV* were used to transform *P. polymyxa* DSM-365 and GfpUV fluorescence was quantified by flow cytometry (Figure 2). The *P. polymyxa* transformants showed higher than background GfpUV fluorescence intensities (Figure 2). The strengths of promoters Ppyk and Ptuf were comparable in *P. polymyxa* and in *P. riograndensis* while, the promoter strength of Pgap was almost two fold lower in *P. polymyxa* than in *P. riograndensis* (Figure 2).

The theta-replicating expression vector pTX carrying a xylose inducible gene expression system was shown to allow for xylose-inducible gene expression in *P. polymyxa* DSM-365 using *mCherry* as reporter gene. After cultivation in Caso broth without added xylose, a background mCherry fluorescence of less than 0.2 was observed (Figure 6A). With 50 mM and 100 mM xylose added as inducer, mCherry fluorescence increased about 2 fold and about 4 fold, respectively.

Results

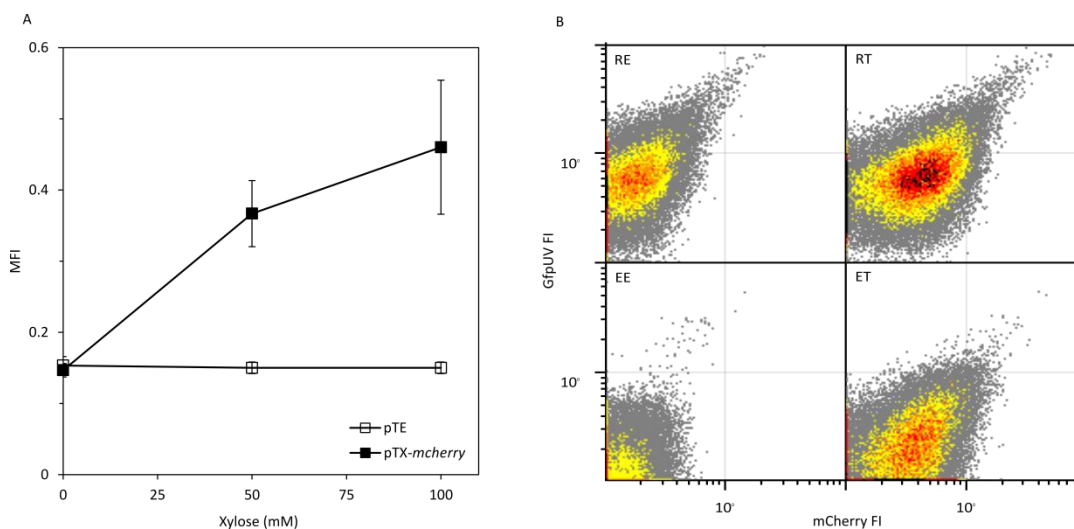


Figure 6. GfpUV and mCherry fluorescence *P. polymyxa* transformed with two compatible expression vectors. Populations of 20,000 cells of *P. polymyxa* DSM-365 transformed with pRE and pTE (EE), pRM2-*gfpUV* and pTE (RE), pTX-*mcherry* and pRE (ET) or pRM2-*gfpUV* and pTX-*mcherry* (RT) cultivated in the presence of a mixture of 100 mM of xylose and mannitol were analysed for GfpUV and mCherry fluorescence by flow cytometry. The figure shows means and standard deviation of biological triplicates.

In the next step, *P. polymyxa* DSM-365 was transformed with the two compatible expression vectors pRM2-*gfpUV* and pTX-*mCherry* or the respective empty vectors pRE and pTE. *P. polymyxa* strains DSM-365(pRE)(pTE), DSM-365(pRM2-*gfpUV*)(pTE), DSM-365(pRE)(pTX-*mcherry*) and DSM-365(pRM2-*gfpUV*)(pTX-*mcherry*) were cultivated in Caso broth and fluorescent reporter gene expression was induced with a mixture of 100 mM xylose and 100 mM mannitol. GfpUV and mCherry fluorescence analysis revealed double fluorescence negative cells for DSM-365(pRE)(pTE) and double fluorescence positive cells for DSM-365(pRM2-*gfpUV*)(pTX-*mcherry*; Figure 6B). DSM-365(pRM2-*gfpUV*)(pTE) only showed GfpUV fluorescence, whereas DSM-365(pRE)(pTX-*mcherry*) only showed mCherry fluorescence (Figure 6B). Taken together, the transformation protocol and the gene expression tools developed for *P. riogradensis* were shown to be transferable to at least one other species of the genus *Paenibacillus*.

2.3.5. Discussion

Here, we optimized a simple and functional method using magnesium aminoclays for transformation of two *Paenibacillus* species. Moreover, efficient constitutive and inducible gene

Results

expression using compatible theta- and rolling circle-replicating vectors developed here enlarged the genetic toolbox for *Paenibacillus*. Besides characterization of these systems using fluorescent reporter genes, biotin-auxotrophic *P. riograndensis* was rendered prototrophic for biotin by inducible heterologous expression of the *bioWAFDBI* operon from *B. subtilis*.

Biotin is required as a co-factor for a diverse group of enzymes called “biotin-dependent family” enzymes [30]. Biotin is essential for *E. coli* although it possesses only a single biotin-containing enzyme, namely acetyl-CoA carboxylase catalyzing the formation of malonyl-CoA as essential precursor for fatty acid biosynthesis. The genome of the biotin auxotrophic *P. riograndensis* SBR5 contains genes putatively encoding pyruvate carboxylase (PRIO_6030) and acetyl-CoA carboxylase (PRIO_2337). Biotin has to be added to the growth medium of auxotrophic *P. riograndensis* since it lacks genes for biotin biosynthesis. Of the proteins encoded in the biotin biosynthesis operon *bioWAFDBI* from *B. subtilis*, 6-Carboxyhexanoate CoA ligase BioW is not required for *de novo* biotin synthesis, but to activate pimelic acid to pimeloyl-CoA. *P. riograndensis* may possess a homolog of BioI since the PRIO_5347 encoded P450 enzyme shares similarity with BioI of *B. subtilis*, but does not possess homologs of BioW, BioA, BioF, BioD and BioB [3]. As shown for other biotin auxotrophs, e.g. *C. glutamicum* ATCC 13032 [17,31], heterologous expression of the complete *bioWAFDBI* operon from *B. subtilis* led to biotin prototrophy of *P. riograndensis*. However, it remains to be shown if expression of all *bio* genes is required or if expression of a subset of these genes would be sufficient: *bioFI* in the case of *C. glutamicum* and possibly *bioAFDB* in the case of *P. riograndensis*. It is known that many root-associated bacteria are dependent on a supply of previously synthesized growth factors from plants. Indeed, biotin is commonly present in the root exudates of higher plants [32]. This may suggest that biotin synthesis by *P. riograndensis* has been lost during evolution.

The major advantage of the magnesium aminoclay method is its simplicity, whereas other methods may be superior with respect to the transformation efficiency. The transformation efficiencies obtained for *P. riograndensis* SBR5 (10^3 per μg of DNA) and *P. polymyxa* DSM-365 (10^2 per μg of DNA) are comparable to those obtained in *E. coli* and *S. mutans* by the magnesium aminoclay method [9]. These transformation efficiencies are sufficient for strain construction, but are too low to generate gene libraries in these species, e.g. when screening libraries of gene knock downs using CRISPR interference [33,34]. Electroporation protocols developed for *P. polymyxa* [7] and *P. larvae* [6] are 100 to 1000 times more efficient, however, even these transformation efficiencies of 10^5 per μg of DNA are too low to generate large gene libraries, which requires

Results

transformation efficiencies in the order of 10^8 to 10^9 per μg of DNA as obtained for *E. coli* [35]. Taken together, the low transformation efficiency by the magnesium aminoclay method is compensated for by its simplicity, the fact that it does not involve the use of expensive material such as electroporation cuvettes or electricity, and the fact that laborious preparation of competent cells is not required since the use of an exponentially growing *Paenibacillus* culture is sufficient.

Biotechnological processes involving recombinant bacteria often face stability problems when using rolling circle-replicating plasmids as is seen also for Bacilli [15,36,37]. Besides their roles in plant growth promotion and bioremediation, Paenibacilli may find biotechnological application in the production of value-added compounds such as (R,R)-2,3-butanediol [38,39] or of antimicrobials such as the lipodepsipeptide fusaricidin [40]. Thus, the more stable theta-replicating plasmids may be valuable for applications using recombinant Paenibacilli. However, it has to be noted that due the lower copy numbers of theta-replicating plasmids as compared to most rolling circle-replicating plasmids, overexpression of the endogenous or heterologous genes in theta-replicating plasmids requires stronger promoters and/or translation efficiency.

In this study, several constitutive promoters of various strengths as well as graded inducible gene expression systems were studied for gene expression in *P. riograndensis*. Based on a bioinformatics analysis of promoter sequences, three promoters expected to be strong and constitutive were chosen. As shown in Figure 2, the expression of *gfpUV* in *P. riograndensis* was three (Ppyk), six (Ptuf) or about ten (PgapA) fold higher than the autofluorescence background and a mean fluorescence intensity of about 1.1 was obtained with expression vector pPgap-*gfpUV* (Figure 2). However, in *P. polymyxa* the *gfpUV* expression from *P. riograndensis* promoter PgapA only led to mean fluorescence intensity of about 0.5 (Figure 2). This is commensurate with the sequence differences between the PgapA promoters from *P. riograndensis* and *P. polymyxa*, with six mismatches in the -10 box and one mismatch in the -35 box (BLAST analysis not shown), thus, high constitutive gene expression in *P. polymyxa* should be based on the endogenous PgapA promoter rather than the one from *P. riograndensis*.

When fully induced, gene expression from the mannitol inducible promoter PmtIR and the xylose inducible promoter PxylA reached higher levels (mean fluorescence intensities of about 2.5 for the mannitol inducible gene expression vectors pRM1-*gfpUV* and pRM2-*gfpUV* and of about 5 for pRX-*gfpUV*; Figure 3) than obtained with PgapA (mean fluorescence intensity of about 1.1; Figure 2). The very high expression levels obtained with fully induced PmtIR and

Results

PxylA come at a cost, namely the requirement to add ≥ 100 mM xylose or ≥ 150 mM mannitol to the growth medium. Neither mannitol nor xylose are gratuitous inducers in *Paenibacillus* since they serve as carbon sources for growth [2].

The induction patterns with respect to the inducer concentrations deviated from perfect linearity which may reflect that inducers were catabolized and their concentrations diminished during the growth of the recombinant strains, although they were added to complex Caso broth rather than minimal media and, thus, were not required as growth substrates. The observed induction patterns may also reflect all-or-none induction and the presence of induced and non-induced sub-populations. In *E. coli*, this phenomenon is known for arabinose inducible gene expression from expression vectors and deletion of the arabinose utilization genes was required for the homogenous gene expression from the plasmid [41], a strategy which may be followed in *Paenibacillus* once gene deletion is possible in this bacterium. Homogenous gene expression may require that genes important for inducer uptake are expressed constitutively and independently from the inducer itself. In *E. coli*, for example, transcribing arabinose uptake gene *araE* from a constitutive promoter from *Lactococcus lactis* instead of its own arabinose inducible promoter enabled homogenous graded arabinose induction [42].

In general, promoters from different *Bacillus* or *Paenibacillus* species are functional in other *Bacillus* or *Paenibacillus* species, e.g. the promoters PxylA from *B. megaterium* and PmtlA from *B. methanolicus* could be used in *Paenibacillus*. On the other hand, *B. subtilis* PmtlA hardly worked in *B. methanolicus* (Table 3). Likewise, PxylA was xylose inducible in *P. polymyxa* DSM-365; however, induced expression of the fluorescence reporter gene was about tenfold lower than in *P. riograndensis* (Figure 6A). Thus, transferability of the gene expression systems is achievable, however, to fully exploit the application potential these systems need to be optimized in the respective hosts.

The genetic toolbox described here forecasts future developments in functional genomics of *Paenibacilli*. Gain-of-function and loss-of-function analyses are important elements of functional genomics and they require genetic systems for gene overexpression and gene deletion. For instance, controlled gene expression is important in gene deletion using CRISPR/Cas9 [43,44] or for CRISPRi/dCas9 mediated gene knockdown [33,34]. A prerequisite for the use of CRISPR technology as well as for gain-of-function analyses in *Paenibacillus* has been achieved in this study by the two vector system for independent mannitol and/or xylose inducible gene expression.

Results

2.3.6. References

1. Beneduzi A, Moreira F, Costa PB, Vargas LK, Lisboa BB, Favreto R, et al. Diversity and plant growth promoting evaluation abilities of bacteria isolated from sugarcane cultivated in the South of Brazil. *Appl. Soil Ecol.* 2013;63:94–104.
2. Beneduzi A, Costa PB, Melo IS, Bodanese-Zanettini MH, Passaglia LMP. *Paenibacillus riograndensis* sp. nov., a nitrogen-fixing species isolated from the rhizosphere of *Triticum aestivum*. *Int. J. Syst. Evol. Microbiol.* 2010;60:128–33.
3. Brito LF, Bach E, Kalinowski J, Rückert C, Wibberg D, Passaglia LM, et al. Complete genome sequence of *Paenibacillus riograndensis* SBR5, a Gram-positive diazotrophic rhizobacterium. *J. Biotechnol.* 2015;207:30–1.
4. Fernandes GDC, Trarbach LJ, Campos SBD, Beneduzi A, Passaglia LMP. Alternative nitrogenase and pseudogenes: unique features of the *Paenibacillus riograndensis* nitrogen fixation system. *Res. Microbiol.* 2014;165:571–80.
5. Sperb ER, Tadra-Sfeir MZ, Sperotto RA, Fernandes GDC, Pedrosa FO, de Souza EM, et al. Iron deficiency resistance mechanisms enlightened by gene expression analysis in *Paenibacillus riograndensis* SBR5. *Res. Microbiol.* 2016;167:501–9.
6. Murray KD, Aronstein KA. Transformation of the Gram-positive honey bee pathogen, *Paenibacillus larvae*, by electroporation. *J. Microbiol. Methods.* 2008;75:325–8.
7. Rosado A, Duarte GF, Seldin L. Optimization of electroporation procedure to transform *B. polymyxa* SCE2 and other nitrogen-fixing *Bacillus*. *J. Microbiol. Methods.* 1994;19:1–11.
8. Bakhiet N, Stahly DP. Studies on transfection and transformation of protoplasts of *Bacillus larvae*, *Bacillus subtilis*, and *Bacillus popilliae*. *Appl. Environ. Microbiol.* 1985;49:577–81.
9. Choi HA, Lee YC, Lee JY, Shin HJ, Han HK, Kim GJ. A simple bacterial transformation method using magnesium- and calcium-aminoclay. *J. Microbiol. Methods.* 2013;95:97–101.
10. Kim S, Lee YC, Cho DH, Lee HU, Huh YS, Kim GJ, et al. A simple and non-invasive method for nuclear transformation of intact-walled *Chlamydomonas reinhardtii*. *PLoS ONE.* 2014;9:1–9.
11. Yoshida N, Ikeda T, Yoshida T, Sengoku T, Ogawa K. Chrysotile asbestos fibers mediate transformation of *Escherichia coli* by exogenous plasmid DNA. *FEMS Microbiol. Lett.* 2001;195:133–7.
12. Yoshida N, Sato M. Plasmid uptake by bacteria: a comparison of methods and efficiencies. *Appl. Microbiol. Biotechnol.* 2009;79:1–8.
13. Biedendieck R, Borgmeier C, Bunk B, Stammen S, Scherling C, Meinhardt F, et al. Systems biology of recombinant protein production using *Bacillus megaterium*. *Methods Enzymol.* 2011; 500:165-95

Results

14. Hanahan D, Harbor CS. Studies on transformation of *Escherichia coli* with plasmids. *J. Mol. Biol.* 1983;166:557–80.
15. Irla M, Heggeset TMBN Ingemar, Paul L, Tone H, Le SB, Brautaset T, et al. Genome-based genetic tool development for *Bacillus methanolicus*: theta- and rolling circle-replicating plasmids for inducible gene expression and application to methanol-based cadaverine production. *Front. Microbiol.* 2016;7:1481.
16. Nguyen HD, Nguyen QA, Ferreira RC, Ferreira LCS, Tran LT, Schumann W. Construction of plasmid-based expression vectors for *Bacillus subtilis* exhibiting full structural stability. *Plasmid.* 2005;54:241–8.
17. Peters-Wendisch P, Götter S, Heider SAE, Reddy GK, Nguyen AQ, Stansen KC, et al. Engineering biotin prototrophic *Corynebacterium glutamicum* strains for amino acid, diamine and carotenoid production. *J. Biotechnol.* 2014;192:346–54.
18. Jakobsen ØM, Brautaset T, Degnes KF, Heggeset TMB, Balzer S, Flickinger MC, et al. Overexpression of wild-type aspartokinase increases L-lysine production in the thermotolerant methylotrophic bacterium *Bacillus methanolicus*. *Appl. Environ. Microbiol.* 2009;75:652–61.
19. Sambrook J. *Molecular cloning: a laboratory manual*. New York: Cold Spring Harbor; 2001.
20. Eikmanns BJ, Thum-schmitz N, Eggeling L, Ludtke K, Sahm H. Nucleotide sequence, expression and transcriptional analysis of the *Corynebacterium glutamicum gltA* gene encoding citrate synthase. *Microbiology.* 1994;140:1817–28.
21. Gibson DG. Programming biological operating systems: genome design, assembly and activation. *Nat. Methods.* 2014;11: 521–6.
22. Han HK, Lee YC, Lee MY, Patil AJ, Shin HJ. Magnesium and calcium organophyllosilicates: synthesis and in vitro cytotoxicity study. *ACS Appl. Mater. Interfaces.* 2011;3:2564–72.
23. Pátek M, Nešvera J. Sigma factors and promoters in *Corynebacterium glutamicum*. *J. Biotechnol.* 2011;154:101–13.
24. Becker J, Schäfer R, Kohlstedt M, Harder BJ, Borchert NS, Stöveken N, et al. Systems metabolic engineering of *Corynebacterium glutamicum* for production of the chemical chaperone ectoine. *Microb. Cell Fact.* 2013;12:110.
25. Altschup SF, Gish W, Pennsylvania T, Park U. Basic local alignment search tool. *J. Mol. Biol.* 1990;215:403–10.
26. Solovyev V, Salamov A. Automatic annotation of microbial genomes and metagenomic sequences. In: Li R W (ed) *Metagenomics and its applications in agriculture, biomedicine and environmental studies*. Nova Science Publishers; 2011.

Results

27. Heravi KM, Altenbuchner J. Regulation of the *Bacillus subtilis* mannitol utilization genes: promoter structure and transcriptional activation by the wild-type regulator (MtlR) and its mutants. *Microbiology*. 2016;160:91–101.
28. Heggeset TMB, Krog A, Balzer S, Wentzel A, Ellingsen TE, Brautaset T. Genome sequence of thermotolerant *Bacillus methanolicus*: features and regulation related to methylotrophy and production of L-lysine and L-glutamate from methanol. *Appl. Environ. Microbiol.* 2012;78:5170–81.
29. Irla M, Neshat A, Brautaset T, Rückert C, Kalinowski J, Wendisch VF. Transcriptome analysis of thermophilic methylotrophic *Bacillus methanolicus* MGA3 using RNA-sequencing provides detailed insights into its previously uncharted transcriptional landscape. *BMC Genomics*. 2015;16:73.
30. Jitrapakdee S, Wallace JC. The biotin enzyme family: conserved structural motifs and domain rearrangements. *Curr. Protein Pept. Sci.* 2003;4:217–29.
31. Ikeda M, Miyamoto A, Mutoh S, Kitano Y, Tajima M, Shirakura D, et al. Development of biotin-prototrophic and -hyperauxotrophic *Corynebacterium glutamicum* strains. *Appl. Environ. Microbiol.* 2013;79:4586–94.
32. Jones PD, Graham V, Segal L, Baillie WJ, Briggs MH. Forms of soil biotin. *Life Sci.* 1962;1:645–8.
33. Cleto S, Jensen JK, Wendisch VF, Lu TK. *Corynebacterium glutamicum* metabolic engineering with CRISPR interference (CRISPRi). *ACS Synth. Biol.* 2016;5:375-85.
34. Tong Y, Charusanti P, Zhang L, Weber T, Lee SY. CRISPR-Cas9 based engineering of actinomycetal genomes. *ACS Synth. Biol.* 2015;4:1020–9.
35. Hanahan BD, Jessee J. Plasmid transformation of *Escherichia coli* and other bacteria. *Methods Enzymol.* 1991;204:63–113.
36. Leonhardt H. Identification of a low-copy-number mutation within the pUBI10 replicon and its effect on plasmid stability in *Bacillus subtilis*. *Gene.* 1990;94:121–4.
37. Leonhardt H, Alonso JC. Parameters affecting plasmid stability in *Bacillus subtilis*. *Gene.* 1991;103:107–11.
38. Yu B, Sun J, Bommareddy RR, Song L, Zeng A. Novel (2R, 3R)-2, 3-butanediol dehydrogenase from potential industrial strain *Paenibacillus polymyxa* ATCC 12321. *Appl. Environ. Microbiol.* 2011;77:4230–3.
39. Adlakha N, Shams S. Efficient production of (R, R)-2, 3- butanediol from cellulosic hydrolysate using *Paenibacillus polymyxa* ICGEB2008. *J. Ind. Microbiol. Biotechnol.* 2015;42:21–28.

Results

40. Kim HR, Park SY, Kim SB, Jeong H, Choi SK, Park SH. Inactivation of the phosphoglucomutase gene *pgm* in *Paenibacillus polymyxa* leads to overproduction of fusaricidin. *J. Ind. Microbiol. Biotechnol.* 2014;41:1405–1414.
41. Datsenko KA, Wanner BL. One-step inactivation of chromosomal genes in *Escherichia coli* K-12 using PCR products. *Proc. Natl. Acad. Sci. USA.* 2000; 97:6640-6645.
42. Khlebnikov A, Datsenko KA, Skaug T, Wanner BL, Keasling JD. Homogeneous expression of the P(BAD) promoter in *Escherichia coli* by constitutive expression of the low-affinity high-capacity AraE transporter. *Microbiology.* 2016;147:3241–3247.
43. Jiang W, Marraffini LA. CRISPR-Cas: new tools for genetic manipulations from bacterial immunity systems. *Annu. Rev. Microbiol.* 2015;69:209:228.
44. Makarova KS. Evolution and classification of the CRISPR–Cas systems. *Nat. Publ. Group.* 2011;9:467–477.

2.4 Differential gene expression of phosphate solubilizing-bacterium Paenibacillus riograndensis SBR5 cultivated in two distinct phosphate sources

Luciana Fernandes de Brito, Marina Gil Lopez & Volker F. Wendisch

Genetics of Prokaryotes, Faculty of Biology & Center for Biotechnology (CeBiTec), Bielefeld University, Universitätsstraße 25, 33615 Bielefeld, Germany

2.4.1. Abstract

Due to the importance of phosphorus (P) in agriculture, the crop inoculation with phosphate solubilizing bacteria (PSB) is a relevant subject of study. *Paenibacillus riograndensis* SBR5 is a promising candidate for crop inoculation because it is capable of performing nitrogen fixation and producing phytopathogen antagonist substances. However, this organism has not been studied extensively. Here, we performed a differential gene expression analysis associated to phenotypic study aiming to evaluate the process of phosphate solubilization (PS) in this organism. SBR5 was cultivated in two distinct P sources: NaH_2PO_4 (soluble phosphate) and hydroxyapatite (insoluble phosphate). Total RNA of SBR5 cultivated in these two conditions was isolated and submitted to sequencing. Moreover, organic acids production and PS by SBR5 were analyzed and its motility was evaluated by the means of flow cytometry. We discovered that the expression of 42 genes was upregulated and 15 genes downregulated in the insoluble phosphate condition. Expression of genes involved in glucose metabolism, including those coding for 2-oxoglutarate dehydrogenase, was downregulated in insoluble phosphate condition. Determination of organic acids concentration showed that the production of tricarboxylic acid cycle-derived organic acids is reduced in this condition, proving that metabolic channeling of glucose towards the tricarboxylic acid cycle is negatively regulated by insoluble phosphates. The cultivation in hydroxyapatite caused the reduction in the motility of SBR5 cells as a response to phosphate depletion in the beginning of its growth. SBR5 was able to solubilize hydroxyapatite, which suggests that this organism is a promising PSB. Our findings are the initial step in the elucidation of the PS process in *P. riograndensis* SBR5, and will be a valuable groundwork for further studies of this organism as a plant growth promoting rhizobacterium.

Results

2.4.2. Introduction

Phosphorus (P), together with nitrogen and potassium, is an essential macronutrient for plant growth. Plant roots are able to absorb P in form of orthophosphates, either H_2PO_4^- or HPO_4^{2-} , but the concentrations of those ions in soil are in the micromolar range [1,2]. This is due to the complex dynamics of P in the soil; this nutrient has a unique characteristic, which is its high fixation in soil. Mineral phosphates can be, for example, found associated with the surface of iron or aluminum oxides that are poorly soluble and accessible [3]. These factors lead to the overloading of chemical P fertilizers and animal manure to the agricultural land that indeed improves soil P fertility and crop production, but causes severe environmental damage in the past decades [4]. Therefore, with increasing demand of agricultural production, P is receiving more attention as a nonrenewable resource [5]. In this context, the phosphate solubilization (PS) performed by organisms in the soil is an interesting target for study. PS ability is well characterized for mycorrhizal fungi [6] and phosphate solubilizing bacteria (PSB), mostly associated to the plant rhizosphere [7]. There is a substantial number of PSB genera widespread in the rhizosphere [8], whereof some are well-established as plant growth promoting rhizobacteria (PGPR) e.g. *Pseudomonas* [9], *Bacillus* [8], *Enterobacter* [10] and *Azotobacter* [11]. The use of PSB as inoculants leads to increased P uptake by the plant and crop yield. Besides providing soluble P to plants, these organisms promote their growth and development by other activities such as nitrogen fixation and production of plant phytohormones [12]. Among the mechanisms utilized by PSB for phosphate solubilization, the production of organic acids is well recognized and is considered to be most common in rhizobacteria. The organic acids excreted by PSB have different modes of action that lead to PS; the mineral ions bound to precipitated phosphates can be chelated by these organic acids or P can be dissolved through the decrease of the pH [13]. Among the genera considered as PSB, *Paenibacillus* has shown to be promising for inoculation purposes. In comparative genomic analysis, it was suggested that a wide group of *Paenibacillus* is able to perform PS by producing the organic acid gluconate [14]. Sixteen *Paenibacillus* species (e. g. *Paenibacillus azotofixans*, *Paenibacillus dendritiformis*, *Paenibacillus elgii*, *Paenibacillus graminis* and *Paenibacillus polymyxa*) showed high conservation of the genes coding for glucose-1-dehydrogenase and gluconate dehydrogenase, which are involved in the synthesis the organic acid gluconate [14].

Results

Paenibacillus riograndensis is a rod-shaped, Gram-positive, motile, nitrogen-fixing bacterium [15]. The strain SBR5 was isolated from the rhizosphere of wheat (*Triticum aestivum*) plants cultivated in Rio Grande do Sul, Brazil [16]. In addition to nitrogen fixing, SBR5 possesses further plant growth promoting activities, such as ability to produce indol-3-acetic acid and phytopathogen antagonist substances [17,18]. The complete genome of *P. riograndensis* SBR5 was sequenced and fully annotated and consists of one chromosome with 7.893.056 bps, containing 6705 protein coding genes, 87 tRNAs and 27 rRNAs genes [19]. Moreover, molecular tools for gene expression in this organism were developed [20]. Hence, *P. riograndensis* SBR5 is a promising target for study and agricultural purposes. SBR5 is poorly characterized and its potential as PSB has not been studied. To elucidate the PS process in *P. riograndensis* SBR5, we performed for the first time for this species a differential gene expression analysis under supplementation with two phosphate sources: soluble and insoluble. The growth and PS activity of SBR5 were investigated and the differences in the global transcriptome profiles in both conditions were analyzed by utilizing RNA sequencing (RNAseq) technology.

2.4.3. Materials and Methods

Strains and growth conditions

The PGPR strain *P. riograndensis* SBR5, which was the object of this study, was obtained from the strain collection of the Department of Genetics at Universidade Federal do Rio Grande do Sul, Brazil. Here, we performed cultivations in order to expose SBR5 to two distinct phosphate sources. The bacterial cells were grown in petri dishes containing LB agar (Lysogeny Broth) and a single colony was picked and transferred to 500 mL shaking flasks containing 50 mL of LB medium. One mL of the bacterial suspension was inoculated into 500 mL shaking flasks containing 50 mL of distinct broth media differing with regard to the P source: 1) Pikovskaya broth (PVK; prepared as Pikovskaya, [21]) with 5g L⁻¹ of Ca₅(PO₄)₃(OH) (hydroxyapatite) as P source (PbI); 2) PVK with 1.6 g L⁻¹ NaH₂PO₄ as P source (PbS). To maintain neutral pH of both media, 12 g L⁻¹ of 3-morpholinopropane-1-sulfonic acid (MOPS) were added. The cells grown in each condition were used to re-inoculate the fresh media. During the cultivations, the cells were routinely shaken at 120 rpm and temperature of 30°C. For each condition tested, six biological replicates were used: three for harvesting of bacterial cells and

Results

total RNA isolation, and three for further determination of growth characteristics. The optical density at 600 nm ($OD_{600 \text{ nm}}$) of the cultivated cells was measured in regular intervals. During each measurement of growth, the pH of the culture broth was measured with pH indicator sticks (Macherey-Nagel, Düren, Germany). The initial $OD_{600 \text{ nm}}$ of the main cultivation was approximately 0.05. Bacterial cells of 3 replications were harvested in the middle of the exponential phase and the harvesting procedure was done according to Irla et al. [22]. Supernatants of the bacterial cultures and cell pellets of the other 3 replications were collected by centrifugation (4,000 rpm) at the time points of 0, 5 and 20 hours for further phenotypic analysis.

RNA isolation and preparation and sequencing of cDNA libraries

In order to isolate the total RNA from SBR5 cells, bacterial cell pellets previously harvested and stored at -80°C were thawed in ice and RNA was extracted individually for each cultivation condition. All the procedures regarding RNA isolation and RNA quality control were done accordingly to Brito et al. [23]. The three replications of extracted RNA samples of each condition were pooled in equal parts and the pool of total RNA was subsequently used for the preparation of cDNA libraries. For each condition, a whole transcriptome library was prepared. The preparation of this library and the cDNA sequencing were carried out according to Mentz et al. [24].

Bioinformatics analysis

The sequence reads obtained in the present study were mapped onto the reference genome of *P. riograndensis* SBR5 [19]. To prepare the reads for mapping, the tool Trimmomatic version 0.33 [25] was used to trim the sequences to a minimal length of 35 base pairs. Trimmed reads were mapped to the reference genome of SBR5 through the software for short read alignment Bowtie [26]. The visualization of mapped reads and the differential gene expression analysis were performed using the software ReadXplorer [27], in which the statistical method DEseq was employed to analyze the resultant RNAseq data [28]. The cut-off values for designating a gene as differentially expressed included a change in expression level (base mean) higher than 30 and an adjusted *P*-value of equal to or less than 0.05. When differentially expressed genes coding for proteins of unknown function were detected, the gene sequences were submitted to BLASTx analysis to identify the protein family conservations [29].

Results

Validation of RNAseq data by real-time quantitative reverse transcription-PCR

In order to validate the data obtained by DEseq analysis, real-time quantitative reverse transcription-PCR (qRT-PCR) was performed utilizing a LightCycler® system (Roche Diagnostics, Penzberg, Germany). The RNA samples utilized to compose the RNA pools for cDNA library preparation in this study were also utilized as templates for qRT-PCR. Therefore, each sample concentration was adjusted to 50 ng RNA μL^{-1} and 1 μL thereof was pipetted into a reaction mix of the SensiFAST™ SYBR® No-ROX Kit (Bioline, Luckenwalde, Germany), following manufacturer's instructions. Differentially expressed genes selected for this assay as well as the characteristics of the primers utilized are listed in Table 1. For evaluation of relative gene expression, 16S rRNA was used as reference control [30]. The melting-curve data-based quantification cycle (Cq) values, from the LightCycler® output files, were used for further calculation. For calculation of relative gene expression, the following equation was used: $\Delta\Delta\text{Cq} = 2^{-(\text{CqPbI} - \text{Cq16S})} / 2^{-(\text{CqPbS} - \text{Cq16S})}$ [31].

Table 1. Oligonucleotide sequences (5'-3') used for amplification of gene fragments of *P. riograndensis* SBR5 in qRT-PCR.

Gene identity	Forward	Reverse	Gene product length [bp]
P.riograndensis_final_1896	GCTGAGCTGATGGGTGAATG	TATCCGGGATGCTCTCCTTG	229
P.riograndensis_final_1897	TCGTCTATGCGCTTGGATCG	AAGTGAACGTCCGCTGATCG	179
P.riograndensis_final_1898	CCGCCAGCAAAGCCTATCTC	GCTACATCATCGCCCAGCTC	154
<i>yusV</i>	GCATCAAGGCTGGCTGAAGG	AGATAGGTGGTCCGGCTCGTC	198
P.riograndensis_final_1900	AGCGGGTCAAGGCCAGAATC	CCGCCACAAGGGTTCTTTGC	243
<i>odhB</i>	TGCCGTGTCTGCCAAGGAAG	ATGCCGAGAATGCCGACCTG	231
<i>odhA</i>	GGCACACCGATCCGGTTAAG	CGGGTGCGAACACGTTGTAG	208
P.riograndensis_final_5412	ATCGGATGCCAGCATTGTAG	AATGTAGCCGATGGCGTTAG	181
P.riograndensis_final_5413	GAACTGAACGACAGCAAAGG	CCGTCTGCATTCCAATGAAG	242
P.riograndensis_final_5640	GTGTGGCAAAGTCCCTGAAC	CAAACATCCAGTGCGGTGTC	210
P.riograndensis_final_5641	CCTATTGGATCGGCAAGTGG	CCGGTGTCACTGTATTCTGG	198
<i>opuAA</i>	CCGAATATGGCCTTGAAGTG	CACTGAAAGCCTCATCCATC	201
P.riograndensis_final_6162	GCGGTGTATGACTGCTTC	TAGCGCCCTCAAGGAGATG	214
P.riograndensis_final_6163	TGCTGCAGTACAGGGAGTTG	TCCTTGCACTGCCGAATTG	157
P.riograndensis_final_6164	CGAGCAAGCACAAACGTAATG	TATTTGCACCCGCTGTGATG	245
Reference control (16S)*	CACGTGTAGCGGTGAAATGC	ACTTCGGCACCAAGGGTATC	184

* Oligonucleotide sequences designed by Sperb et al. [30].

Results

Phenotypic Analysis

For quantification of glucose and organic acids concentration in the supernatants of SBR5, high performance liquid chromatography system (HPLC, 1200 series, Agilent Technologies Deutschland GmbH, Böblingen, Germany) was used as in Zahoor et al. [32]. Quantification was done by calibration with external standards. By this method glucose, gluconate, oxoglutarate, acetate, citrate, succinate, oxalate and malate were determined. 2-Oxoglutarate dehydrogenase activity was measured accordingly to Nguyen et al. [33]. Furthermore, the solubilization efficiency of SBR5 cultivated in the different conditions was determined through the quantification of orthophosphates present in the supernatants. This assay was performed by the means of the molybdenum-blue method, as described by Murphy and Riley [34]. Lastly, to analyze the motility of SBR5 cells, the cells were cultivated as described above (in PbS, PbI and LB medium) and collected 5 hours after inoculation, then centrifuged for 10 minutes at 4,000 rpm. The pellets were washed two times in NaCl 0.89 % solution and the OD_{600nm} was adjusted to 0.5. The cell suspensions were incubated with 10 µg mL⁻¹ of Alexa Fluor® 594 dye (Thermo Fisher Scientific, Waltham, USA), prepared accordingly to manufacturer's instructions, for 30 minutes at room temperature then washed two times in NaCl 0.89 % solution. To quantify the fluorescence intensities in the cell suspensions, they were submitted to flow cytometry (Beckman Coulter, Brea, US) and the data analyzed in the Beckman Coulter Kaluza® Flow Analysis Software. The settings for the emission signal and filters within the flow cytometer for detection of Alexa Fluor® 594 dye fluorescence was 620/525 bandpass FL1 filter.

2.4.4. Results and Discussion

Phosphate solubilizing activity by P. riograndensis SBR5

The pH values of the cultivation broth of the SBR5 cultures grown in the two determined conditions were lower than the initial pH (Figure 1). However, in PbI medium the pH decreased more substantially (from 7 ± 0 to 4 ± 0) in comparison to PbS medium (from 7 ± 0 to 6 ± 0) (Figure 1). In many cases, acidification is the main mechanism involved in the phosphate

Results

solubilization. Several authors have suggested that a decrease of pH values due to the production of organic acids and the release of protons by PSB is a basic principle of their PS activity [8,35]. The decrease of pH as a mechanism to perform PS has been reported in fungi [36], and it is mostly related to the production of organic acids, as in *Aspergillus* and *Penicillium* [37]. Furthermore, *P. riograndensis* SBR5 grew slightly better in PbS, with NaH_2PO_4 as P source, in comparison to PbI, where hydroxyapatite was a P source (Figure 1). This might be due to the fact that hydroxyapatite is initially insoluble in the medium, which led to the P deficiency at the beginning of the growth. This result is in agreement with studies on other PSB strains, such as *Pseudomonas aeruginosa* and *Burkholderia multivorans*, which reported that the final cell biomass of PSB strains under sufficient phosphate condition is higher than under phosphate depletion condition [38,39].

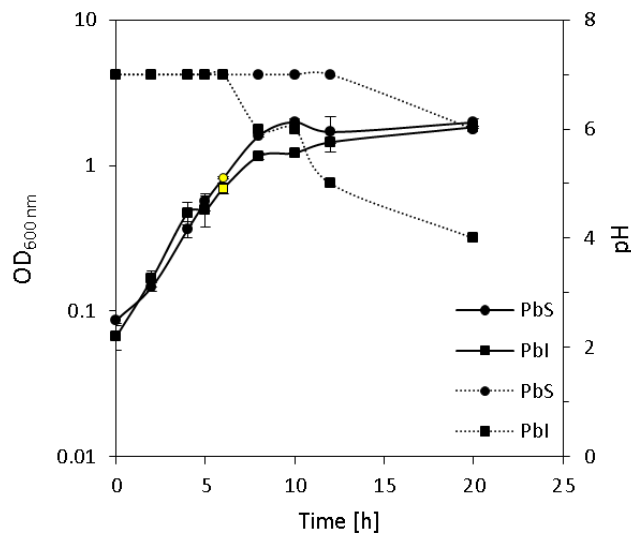


Figure 1. Growth of SBR cells and pH values in PbI and PbS media. The time point of the cell harvesting for RNA isolation and supernatant collection for further analytical steps is depicted with yellow symbols.

In the present study, the P source in PbI was 5 g L^{-1} hydroxyapatite, which was not readily available for bacterial growth. In the moment of inoculation, the medium PbI contained about $20 \mu\text{g P-PO}_4^{-3} \text{ mL}^{-1}$ of orthophosphates (Figure 2). This is half of the concentration of orthophosphates utilized by SBR5 in PbS, which was approximately $40 \mu\text{g P-PO}_4^{-3} \text{ mL}^{-1}$. The initial low concentration of available P contributed to the induction of PS by SBR5 in PbI medium. It is a general phenotype of PSB that the PS activity is induced by low levels of

Results

exogenous soluble phosphate and inhibited by its high levels [39,40]. Increase of orthophosphate concentration during incubation was detected in the PbI medium, containing hydroxyapatite. The PS activity of *P. riograndensis* SBR5 led to a liberation of $300 \mu\text{g P-PO}_4^{-3} \text{ mL}^{-1}$ of orthophosphates in PbI medium (Figure 2). This value is higher than values observed for other *Paenibacillus* species: $80 \mu\text{g mL}^{-1}$ by *P. polymyxa* and $130 \mu\text{g mL}^{-1}$ by *Paenibacillus mucilaginosus* from CaHPO_4 and phosphorite after 3 and 5 days of incubation, respectively [41,42], showing that *P. riograndensis* SBR5 is a promising PSB. Moreover, the reverse correlation between pH value of the culture (Figure 1) and the released orthophosphate concentration (Figure 2) indicates that organic acid production by *P. riograndensis* SBR5 may play a role in the solubilization of insoluble phosphate.

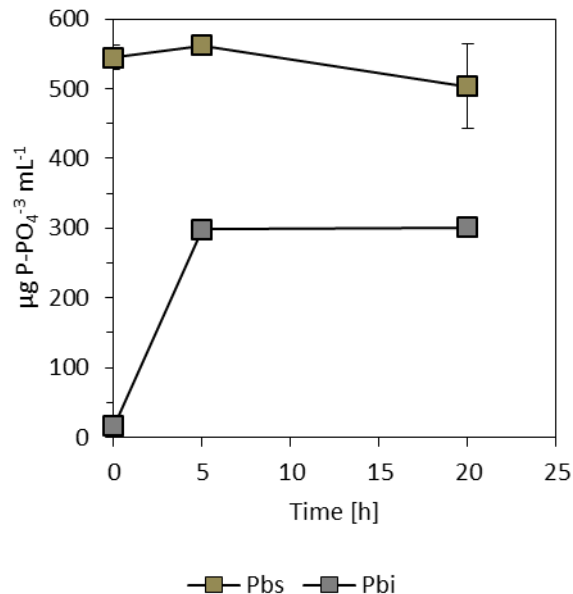


Figure 2. Concentration of orthophosphates in the supernatant and of *P. riograndensis* SBR5 cultivated in PVK broth (PbI) in comparison to cultivation in PVK broth having NaH_2PO_4 as P source (PbS). The concentration of orthophosphates in the supernatants was determined by the molybdenum-blue method [34].

The phosphate in PbS was not completely utilized (Figure 2), but supported the growth of *P. riograndensis* SBR5 (Figure 1), indicating that PbS provided sufficient supply of P for SBR5. Moreover, the decrease of pH value in the culture grown in PbS medium was lower in comparison to that in the PbI medium (Figure 1). It is known that the PS of PSB can be repressed by soluble phosphate in the mechanism of a feedback inhibition [39]. Sensitivity to soluble

Results

phosphate is a severe limitation to the extensive application of PSB. However, the molecular mechanism of soluble phosphate regulation on phosphate-solubilizing activity of PSB remains unclear. Hence, the regulation of PS in *P. riograndensis* SBR5 by different concentrations of soluble phosphate is still to be elucidated.

Differential gene expression analysis and validation of expression pattern by qRT-PCR

Gene expression analysis regarding the P metabolism and PS in bacteria was performed by the means of microarray [43] and RNAseq technologies [39]. Here, we carried out the differential gene expression analysis of *P. riograndensis* SBR5 cultivated in two distinct P conditions: one soluble P source (NaH₂PO₄, PbS medium) and other insoluble (hydroxyapatite, PbI medium). Sequencing of cDNA libraries generated from RNA obtained in those two conditions resulted in 2,729,614 reads for PbS sample and 2,773,600 reads for PbI. Of the resultant reads, 2,720,143 and 2,685,108 reads of PbS and PbI libraries, respectively, were mapped onto the genome of SBR5. The differential gene expression analysis was carried out with the statistical method DEseq [28]. Our DESeq analysis revealed the expression of 42 genes was upregulated (Table 3) and 15 genes downregulated in the insoluble phosphate condition (Table 2).

Table 2. List of genes upregulated in *P. riograndensis* SBR5 cultivated in PbI in comparison to cultivation in PbS. Gene names in bold indicates genes chosen for RT-qPCR analysis; gene products in italic represents BLAST analysis results.

Feature	Product	Fold	
		change	P-value
P.riograndensis_final_1123	<i>No putative conserved domains</i>	3.97	0.00
P.riograndensis_final_1182	YhgE/Pip N-terminal domain protein	3.41	0.00
<i>yugH</i>	Putative aminotransferase YugH	4.09	0.00
P.riograndensis_final_1553	<i>No putative conserved domains</i>	3.19	0.01
	Non-ribosomal peptide synthase/amino acid adenylation		
P.riograndensis_final_1679	enzyme	3.10	0.01
P.riograndensis_final_1712	Glutamine--scyllo-inositol transaminase	3.26	0.01
P.riograndensis_final_1811	S-layer domain-containing protein	4.07	0.00
P.riograndensis_final_1812	ABC-type multidrug transport system	4.54	0.00
P.riograndensis_final_1813	ABC transporter	5.15	0.00
P.riograndensis_final_1896	Periplasmic-binding protein	3.65	0.00

Results

P.riograndensis_final_1897	Transport system permease	4.54	0.00
P.riograndensis_final_1898	Transport system permease	3.31	0.01
	Probable siderophore transport system ATP- binding		
<i>yusV</i>	protein YusV	4.62	0.00
P.riograndensis_final_1900	<i>Ferric iron reductase protein FluF</i>	5.15	0.00
P.riograndensis_final_2070	Trypsin	3.25	0.01
P.riograndensis_final_2763	<i>No putative conserved domains</i>	3.65	0.01
<i>fabG</i>	3-Ketoacyl-ACP reductase	3.20	0.01
P.riograndensis_final_2959	<i>No putative conserved domains</i>	4.46	0.00
P.riograndensis_final_3118	<i>Heat induced stress protein YflT</i>	3.03	0.01
P.riograndensis_final_3123	General stress protein 16O	3.29	0.01
<i>treA</i>	Trehalose-6-phosphate hydrolase	3.42	0.01
	<i>Periplasmic-binding component of alginate-specific ABC</i>		
P.riograndensis_final_345	<i>uptake system-like</i>	4.94	0.00
P.riograndensis_final_346	<i>Carbohydrate Binding protein</i>	3.47	0.01
P.riograndensis_final_3666	PAS domain S-box protein	3.57	0.01
P.riograndensis_final_3815	<i>No putative conserved domains</i>	4.05	0.00
P.riograndensis_final_4161	<i>Carbohydrate/starch-binding protein</i>	4.65	0.00
P.riograndensis_final_4326	<i>No putative conserved domains</i>	3.73	0.00
P.riograndensis_final_4843	<i>General stress protein YciG</i>	4.80	0.00
<i>rplU</i>	50S ribosomal protein L21	3.00	0.01
P.riograndensis_final_5412	Phosphate binding protein	4.71	0.00
P.riograndensis_final_5413	<i>Copper amine oxidase N-terminal domain</i>	4.10	0.01
P.riograndensis_final_5808	Transcription cofactor	4.13	0.00
P.riograndensis_final_5813	<i>No putative conserved domains</i>	3.65	0.00
P.riograndensis_final_5814	<i>No putative conserved domains</i>	3.55	0.00
P.riograndensis_final_5825	<i>Uncharacterized membrane protein YtjA</i>	4.09	0.00
P.riograndensis_final_602	<i>CsbD-like protein</i>	3.84	0.00
P.riograndensis_final_603	<i>No putative conserved domains</i>	4.02	0.00
P.riograndensis_final_6178	<i>Putative flagellar system-associated repeat</i>	3.05	0.01
P.riograndensis_final_6290	<i>Putative effector of murein hydrolase LrgA</i>	3.04	0.01
<i>ywbG</i>	Uncharacterized protein YwbG	4.33	0.00
<i>yunF</i>	UPF0759 protein YunF	3.00	0.01
P.riograndensis_final_635	<i>Carbohydrate/starch-binding protein</i>	3.08	0.01

Results

Table 3. List of genes downregulated in *P. riograndensis* SBR5 cultivated in PbI in comparison to cultivation in PbS. Gene names in bold indicates genes chosen for RT-qPCR analysis; gene products in italic represents BLAST analysis results.

Feature	Product	Fold change	P-value
P.riograndensis_final_2300	Transcriptional regulator TenI	-5.00	0.00
P.riograndensis_final_2303	Thiazole biosynthesis protein ThiH	-3.11	0.01
P.riograndensis_final_3056	<i>No conserved domain</i>	-4.81	0.00
<i>odhB</i>	Dihydrolipoyllysine-residue succinyltransferase component of 2-oxoglutarate dehydrogenase complex	-3.16	0.01
<i>odhA</i>	2-Oxoglutarate dehydrogenase E1 component	-3.03	0.01
P.riograndensis_final_5637	<i>No conserved domain</i>	-4.56	0.00
P.riograndensis_final_5640	ABC transporter, substrate-binding protein, QAT family	-3.92	0.00
P.riograndensis_final_5641	Glycine betaine transport system permease protein opuAB	-4.59	0.00
<i>opuAA</i>	Glycine betaine transport ATP-binding protein OpuAA	-5.04	0.00
P.riograndensis_final_6139	<i>Cobalt-precorrin-8X methylmutase</i>	-4.75	0.00
P.riograndensis_final_6151		-3.43	0.01
P.riograndensis_final_6162	Flagellar capping protein	-3.95	0.00
P.riograndensis_final_6163	<i>FlaG protein</i>	-5.70	0.00
P.riograndensis_final_6164	Flagellin	-4.00	0.00
P.riograndensis_final_6184	<i>No conserved domain</i>	-3.17	0.01

The results obtained in the RNAseq analysis were confirmed by the analysis of gene expression patterns in the two distinct P sources conditions by q-RT-PCR, when 15 genes among up/downregulated genes were selected. Seven out of the 15 genes exhibited constant up-regulation and 8 out of the 15 genes showed constant down-regulation when hydroxyapatite was used as P source. The expression patterns of the 15 candidate genes detected by q-RT-PCR were in accordance to the gene expression patterns obtained in the RNAseq analysis (Figure 3), which demonstrates the reliability of the high throughput RNAseq technology.

Results

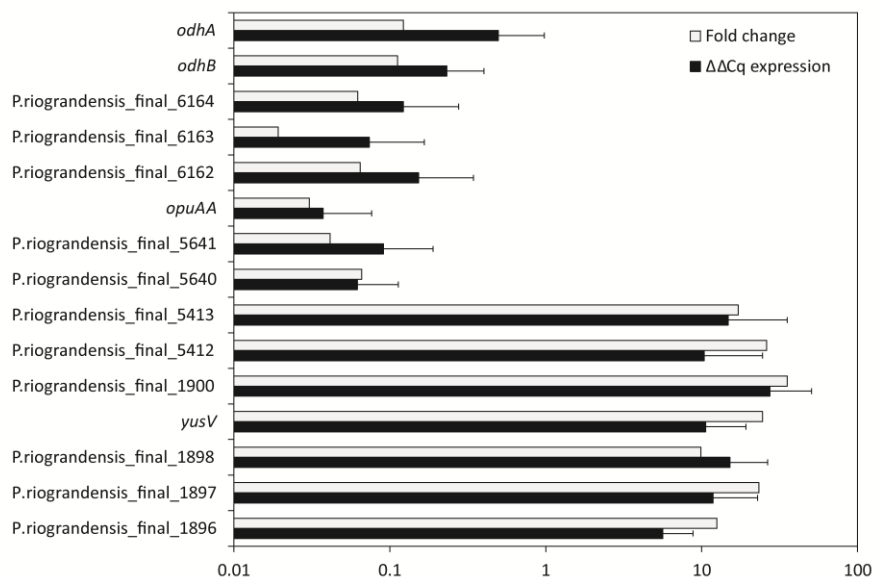


Figure 3. Relative gene expression levels (mean $\Delta\Delta Cq$ expression and standard deviation of biological triplicates) obtained in qRT-PCR in comparison to their differential gene expression (fold change) obtained RNAseq analysis of *P. riograndensis* SBR5 grown in PVK broth (PbI) in comparison to cultivation in PVK broth with phosphate source replaced by NaH_2PO_4 (PbS).

Results of transcriptome analysis showed that in *P. riograndensis* SBR5 the expression two genes related to carbon metabolism was downregulated in SBR5 cultivated in PbI condition, the genes forming the *odhA* and *odhB* complex that codes for 2-oxoglutarate dehydrogenase (2-OGDH) (Table 3). Moreover, the genes *P.riograndensis_final_346*, *P.riograndensis_final_635* and *P.riograndensis_final_4161* that code for carbohydrate binding proteins, were upregulated in PbI condition (Table 2). In the PGPR *B. multivorans*, the expression of genes related to carbon metabolism, including genes encoding sugar ABC transporters as well as 2-OGDH, was upregulated when P was depleted in the medium [39]. The switch of carbon metabolism pathways is closely related to the concentration of soluble phosphate [44]. Furthermore, the expression of genes involved in stress response (*P.riograndensis_final_3118*, *P.riograndensis_final_3123* and *P.riograndensis_final_4843*) was upregulated in PbI condition (Table 2). As discussed before, P was not readily available at the beginning of the cultivation of SBR5 in that condition (Figure 2). Similarly, phosphate depletion led to expression of σ^B -mediated general stress response genes in *Bacillus subtilis* [45]. *B. subtilis* responds to phosphate starvation stress by regulating genes encoding the phosphate starvation Pho proteins [46]. The *pho* regulon is controlled by the two-component PhoP-PhoR signal transduction system [47].

Results

Although expression of genes coding for PhoP-PhoR was not up-regulated in SBR5 in P depletion condition (PbI), they are present in the genome sequence of *P. riograndensis* SBR5 (P.riograndensis_final_2307-2308) (Genbank accession LN831776). Apart from induction of stress response, PbI condition seems to influence the synthesis of flagella. The expression of an operon comprising genes coding for a flagellar capping protein (P.riograndensis_final_6162), a FlaG protein (P.riograndensis_final_6163) and a flagellin protein (P.riograndensis_final_6164) was downregulated in this condition (Table 3). Inorganic phosphate is part of ATP which is a fundamental molecule for cell energy storage, and it plays significant role in flagella synthesis and movement, which are high energy-consuming processes [48,49]. It might mean that low P availability in PbI medium leads to induction of energy saving processes manifested by hindrance of flagella synthesis. Moreover, an expression of an operon that includes two genes related to iron and siderophore metabolism (*yusV*-P.riograndensis_final_1900) was upregulated in SBR5 cultivated in PbI medium (Table 2). P.riograndensis_final_1900 encodes a protein that belongs to a ferric reductase protein family and YusV is a siderophore transporter protein. In microbes, assimilatory ferric reductases are key enzymes of the iron assimilatory pathway [50]. P solubilization mechanisms employed by soil bacteria and fungi also include the production of siderophores, due to their chelating properties [51]. However, the upregulation of expression of siderophore-related genes by SBR5 cultivated in PbI observed in the present study needs to be further investigated, because hydroxyapatite is a calcic P source (not an iron phosphate). Furthermore, in a previous study it was suggested that SBR5 possesses genes involved in the transport of siderophore, but not in its production [30]. Finally, one gene encoding pyrroline-5-carboxylase reductase and an operon comprising genes related to the transport of glycine betaine were downregulated in SBR5 grown in PbI (Table 3). Proline and glycine betaine are among the principal compatible solutes accumulated as osmotic response in bacteria [52]. The accumulation of the osmoprotectant glycine betaine from exogenous sources provides a high degree of osmotic tolerance to *B. subtilis* [53]. The expression of these genes indicates that PbI medium caused high external osmolality leading to the induction of osmoadaptation in *P.riograndensis* SBR5.

Phenotypic analysis regarding the phosphate solubilization activity by P. riograndensis SBR5

Phenotypic analysis was performed based on the currently available genomic and transcriptomic databases [19,23] and on the gene expression analysis performed in the present

Results

study. We aimed to relate some of the differentially expressed genes of *P. riograndensis* SBR5, cultivated with two distinct P sources, to the physiological analysis of PS processes. The up/downregulation of expression of genes related to carbon metabolism, such as upregulation of P.riograndensis_final_346, P.riograndensis_final_635 and P.riograndensis_final_4161, encoding carbohydrate binding proteins, and downregulation *odhA* and *odhB*, encoding 2-OGDH, was observed during growth of SBR5 with 5g L⁻¹ hydroxyapatite as P source (Tables 2 and 3). This result indicated that *P. riograndensis* SBR5 changes its carbon metabolism in the presence of hydroxyapatite, when P is not readily available. Moreover, the excretion of organic acids by PSB is considered a crucial factor in PS [13]. Based on that, we decided to quantify the production of organic acids and consumption of glucose in SBR5 in the determined conditions. The production of oxalate and malate, which were previously related to PS in *Pseudomonas* [54], was not observed in *P. riograndensis* SBR5 in P depletion conditions. Nevertheless, an increase of approximately 50% of total organic acids was observed when SBR5 was cultivated in PbI (Figure 4). This is in accordance with our observation regarding the acidification of the growth medium in PbI condition (Figure 1). More importantly, the composition of the organic acids produced by SBR5 in the determined conditions was different. When cultivated in PbI, the production of acetate and gluconate in SBR5 were greatly increased in comparison to growth in PbS (Figure 4). Gluconate and acetate are known as agents active in PS. Gluconate is produced by the majority of the PSB, being often the most quantitatively produced organic acid for PS means [35,54–56]. The production of acetate by PSB isolates to perform PS has also been reported [57].

Results

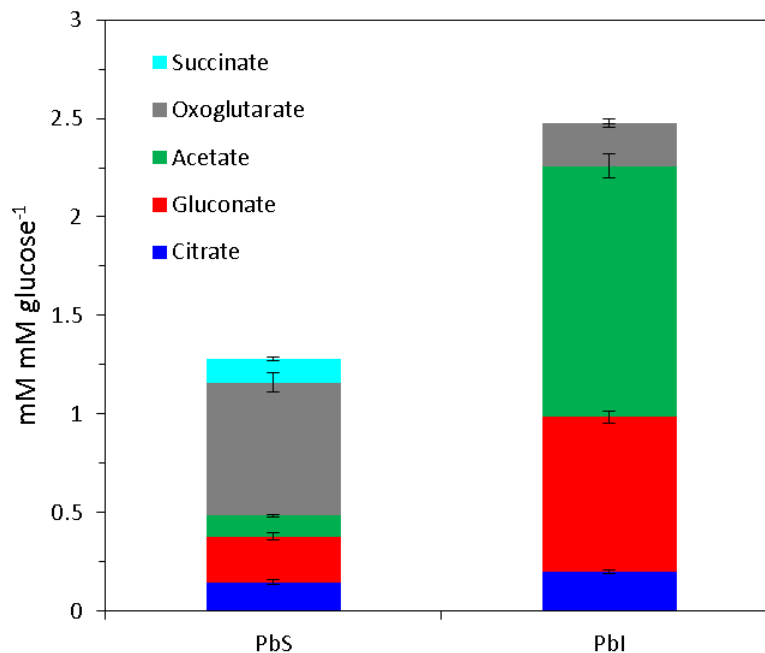


Figure 4. Yield of organic acids in mM mM glucose⁻¹ produced by *P. riograndensis* SBR5 cultivated in PVK broth (PbI) in comparison to cultivation in PVK broth phosphate source replaced by NaH₂PO₄ (PbS). The quantification of glucose and organic acids was determined by HPLC analysis of the supernatants of SBR5 collected at 20 hours of growth.

Genes encoding 2-OGDH, forming a complex *odhAB*, were downregulated in SBR5 at 5g L⁻¹ of hydroxyapatite (Table 3). This was confirmed by analysis of enzymatic activity of 2-OGDH which was significantly lower in cells grown in PbI than in PbS grown cells (Supplementary Figure S1). Interestingly, the accumulation of oxoglutarate dropped drastically in PbI in comparison to PbS (Figure 4). 2-OGDH is a key enzyme that catalyzes the step in tricarboxylic acid (TCA) cycle in which oxoglutarate is converted to succinyl CoA [33]. Thereby, it is suggested that the metabolic flux towards the TCA cycle is reduced when SBR5 is cultivated PbI medium which leads to general decrease of accumulation of TCA metabolites e.g. oxoglutarate and succinate (Figure 5). Low production of oxoglutarate in contrast to high production of gluconate was also observed in soil bacterial isolates that perform PS [57]. Furthermore, a yield about 0.12 mM mM glucose⁻¹ of succinate was detected by HPLC when supernatant of SBR5 cultivated in PbS was analyzed, but no succinate was detected in PbI (Figure 4). Succinate is a product of a step in TCA cycle that follows the reaction catalyzed by 2-OGDH (Figure 5) and it is also one of the major organic acids present in root exudates of plants in rhizosphere. Repression of glucose utilization by succinate is termed as succinate-mediated

Results

catabolite repression [58]. Patel et al. [59] showed that succinate and malate individually and as mixtures repressed gluconate production and PS in *P. aeruginosa*. It is also a component that represses PS phenotype in *Klebsiella pneumoniae* [60,61]. Based on that and on our findings, the reduction of the metabolic flux towards the TCA cycle might be one strategy utilized by SBR5 to perform PS. However, more analytical studies must be performed in order to better explain this process.

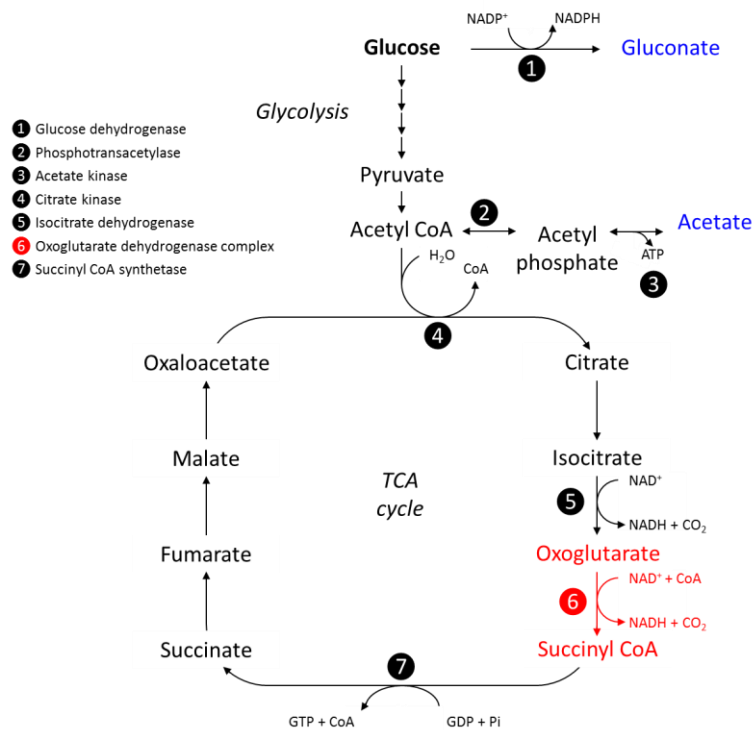


Figure 5. Scheme of pathways in central carbon metabolism that may be involved in the production of organic acids in *P. riograndensis* SBR5. Highlighted in blue are the compounds accumulated in PbI medium, in red is the enzymatic process activated and compounds accumulated in PbS medium. Source: www.genome.jp/kegg/pathway

Furthermore, we have evaluated the motility of SBR5 cultivated in the determined conditions. *P. riograndensis* SBR5 cells cultivated in PbS, PbI or LB (control) medium were stained with Alexa Fluor® 594 dye and subsequently analyzed by flow cytometry. Ten thousand cells of each treatment were analyzed and PbS- and PbI-cultivated cells presented different behavior. The cells grown in PbS showed similar fluorescence to the cells grown in LB medium (Figure 6). In contrast, the cells cultivated in PbI presented a negative peak shift in the flow

Results

cytometry histogram overlay, evidencing reduced fluorescence intensity (Figure 6). Flagellar filaments can be readily stained with amino-specific Alexa Fluor® dye; the cell bodies also were labeled, but flagellated cells present higher fluorescence [62]. This result supports the findings in the RNAseq/qRT-PCR data in which flagella-related genes were downregulated during PbI cultivation. In condition of insufficient P source, flagella-related genes were downregulated in the PSB *B. multivorans* [39]. Here, as mentioned above, P was not readily available to *P. riograndensis* SBR5 in the beginning of its growth (Figure 2). Downregulation of flagella-related genes at PbI medium might be also due to the depletion of P which may influence ATP formation and energy storage processes [63].

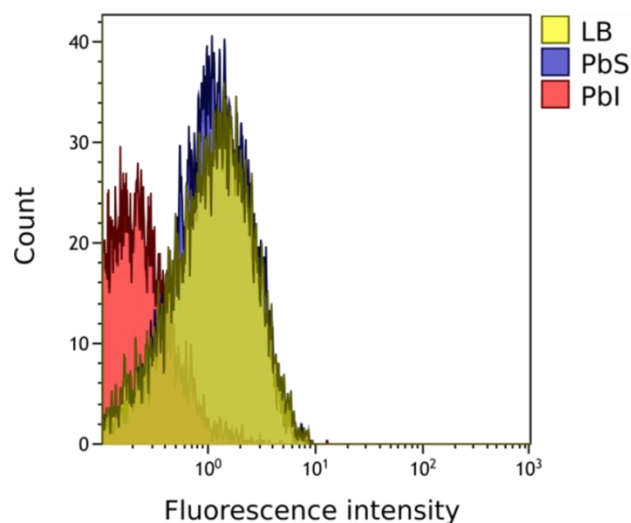


Figure 6. Flow cytometry histograms of 10,000 *P. riograndensis* SBR5 cells cultivated in PVK broth (PbI) in comparison to cultivation in PVK broth phosphate source replaced by NaH₂PO₄ (PbS). SBR5 cells were cultivated in LB medium as a control and all the cells were stained with Alexa Fluor® 594 dye.

2.4.5. Conclusion

The differential gene expression results of the present study revealed a highly complex transcriptional response of *P. riograndensis* SBR5 to two distinct P sources, soluble and insoluble. We showed two important aspects of PS by SBR5: in one hand, *P. riograndensis* SBR5 changes its carbon metabolism characteristics in presence of insoluble phosphate by the reduction of the metabolic flux towards the TCA cycle. On the other hand, it shows signs of stress response in presence of insoluble phosphate, by expression stress response genes and drastic reduction of its motility for propose of energy saving. We showed that the production of

Results

organic acids might be the most important strategy utilized by SBR5 to perform PS. The findings of our study will help us to understand the molecular mechanism of insoluble phosphate regulation on PSB physiological activities by *P.riograndensis* SBR5, especially PS, which provides the first step in the elucidation of PS process in this organism that could further improve the scope of its application as crop inoculant.

2.4.6. References

1. Shin H, Shin HS, Dewbre GR, Harrison MJ. Phosphate transport in Arabidopsis: Pht1;1 and Pht1;4 play a major role in phosphate acquisition from both low- and high-phosphate environments. *Plant J.* 2004;39:629–42.
2. Ai P, Sun S, Zhao J, Fan X, Xin W, Guo Q, et al. Two rice phosphate transporters, OsPht1;2 and OsPht1;6, have different functions and kinetic properties in uptake and translocation. *Plant J.* 2009;798–809.
3. Shen J, Yuan L, Zhang J, Li H, Bai Z, Chen X. Phosphorus dynamics: from soil to plant. *Plant Physiol.* 2011;156:997–1005.
4. Vance CP, Vance CP, Uhde-Stone C, Allan DL. Phosphorus acquisition and use: critical adaptations by plants for securing a nonrenewable resource. *New Phytol.* 2003;423–47.
5. Cordell D, Drangert J, White S. The story of phosphorus: global food security and food for thought. *Global Environ. Chang.* 2009;19:292–305.
6. Delavaux CS, Smith-Ramesh LM, Kuebbing SE. Beyond nutrients: a meta-analysis of the diverse effects of arbuscular mycorrhizal fungi on plants and soils. *Ecology* [accepted].
7. Rodríguez H, Fraga R. Phosphate solubilizing bacteria and their role in plant growth promotion. *Biotechnol. Adv.* 1999;17:319–39.
8. Chen YP, Rekha PD, Arun AB, Shen FT, Lai W, Young CC. Phosphate solubilizing bacteria from subtropical soil and their tricalcium phosphate solubilizing abilities. *Appl. Soil Ecol.* 2006;34:33–41.
9. Wani PA, Khan MS, Zaidi A. Synergistic effects of the inoculation with nitrogen-fixing and phosphate-solubilizing rhizobacteria on the performance of field-grown chickpea. *J. Plant Nutr. Soil Sci.* 2007;170:283–7.
10. Chung H, Park M, Madhaiyan M, Seshadri S, Song J, Cho H, et al. Isolation and characterization of phosphate solubilizing bacteria from the rhizosphere of crop plants of Korea. *Soil Biol. Biochem.* 2005;37:1970–4.

Results

11. Kumar V, Behl RK, Narula N. Establishment of phosphate-solubilizing strains of *Azotobacter chroococcum* in the rhizosphere and their effect on wheat cultivars under green house conditions. *Microbiol. Res.* 2001;156:87–93.
12. Zaidi A, Khan M, Ahemad M, Oves M. Plant growth promotion by phosphate solubilizing bacteria. *Acta Microbiol. Immunol. Hung.* 2009;56:263–284.
13. Rashid M, Khalil S, Ayub N, Alam S, Latif F. Organic Acids Production and Phosphate Solubilization by Phosphate Solubilizing Microorganisms (PSM) Under *in vitro* conditions. *Pak. J. Biol. Sci.* 7:187-96.
14. Xie J, Shi H, Du Z, Wang T, Liu X, Chen S. Comparative genomic and functional analysis reveal conservation of plant growth promoting traits in *Paenibacillus polymyxa* and its closely related species. *Nat. Publ. Group.* 2016;6:21329.
15. Beneduzi A, Costa PB, Melo IS, Bodanese-zanettini MH, Passaglia LMP. *Paenibacillus riograndensis* sp . nov ., a nitrogen- fixing species isolated from the rhizosphere of *Triticum aestivum*. *Int. J. Syst. Evol. Microbiol.* 2010;60:128–33.
16. Beneduzi A, Peres D, Costa PB da, Zanettini MHB, Passaglia LMP. Genetic and phenotypic diversity of plant-growth-promoting bacilli isolated from wheat fields in southern Brazil. *Res. Microbiol.* 2008;159:244–50.
17. Fernandes GDC, Trarbach LJ, Campos SBD, Beneduzi A, Passaglia LMP. Alternative nitrogenase and pseudogenes : unique features of the *Paenibacillus riograndensis* nitrogen fixation system. *Res. Microbiol.* 2014;165:571–580.
18. Bach E, Dubal G, Carvalho GD, Brito B, Maria L, Passaglia P. Evaluation of biological control and rhizosphere competence of plant growth promoting bacteria. *Appl. Soil Ecol.* 2016;99:141–149.
19. Brito LF, Bach E, Kalinowski J, Rückert C, Wibberg D, Passaglia LM, et al. Complete genome sequence of *Paenibacillus riograndensis* SBR5, a Gram-positive diazotrophic rhizobacterium. *J. Biotechnol.* 2015;207:30–1.
20. Brito LF, Irla M, Walter T, Wendisch VF. Magnesium aminoclay-based transformation of *Paenibacillus riograndensis* and *Paenibacillus polymyxa* and development of tools for gene expression. *Appl. Microbiol. Biotechnol.* 2017;735–47.
21. Pikovskaya, RI. Mobilization of phosphorus in soil in connection with the vital activity of some microbial species. *Microbiologiya.* 1948;17:362–70.
22. Irla M, Neshat A, Brautaset T, Rückert C, Kalinowski J, Wendisch VF. Transcriptome analysis of thermophilic methylotrophic *Bacillus methanolicus* MGA3 using RNA-sequencing provides detailed insights into its previously uncharted transcriptional landscape. *BMC Genomics.* 2015;1–22.

Results

23. Brito LF, Irla M, Kalinowski J, Wendisch VF. Detailed transcriptome analysis of the plant growth promoting *Paenibacillus riograndensis* SBR5 using RNAseq technology. BMC Genomics [submitted].
24. Mentz A, Neshat A, Pfeifer-sancar K, Pühler A, Rückert C, Kalinowski J. Comprehensive discovery and characterization of small RNAs in *Corynebacterium glutamicum* ATCC 13032. BMC Genomics. 2013;14:714.
25. Bolger AM, Lohse M, Usadel B. Trimmomatic: A flexible trimmer for Illumina sequence data. Bioinformatics. 2014;30:2114–20.
26. Langmead B, Trapnell C, Pop M, Salzberg SL. Ultrafast and memory-efficient alignment of short DNA sequences to the human genome. Genome Biol. 2009;10:R25.
27. Hilker R, Stadermann KB, Doppmeier D, Kalinowski J, Stoye J, Straube J, et al. ReadXplorer - Visualization and analysis of mapped sequences. Bioinformatics. 2014;30:2247–2254.
28. Anders S, Huber W. Differential expression analysis for sequence count data. Genome Biol. 2010;11:R106.
29. Altschup SF, Gish W, Pennsylvania T, Park U. Basic local alignment search tool. J. Mol. Biol. 1990;215:403–10.
30. Sperb ER, Tadra-sfeir MZ, Sperotto RA, Fernandes GDC, Pedrosa FO, de Souza EM, et al. Iron deficiency resistance mechanisms enlightened by gene expression analysis in *Paenibacillus riograndensis* SBR5. Res. Microbiol. 2016;167:501–9.
31. Haimes J, Kelley M. Demonstration of a $\Delta\Delta Cq$ calculation method to compute relative gene expression from qPCR data. GE Healthcare; 2014.
32. Zahoor A, Otten A, Wendisch VF. Metabolic engineering of *Corynebacterium glutamicum* for glycolate production. J. Biotechnol. 2014;192:366–375.
33. Nguyen AQD, Schneider J, Reddy GK, Wendisch VF. Fermentative production of the diamine putrescine: system metabolic engineering of *Corynebacterium glutamicum*. Metabolites. 2015;211–231.
34. Murphy J, Riley J. A single-solution method for the determination of soluble phosphate in sea water. J. Mar. Biol. Assoc. UK. 1958;37:9–14.
35. Marra LM, Oliveira-longatti SMD, Soares CRFS, Lima JMD, Olivares FL, Moreira FMS. Initial pH of medium affects organic acids production but do not affect phosphate solubilization. Braz. J. Microbiol. 2015;375:367–375.
36. Whitelaw MA. Growth promotion of plants inoculated with phosphate-solubilizing fungi. Adv. Agron. 2000;69:99–151.

Results

37. Li Z, Bai T, Dai L, Wang F, Tao J, Meng S. A study of organic acid production in contrasts between two phosphate solubilizing fungi: *Penicillium oxalicum* and *Aspergillus niger*. Nat. Publ. Group. 2016;1–8.
38. Buch A, Archana G, Kumar GN. Metabolic channeling of glucose towards gluconate in phosphate-solubilizing *Pseudomonas aeruginosa* P4 under phosphorus deficiency. Res. Microbiol. 2008;159:635–642.
39. Zeng Q, Wu X, Wang J, Ding X. Phosphate solubilization and gene expression of phosphate-solubilizing bacterium *Burkholderia multivorans* WS-FJ9 under different levels of soluble phosphate. J. Microbiol. Biotechnol. 2017;27:844–855.
40. Mikanová O, Nováková J. Evaluation of the P-solubilizing activity of soil microorganisms and its sensitivity to soluble phosphate. Rost. Vyroba. 2002;48:397–400.
41. Wang Y, Shi Y, Li B, Shan C, Ibrahim M, Jabeen A, et al. Phosphate solubilization of *Paenibacillus polymyxa* and *Paenibacillus macerans* from mycorrhizal and non-mycorrhizal cucumber plants. Afr. J. Microbiol. Res. 2012;6:4567–4573.
42. Hu X, Chen J, Guo J, Hangzhou X. Two phosphate- and potassium-solubilizing bacteria isolated from Tianmu Mountain, Zhejiang, China. Microbiol. Biotechnol. 2006;22:983–90.
43. Bianco C, Defez R. Improvement of phosphate solubilization and *Medicago* plant yield by an indole-3-acetic acid-overproducing strain of *Sinorhizobium meliloti*. Appl. Environ. Microbiol. 2010;76:4626–32.
44. Thomas L, Hodgson DA, Wentzel A, Nieselt K, Ellingsen TE, Moore J, et al. Metabolic switches and adaptations deduced from the proteomes of *Streptomyces coelicolor* wild type and *phoP* mutant grown in batch culture. Mol. Cell. Proteomics. 2012;11:M111.013797.
45. Prágai Z, Allenby NEE, O'Connor N, Dubrac S, Rapoport G, Msadek T, et al. Transcriptional regulation of the *phoPR* operon in *Bacillus subtilis*. J. Bacteriol. 2004;186:1182–90.
46. Prágai Z, Harwood CR. Regulatory interactions between the Pho and α^B -dependent general stress regulons of *Bacillus subtilis*. Microbiol. Read. Engl. 2002;148:1593–602.
47. Shi L, Hulett FM. The cytoplasmic kinase domain of PhoR is sufficient for the low phosphate-inducible expression of Pho regulon genes in *Bacillus subtilis*. Mol. Microbiol. 1999;31:211–222.
48. Guttenplan SB, Kearns DB. Regulation of flagellar motility during biofilm formation. FEMS Microbiol. Rev. 2013;37:849–871.
49. Rashid MH, Kornberg A. Inorganic polyphosphate is needed for swimming, swarming, and twitching motilities of *Pseudomonas aeruginosa*. Proc. Natl. Acad. Sci. USA. 2000;97:4885–90.
50. Schro I, Johnson E, Vries SD. Microbial ferric iron reductases. FEMS Microbiol. Rev. 2003;27:427–47.

Results

51. Sharma SB, Sayyed RZ, Trivedi MH, Gobi TA. Phosphate solubilizing microbes: sustainable approach for managing phosphorus deficiency in agricultural soils. Springerplus. 2013;2:587.
52. Sleator RD, Hill C. Bacterial osmoadaptation: the role of osmolytes in bacterial stress and virulence. FEMS Microbiol. Rev. 2002;26:49–71.
53. Kappes RM, Kempf B. Three transport systems for the osmoprotectant glycine betaine operate in *Bacillus subtilis*: characterization of OpuD. J Bacteriol. 1996;178:5071–79.
54. Vyas P, Gulati A. Organic acid production in vitro and plant growth promotion in maize under controlled environment by phosphate-solubilizing fluorescent *Pseudomonas*. BMC Microbiol. 2009;9:174.
55. Shahid M, Hameed S. Root colonization and growth promotion of sunflower (*Helianthus annuus* L.) by phosphate solubilizing *Enterobacter* sp. Fs-11. World J. Microbiol. Biotechnol. 2012;28:2749–58.
56. Yi Y, Huang W, Ge Y. Exopolysaccharide: A novel important factor in the microbial dissolution of tricalcium phosphate. World J. Microbiol. Biotechnol. 2008;24:1059–65.
57. Mardad I, Serrano A, Soukri A. Solubilization of inorganic phosphate and production of organic acids by bacteria isolated from a Moroccan mineral phosphate deposit. Afr. J. Microbiol. Res. 2013;7:626–635.
58. Bringhurst RM, Gage DJ. Control of inducer accumulation plays a key role in succinate-mediated catabolite repression in *Sinorhizobium meliloti*. J. Bacteriol. 2002;184:5385–92.
59. Divya K, Patel, Prayag Murawala, G. Archana, G. Naresh Kumar. Repression of mineral phosphate solubilizing phenotype in the presence of weak organic acids in plant growth promoting fluorescent *Pseudomonas*. Bioresour. Technol. 2011;102:3055–61.
60. Rajput MS, Iyer B, Pandya M, Jog R. Derepression of mineral phosphate solubilization phenotype by insertional inactivation of *iclR* in *Klebsiella pneumoniae*. PLoS One. 2015;10(9):e0138235.
61. Rajput MS, Naresh Kumar G, Rajkumar S. Repression of oxalic acid-mediated mineral phosphate solubilization in rhizospheric isolates of *Klebsiella pneumoniae* by succinate. Arch. Microbiol. 2013;195:81–8.
62. Turner L, Ryu WS, Berg HC. Real-time imaging of fluorescent flagellar filaments. J. Bacteriol. 2000;182:2793–2801.
63. Guttenplan SB, Shaw S, Kearns DB. The cell biology of peritrichous flagella in *Bacillus subtilis*. Mol. Microbiol. 2013;87:211–229.

3. DISCUSSION

3.1. Basis for the characterization of Paenibacillus riograndensis SBR5: complete genome sequence and genome-wide transcriptome analysis

The main goal of this thesis was to expand the knowledge on the plant growth promoting rhizobacterium (PGPR) *P. riograndensis* SBR5. Before the studies presented in this thesis were started, a draft genome sequence of SBR5 was published [1]. This sequence exhibited the following features: a chromosome of 7,370,000 base pairs (no plasmid was found), with a G+C content of 55.1%, 7,467 detected open reading frames and 16 detected tRNA genes. The draft genome sequence of SBR5 was so far used as a reference to elucidate the transcriptional profile of nitrogen fixation in *P. riograndensis*, revealing that this organism has a unique nitrogen fixation system which allows it to fix nitrogen under molybdenum absence [2]. However, the draft genome sequence of SBR5 was comprised of 2,276 contigs that were not assembled which was a severe hindrance to conducting genome-based studies [1]. Based on that, the genome of *P. riograndensis* SBR5 was sequenced and fully annotated in the present thesis (Chapter 2.1). This resulted in 198 contigs that were assembled into one single contig comprising a circular chromosome of 7,893,056 base pairs. Besides that, the detected G+C content was 50.97%, 6,705 coding sequences (CDS) were identified and 87 tRNA and 27 rRNA genes were found to be organized in 9 putative operons (Chapter 2.1). The major difference between the complete genome sequence described in this thesis and the draft genome sequence previously reported [1] was in size, with a difference of 523,056 base pairs scattered over the whole genome (Chapter 2.1). The collection of information through analysis of bacterial genomes has become essential to systematize the knowledge on PGPR applications [3]. Therefore, the number of genome sequences of PGPR is growing, e. g. genomes of *Burkholderia phytofirmans* [4], *Pseudomonas* sp. [5], *Bacillus* sp. [6] and *Bacillus amyloliquefaciens* [7] were sequenced recently. Sequencing of PGPR genomes is an important approach to gain insight into PGPR physiology. The availability of PGPR genome sequences enabled comparative genomic studies which revealed that the presence of plant growth promotion (PGP)-related genes are features present in different functional groups of bacteria, such as animal pathogens, phytopathogens, saprophytes, endophytes and symbionts, with a number of detected PGP genes increasing along this lineup [8]. Genome-based analysis and its physiological confirmation were performed to demonstrate a high

genetic conservation of PGP features in *Paenibacillus* species, such as indole-3-acetic acid (IAA) production, phosphate solubilization (PS) and metabolism, and nitrogen fixation [9]. The association between genome sequence and physiological properties contributed to the discovery of production of biocontrol-related cyclic lipopeptides in the PGPR *Pseudomonas fluorescens* [10]. Here, besides improving the current genomic information, the complete genome sequence of *P. riograndensis* SBR5 served as basis for the detection of *ara* genes related to its arabinose metabolism and two genes encoding its erythromycin and kanamycin resistances (Chapter 2.1). Moreover, the genome-based evidence for a biotin autotrophy of SBR5 was achieved because homologues to the *bioWAFDBI* operon coding for biotin biosynthesis pathway of *Bacillus subtilis* [11] were not detected in the genome of *P. riograndensis* (Chapter 2.1). To complement the dataset obtained in the complete genome sequence of SBR5, a genome-wide transcriptome analysis (also called transcriptome landscape analysis) was performed in the present thesis, revealing the transcriptomic profile of this organism. In Chapter 2.2, many features of the transcriptome of SBR5 were characterized, such as transcriptional abundances of genes, operon structures, presence of *cis*-regulatory elements, presence of novel transcripts as well as transcription start sites (TSS), promoter motifs and ribosome binding site (RBS) of thousands of annotated genes in the genome of *P. riograndensis* SBR5. This kind of analysis was previously performed for bacteria with industrial relevance, like *Corynebacterium glutamicum* and *Bacillus methanolicus* [12,13] and the use of transcriptome data is highly valuable, for example, in the development of genetic tools for bacteria [14]. Here, the complete genome sequence and transcriptomic landscape analysis of *P. riograndensis* SBR5 were essential groundwork for the development of gene expression tools, vitamin-related physiological analysis and differential gene expression analysis of PS in this organism.

3.2. Transformation method and the use of genomic data to develop genetic tools for P. riograndensis SBR5

The first step in the development of molecular biology tools for microorganisms is establishment of method for vector transformation into bacterial cell. The most common transformation methods are based on several physical or biological processes such as heat shock, electroporation, use of protoplasts or conjugation [15,16]. However, those examples do not exhaust all possibilities. One of the alternatives is for example Yoshida effect. It occurs when a

Discussion

colloidal solution consisting of nano-sized needle-shaped material and bacterial cells is contacted by sliding friction, this complex grows larger and penetrates bacterial cells due to the driving force derived from the sliding friction [17]. This effect is named after its author and is the base of the bacterial transformation method applied on *Paenibacillus* in the present thesis. The Yoshida effect has been applied for the transformation of *Escherichia coli* DH5 α before [18]. However, the referred transformation effect employs the use of chrysotile asbestos fibers, which have carcinogenic properties [19]. For this reason, the use of aminoclays appears as an alternative. The aminoclays were synthesized for the first time in 1997 [20] and consist of aminopropyl-functionalized magnesium phyllosilicates that can be used to construct composites with biomolecules such as DNA [21], which makes them applicable for transformation based on the Yoshida effect. Aminoclays are considered non-toxic; they are used in medicine because they are capable of interacting with negatively charged drug molecules to produce a drug-clay complex that improves the absorption of poorly absorbable drugs after oral administration [22]. Besides being a non-toxic material, the aminoclay protects DNA biomolecules from digestion by nucleases and acts not only as a vehicle for plasmid DNA penetration into the cells but also as a shield for the plasmid DNA against various biological or physical-chemical stresses, such as enzymatic cleavage [23–25]. The transformation method mediated by aminoclay was first applied in bacteria by Choi et al. [26] in *E. coli* and *Streptococcus mutans*, when the aminoclay wrapping of the DNA molecule was shown to be more efficient than that of the Yoshida effect [26]. Moreover, the use of aminoclays enabled a nuclear transformation of DNA into the eukaryotic microalgae *Chlamydomonas reinhardtii* [27]. In Chapter 2.3, this recently developed transformation method was established for *P. riograndensis* SBR5. Strain SBR5 is a recalcitrant organism, and was previously transformed by the means of electroporation resulting in approximately 10^4 transformants μg^{-1} of plasmid DNA [28]. However, although lesser transformation efficiency was obtained in the present study (10^3 transformants μg^{-1} of plasmid DNA), the aminoclay-mediated method is less laborious and less expensive in comparison to the electroporation [26]. Moreover, the aminoclay-mediated bacterial transformation method established here for *P. riograndensis* enabled the further development of gene expression tools for this organism. Finally, this method was also established in other *Paenibacillus* species (*Paenibacillus polymyxa* DSM-365), yielding 10^2 transformants μg^{-1} of plasmid DNA (Chapter 2.3).

Discussion

Until now, no expression system was available for *P. riograndensis* SBR5. Nevertheless, once *P. riograndensis* SBR5 was transformable, the tools for gene expression could be developed. A set of plasmid vectors for other bacilli strains was previously established, one rolling circle replicating and one theta replicating plasmid, pRE and pTE, respectively [14,29]. As described in Chapter 2.3, the complete genome sequence of SBR5 was used to identify sequences of three constitutive promoter sequences, which were cloned into the rolling circle replicating plasmid pRE. These promoters belong to the genes *gapA*, *pyk*, and *tuf1*, coding for glyceraldehyde-3-phosphate dehydrogenase, pyruvate kinase, and elongation factor Tu, respectively. Furthermore, two inducible systems were developed for *P. riograndensis* SBR5 in the present thesis. The first one utilized a theta replicating plasmid pTE harboring a xylose inducible promoter of a *xylA* gene and a *xylR* regulator, both derived from *Bacillus megaterium* [30]. The use of this xylose inducible promoter is well established, being functional in *Staphylococcus aureus* [31] and in different bacilli: *B. megaterium* [30], *B. subtilis* [32], *Brevibacillus choshinensis* [33], and *B. methanolicus* [12]. The second inducible system utilized the pRE plasmid to carry a mannitol inducible promoter. BLAST analysis [34] on the complete genome sequence of SBR5 led to the identification a promoter of the mannitol PTS system *mtlA* gene (*P.riograndensis_final_1805*). However, the best mannitol promoter utilized in this thesis originated from the methylotrophic bacterium *B. methanolicus* and belongs to a *mtlR* gene that encodes the transcriptional regulator MtlR [35,36]. The transcriptional regulator *mtlR* gene transcripts are more abundant during growth of *B. methanolicus* on mannitol in comparison to growth on its commonly used carbon source, methanol [35,37]. This mannitol inducible rolling circle replicating plasmid was previously developed based on the information available on the transcriptomic landscape of *B. methanolicus*, which was used for identification of its TSS and -10 and -35 hexamers location [12,36].

Altogether, a theta replicating xylose inducible system and a rolling circle replicating mannitol inducible system were used to control the expression of *crimson* and *gfpUV* reporter genes, respectively, in *P. riograndensis* SBR5, resulting in the first dual inducible vector system for this organism (Chapter 2.3). Irla et al. [14] used transcriptome landscape analysis of *B. methanolicus* [12] to develop a mannitol (*mtlR*) inducible gene expression system, and that system could be transferred to *P. riograndensis* SBR5 in this thesis (Chapter 2.3). Similarly, the transcriptome landscape analysis presented in Chapter 2.2 can also be utilized to further identify more inducible systems and to develop expression tools for other bacteria. Despite the fact that

Discussion

the use of *gapA*, *pyk*, and *tuf1* constitutive promoters identified in this thesis led to the increase in the expression of *gfpUV* reporter gene in SBR5 (in comparison to promoterless control), the selection of those promoters was based on their strength in *C. glutamicum* [38] and their -10 and -35 hexamers were predicted with the Bacterial Promoter Prediction (BPROM) tool on the SoftBerry platform [39] (Chapter 2.3). The the data on highly expressed genes generated in the transcriptome landscape analysis show that transcripts of *tuf1*, *gapA* and *pyk*, have abundancies of 3,154, 1,106 and 484, respectively, which places them as 78th, 256th, 575th most abundant transcripts of *P. riograndensis* SBR5 (Chapter 2.2). Hence, it would be interesting to test putative strong constitutive promoters predicted on the basis of the transcriptome landscape data. For instance, the gene *P.riograndensis_final_1999* coding for PTS maltose transporter subunit IIBC is an interesting target for further investigation, because it was among the most abundantly transcribed genes under the growth conditions used in Chapter 2.2. Since a database of gene transcriptional abundancies of SBR5 is available (NCBI Gene Expression Omnibus, accession GSE98766) and TSS belonging to more than one thousand annotated genes of SBR5 were identified in the present thesis, this knowledge can be used to identify more constitutive promoters, not only for *P. riograndensis* SBR5, but for other PGPR species. Similar approach was used before for example by Luo et al. [40] where the analysis of the expression levels of almost 6,000 genes of *Streptomyces albus* in different growth conditions and at different time points allowed the identification of 32 genes with most abundant transcripts. The characterization of their promoters showed that their strengths ranged from 200 to 1300% of the before commonly used promoter of the erythromycin resistance gene *ermE* [40]. Similarly, this approach was applied for *B. amyloliquefaciens* [41], *Bacillus thuringiensis* [42] and *Lactococcus lactis* [43].

Furthermore, regulatory elements other than promoters can be predicted based on the transcriptomic data obtained in the scope of this thesis (Chapter 2.2). The promoter of the gene *pyk* was used to characterize a thiamine pyrophosphate (TPP) riboswitch functionality in strain SBR5. In this case, the detection of the native TSS of the *pyk* gene based on the transcriptomic data allowed the exchange the native 5' untranslated region (5' UTR) of the respective promoter by the 5' UTR containing the TPP riboswitch (see below 3.3.2). Furthermore, the prediction of the putative TPP riboswitch in the genome of *P. riograndensis* SBR5 was based on the presence of a 5'UTR of the gene *thiC* (*P.riograndensis_final_150*) which is 240 base pairs longer than a mean 5'UTR in the transcriptome of *P. riograndensis* SBR5. The identification and confirmation of biological activity of TPP riboswitch represents not only a value for understanding basic

physiology of *P. riograndensis* but can be used in the future for construction of advanced regulatory tools useful e. g. as regulatory circuits [44].

Gene knockout methodology has been developed for *Paenibacillus* species [45]. In the characterization of a given gene, the most straightforward approach is to create a knockout strain and to characterize the phenotype of the mutant; e. g. gene deletion was used to characterize the *nif* cluster in *Paenibacillus* sp [46] and also an antagonistic activity against *Fusarium graminearum* in *P. polymyxa* [47]. However, one important limitation of the characterization of *P. riograndensis* SBR5 is the lack of a method to perform modifications in its chromosome. In *P. polymyxa*, homologous recombination was used for gene deletion [45]. This strategy is based on the replacement of a chromosomal sequence with selectable antibiotic resistance gene that is flanked with suitable homology regions to the genome. This is accomplished by Red-mediated recombination in these homology regions [48]. Moreover, gene knockout mutants of *Paenibacillus alvei* were constructed by retrotransposition utilizing the commercially available bacterial mobile group II intron L1.LtrB of *Lactococcus lactis* [49]. Another interesting approach, never performed in *Paenibacillus* species so far, is the gene knockout or knockdown mediated by CRISPR-Cas9 or CRISPRi-dCas9 systems, respectively [50–52]. The progress in development of different genome modification strategies in *Paenibacillus* species indicates that soon one of the newly created methods could be successfully applied for SBR5. This is possible because all the genome modification strategies mentioned above are enabled by the development of the gene expression toolbox as well as the availability of the complete genome sequence and genome-wide transcriptome obtained in the present thesis. It is noteworthy that the dual inducible system developed for *P. riograndensis* SBR5 could be transferred to *P. polymyxa* DSM-365 (Chapter 2.3). Hence, the gene expression toolbox developed in the present thesis opens doors for the development of genome modification also for other members of *Paenibacillus*.

3.3 Application of the omics and gene expression toolbox in P. riograndensis SBR5: analysis of two B-group vitamins

Water-soluble B-group vitamins are among many types of molecules that facilitate interactions of PGPR with plants. They can act synergistically with other biologically active substances in the stimulation of growth of plants and soil microorganisms [53,54]. Bacterial vitamin production can be one of several factors affecting microbial competition for root

Discussion

colonization [55], contributing also to rhizobial plant colonization [56]. The B-group of vitamins consists of thiamine, riboflavin, niacin, pantothenic acid, pyridoxine, biotin, folic acid and cobalamin, and the production of B-group vitamins has been observed in the plant beneficial *P. fluorescens* [56], *Azospirillum* spp. [57] and mycorrhizal fungi [58]. Revillas et al. [59] proposed that, because exogenous applications of B-group vitamins affects plant cellular functions, the production of these vitamins by PGPR, such as *Azotobacter* spp., is a mechanism that explains positive effects of these bacteria on plants and their interactions with other microorganisms in the rhizosphere. PGP was also related to secretion of B-group vitamins by *P. fluorescens* [60]. In Chapter 3.1 the importance of genome-based findings for the analysis of PGPR are pointed out. However, many of these predictions are not tested so far and the association between genome sequence and biological function of the predicted metabolite is lacking. Hence, the database generated in this thesis and gene expression tools for *P. riograndensis* SBR5 were used to characterize the features related to two members of the B-group of vitamins in SBR5: biotin (B₇) and thiamine (B₁).

3.3.1 Characterization of biotin auxotrophy in *P. riograndensis* SBR5

Biotin plays a major role in plant and bacterial survival. For some bacteria, which belong to the PGPR group, the biotin production can be observed and is seen as a factor in the stimulation of plant growth and rhizosphere microbiota improvement, e. g. for *P. fluorescens*, *Azospirillum* spp. and *Azospirillum brasilense* [56,57,61]. Biotin biosynthesis genes have been detected in various bacterial species. For instance, in *Lysinibacillus sphaericus*, *bio* genes are organized in two operons *bioDAYB* and *bioXWF* located at different positions in the chromosome [62]. Nevertheless, the most known models of this process were described for *E. coli* and *B. subtilis* [63] and a general biotin biosynthesis pathway for these organisms is presented in Chapter 1.

Incomplete biotin pathways occur in soil bacteria. In the symbiotic nitrogen fixing *Sinorhizobium meliloti*, several of the key biotin synthesis genes are either missing or only function at very low rates. The *bio* genes are found at two different locations of its chromosome. The gene *bioF* is transcribed separately and the *bioB* gene is co-transcribed with two genes linked to biotin recycling or transport [64]. Although a *bioH* gene is probably present in the genome of this microbe, no genetic locus has been assigned to it yet [64]. In the Gram-positive bacterium

Discussion

C. glutamicum, three functional *bio* genes (*bioAD*, *bioB*) are found in two regions within the chromosome, but no functional *bioC*, *bioH* or *bioF* homologues have been reported [65–67]. Here, the complete genome sequence of *P. riograndensis* SBR5 revealed the absence of most genes belonging to the biotin biosynthesis pathway. Only a gene with sequence 34% identical to the *bioI* gene of *B. subtilis*, which codes for the cytochrome P450 (P.riograndensis_final_5347) was found in the genome of SBR5 (Chapter 2.1). The transcriptome data analysis of *P. riograndensis* SBR5 shows that this homologue may be not active because it was transcribed at relatively low level. The transcriptional abundance of P.riograndensis_final_5347 (measured in Reads Per Kilobase per Million mapped reads- RPKM value) was 86.96, which means that it is part of the transcripts considered to belong to low transcribed genes (Chapter 2.2). Moreover, the growth of *P. riograndensis* SBR5 is enabled by the addition of biotin to the minimal medium, but inhibited when biotin is not present (Chapter 2.3), similarly to what was observed for *S. meliloti* [68] and *C. glutamicum* [67]. Those findings indicate that SBR5 is, like the above mentioned organisms, a biotin auxotrophic bacterium. It can be expected that, in natural environments, biotin is not freely available and the possession of biotin biosynthesis genes might be a selective advantage [69]. However, the loss of the biotin biosynthesis ability by bacteria inhabiting the rhizospheric portion of soil might occur due to the provision of biotin from the plant root exudation [70,71]. The presence of biotin among other vitamins in root exudates has been detected by both an indirect method (i.e. by measuring the growth of auxotrophic bacteria) [68] or by direct analysis of rooting media under sterile conditions [53,72]. The release of vitamins (including biotin) by plant roots promotes the growth of rhizosphere bacteria [55,70,72].

Furthermore, the biotin biosynthesis genes of *C. glutamicum* were analyzed by complementation studies, the heterologous expression of *bioF* from *E. coli* enabled the production of biotin from pimelic acid and the expression of the whole operon *bioWAFDBI* from *B. subtilis* rendered a biotin prototrophy in *C. glutamicum* [67]. To overcome the biotin auxotrophy limitation in plant colonization, the *S. meliloti* strains were constructed by conjugating the *E. coli* biotin synthesis genes into the genome of this symbiotic nitrogen fixing bacterium, which led to establishment of biotin production in that strain [68]. The complementation analysis of the biotin synthesis genes, as in the above mentioned bacteria, was also performed for *P. riograndensis* SBR5 in the present thesis to confirm its biotin auxotrophy. The heterologous expression of biotin synthesis genes in SBR5 was enabled by the gene expression tools developed in this thesis. A rolling-circle plasmid was used to express the

Discussion

bioWAFDBI operon from *B. subtilis*, driven by the mannitol inducible promoter from *B. methanolicus*, in order to enable the growth of a recombinant *P. riograndensis* in minimal medium without biotin supplementation (Chapter 2.3). The complete genome sequence and the heterologous expression of *bioWAFDBI* operon in *P. riograndensis* SBR5 were used to establish a biotin prototrophic *P. riograndensis* strain (Chapter 2.3). This way a novel gene expression tool was tested for expression of a relevant pathway in the PGPR *P. riograndensis*, which shows the usability of molecular biology tools for physiological studies. Furthermore, new insight into the physiology of *P. riograndensis* regarding its biotin metabolism was gained, and confirmed by both genomic analysis and functional studies.

3.3.2. A functional thiamine pyrophosphate riboswitch present in *P. riograndensis* SBR5

Riboswitches are RNA elements which are mostly present in the 5' UTR of bacterial mRNA that sense and bind to a specific small metabolites. Upon metabolite binding to a specific mRNA structure, the aptamer, substantial structural changes occur and result in an “on”- or “off”-switch of the gene expression. These regulatory elements are some of the means of controlling cellular processes in response to environmental conditions [73]. In biotechnology, *thiamine pyrophosphate* (TPP) riboswitches are interesting and attractive target structures for developing antibacterial compounds. They form the most extensive riboswitch class with representatives found in bacteria, fungi and plants [74–76]. In Chapter 2.2 *cis*-regulatory elements, found in the transcriptome of *P. riograndensis* are described. These RNA aptamers can be used in synthetic biology to control gene expression and are an interesting target for development of genetic tools [77]. Therefore, the existence of an available database of *cis*-regulatory elements found in the transcriptome of *P. riograndensis* SBR5 is important for further gene expression studies. A TPP riboswitch of SBR5 was detected and characterized (Chapter 2.2). This riboswitch belongs to the 5' UTR of the *thiC* gene that encodes a putative phosphomethylpyrimidine synthase (*P.riograndensis*_final_150) with identities up to 70% to the respective *E. coli* enzyme. The exact function of ThiC in SBR5 is still to be investigated, but the *E. coli* enzyme participates in thiamine synthesis by converting aminoimidazole ribotide to hydroxymethylpyrimidine phosphate, which is subsequently phosphorylated by the bifunctional hydroxymethylpyrimidine phosphate kinase ThiD to yield hydroxymethyl-pyrimidine pyrophosphate [78]. When cloned into the plasmid pPyk-*gfpUV* (Chapter 2.3) as a replacement of the 5' UTR of *pyk* promoter, the

Discussion

putative TPP riboswitch caused an off-switch of *gfpUV* expression when thiamine was added in the culture medium, showing that this riboswitch is indeed functional in this organism (Chapter 2.2). This finding can be used to develop one more gene expression control mean for *P. riograndensis* SBR5.

Thiamine is indispensable for the activity of the carbohydrate and branched-chain amino acid metabolic enzymes [79]. TPP is the active form of this vitamin and functions as a co-factor of a number of important enzymes in carbohydrate and amino acid metabolism [80]. The production of thiamine is observed in several groups of PGPR, including *Azotobacter*, *Pseudomonas* and *Azospirillum* [81] and its importance in PGPR is described in Chapter 3.3. Thiamine acts as cofactor of 2-oxoglutarate dehydrogenase (2-OGDH) in the tricarboxylic acid (TCA) cycle [79]. The differential gene expression analysis showed that the gene encoding (2-OGDH) was upregulated in *P. riograndensis* SBR5 at sufficient phosphate supplementation in PbS medium (Chapter 2.4). In the same condition, the gene *P.riograndensis_final_2303* coding for the ThiH protein was upregulated as well (Table 1); in *E. coli*, it is part of the thiamine synthesis chain of reactions in which hydroxyethyl-thiazole phosphate is formed [78] (Chapter 1: Figure 6). These findings suggest that thiamine might be important in the phosphate metabolism of *P. riograndensis* SBR5. Moreover, although the production of thiamine by SBR5 was not measured, the analyzed data on the transcript abundance revealed a RPKM value of 1,961 for the transcripts of the *thiC* gene, which is associated with high expression (Table 1); only 216 genes in the genome of SBR5 were part of this group (Chapter 2.2), showing one more time the importance of thiamine in the metabolism of SBR5. Although only *thiH* gene was differentially expressed in PbI condition (Chapter 2.4), genes putatively involved in thiamine biosynthesis by *P. riograndensis* SBR5 are present in its genome sequence and also were transcribed in both landscape and differential transcriptome analysis (Table 1). In Chapter 1, thiamine biosynthesis in *E.coli* is described. Some thiamine biosynthesis genes in *E. coli* are comprised in the operons *thiCEFSGH* and *thiMD*, and the genes *thiL* and *thiI* are transcribed monocistronically [82]. Homologues of the genes belonging to the *E. coli* operon *thiMD*, involved in thiamine salvage [83], were also co-transcribed in SBR5 (Chapter 2.2: Additional file 8). However, the rest of the transcribed thiamine-related genes detected here are not part of operon structures, those are homologues of the *E. coli* genes *thiC*, *thiD*, *thiG*, *thiH* and *thiL* (*P.riograndensis_final_3765*) (Table 1). Moreover, the gene *iscS* that may play a role in the sulfur transfer chemistry in thiamine and 4-thiouridine biosynthetic pathways [84] is also transcribed by SBR5 (Table 1). The

Discussion

genes *thiF* and *thiS* that participate in the formation of the TPP precursor hydroxyethyl-thiazole phosphate in *E. coli* [78] have no detected homologues in SBR5 genome. The description of the genes possibly involved in thiamine biosynthesis in SBR5 is lacking. However, first steps in this direction have been made in this thesis.

Table 1. Gene transcription abundancies (RPKM) of genes probably involved in thiamine biosynthesis by SBR5 in the cultivation conditions of the transcriptome landscape analysis (TLA; Chapter 2.2), PbI or PbS conditions (Chapter 2.4). Transcript abundance is considered low for transcripts with RPKM values < 100, intermediate with RPKM between 100 and 1,000 and high for transcripts with RPKM between 1,000 and 10,000.

Locus	Gene ID	Product	RPKM		
			TLA	PbI	PbS
P.riograndensis_final_150	<i>thiC</i>	Phosphomethyl-pyrimidine synthase	1961	54	289
P.riograndensis_final_2302	<i>thiG</i>	Thiazole synthase	162	26	226
P.riograndensis_final_2303*	<i>thiH</i>	Thiazole biosynthesis protein ThiH	151	23	225
P.riograndensis_final_2996	<i>thiE</i>	Thiamine-phosphate synthase	75	10	68
P.riograndensis_final_2997	<i>thiD</i>	Hydroxymethyl-pyrimidine kinase	101	14	107
P.riograndensis_final_2998	<i>thiM</i>	Hydroxyethyl-thiazole kinase	110	13	67
P.riograndensis_final_3765	-	Thiamine pyrophosphokinase	782	43	70
P.riograndensis_final_5101	<i>thiI</i>	Probable sulfurtransferase	55	66	53
P.riograndensis_final_5210	<i>iscS</i>	Cysteine desulfurase	58	71	99

Gene significantly upregulated* in PsI condition accordingly to DESeq analysis (Chapter 2.4).

Contrary to the biotin biosynthesis pathway, the characterization of thiamine production in SBR5 is not complete. However, the availability of novel gene expression tools described in Chapter cc will facilitate the elucidation of this pathway in the future. Understanding of the vitamin biosynthesis pathways and their regulation in PGPR is extremely important because it can help to evaluate the usability of potential PGP species. The characterization of biotin auxotrophy and regulation of thiamine biosynthesis performed for *P. riograndensis* will be of a high value once other PGPR are characterized.

3.4. First insights on the phosphate solubilization process in *P. riograndensis* SBR5

The importance of P in agriculture, its environmental impact and the contribution of PSB to the development of sustainable agriculture were described in Chapter 1. Taking this into consideration, the PS activity by *P. riograndensis* SBR5 is a crucial PGP feature to be studied.

Discussion

However, prior to this thesis, no scientific effort to characterize this process in SBR5 was done. Here, it was shown that *P. riograndensis* SBR5 is part of a group of bacteria capable of solubilizing phosphates. *Paenibacillus* members that present PS activity has been isolated from the rhizosphere of a variety of crops [85–87]. In some *Paenibacillus* species like *Paenibacillus mucilaginosus* [86], *Paenibacillus elgii* [88], *Paenibacillus kribbensis* [89], *P. polymyxa*, *Paenibacillus macerans* [90] and *Paenibacillus xylanilyticus* [91], the PS ability has been confirmed. The PS activity of *P. macerans* and *P. polymyxa* led to liberation of approximately 80 $\mu\text{g mL}^{-1}$ of solubilized phosphate after 3 days of incubation in liquid medium from $\text{Ca}_3(\text{PO}_4)_2$ and CaHPO_4 , respectively, where those insoluble phosphates were a sole phosphorus (P) sources [90]. Moreover, *P. mucilaginosus* was able to liberate 130 $\mu\text{g mL}^{-1}$ of solubilized P from phosphorite rocks as sole P source after 5 days of incubation in liquid medium [86]. *P. riograndensis* SBR5 was shown to perform PS in the present study, when it was able to solubilize approximately 300 $\mu\text{g mL}^{-1}$ of phosphate from hydroxyapatite in liquid medium after 20 hours of incubation (Chapter 2.4).

In the past decades, enzymatic processes have been characterized to be responsible for PS in bacteria. PS promoted by acid phosphatase was observed in *Pseudomonas* sp. [92], *Burkholderia cepacia* [93], *Enterobacter aerogenes*, *Enterobacter cloacae*, *Citrobacter freundii*, *Proteus mirabilis* and *Serratia marcescens* [94]. Moreover, phytase activity was observed in *Pseudomonas putida* and *Pseudomonas mendocina* [95] and phosphonate activity was detected in *Klebsiella aerogenes* [96] and *P. fluorescens* [97]. However, although *P. riograndensis* SBR5 possesses some of those PS-related enzymes an upregulation of none of their coding gene transcripts was observed in the differential gene expression analysis under PS conditions (Chapter 2.4). However, the complete genome sequence of SBR5 allowed the detection of some candidate genes coding for enzymes that promote PS and enzymes related to P metabolism, e. g. an alkaline phosphatase (*P.riograndensis_final_731*). The Pst phosphate-specific transport system is a major phosphate transport system characterized in *B. subtilis*. The *pst* operon of *B. subtilis* is composed of *pstS*, *pstC*, *pstA*, *pstB1* and *pstB2*. PstS is a binding protein, PstC and PstA are two integral inner membrane proteins and PstB1 and PstB2 are ATP binding proteins [98,99]. Those genes were found in the genome of *P. riograndensis* SBR5 (*P.riograndensis_final_3645-3648*), and were expressed in both landscape and differential gene expression analysis, but at low levels (Table 2). Moreover, PhoP-PhoR is a two-component signal-transduction system that directly regulates the *pho* regulon-related alkaline phosphatase genes (Shi and Hulett, 1999). The

Discussion

complete genome sequence of *P. riograndensis* SBR5 revealed the presence of genes coding for PhoP-PhoR system (P.riograndensis_final_2307-2308), but as in *pst* genes, their transcription abundancies in the transcriptome landscape analysis was low (Table 2). The genes for phosphonate uptake and degradation in *E. coli* were shown to be organized in an operon of seventeen genes named, in alphabetical order, *phnA* to *phnQ* [100]. Out of those genes, only the alkalylphosphonate utilization protein-coding gene *phnA* (P.riograndensis_final_6464) was found in the genome sequence of SBR5, showing that this organism may be not able to metabolize phosphonates. Moreover, no phytase coding gene was found in the genome of SBR5. Hence, *P. riograndensis* SBR5 may utilize other mechanism to solubilize phosphate in organic soils.

Furthermore, the documented PS by PGPR has been frequently related to the releasing of organic acids. The production of organic acids by PSB has been well documented and is regarded a major mechanism utilized by bacteria to solubilize phosphates. Various studies have identified production of organic acids such as: malate and gluconate by *Enterobacter* sp. [101]; gluconate, succinate, citrate and malate by *Pseudomonas poae* [102]; and citrate, lactate and propionate by *B. megaterium* [103] in presence of insoluble phosphate. Here, *P. riograndensis* SBR5 presents PS activity when cultivated in PbI (insoluble hydroxyapatite as sole P source), and increase two and three times of the production of gluconate and acetate, respectively, in this condition compared to PbS (Chapter 2.4, Figure 4). The gene encoding the enzyme glucose dehydrogenase is present in the genome of *P. riograndensis* SBR5 (P.riograndensis_final_6601). Glucose dehydrogenase oxidizes glucose to convert it to gluconate [104]. There is a high conservation of this gene in *Paenibacillus* species [9]. Although gluconate was highly produced in PbI condition, P.riograndensis_final_6601 was lowly transcribed in both landscape and differential transcriptome analysis (Table 2). Phosphotransacetylase and acetate kinase are enzymes involved in the reversible interconversion of acetyl-CoA to acetate (Chapter dd: Figure 5; [105]). The genes P.riograndensis_final_3937 and P.riograndensis_final_4369 (coding for phosphotransacetylase and acetate, respectively) were not differentially expressed, but their transcription abundancies were intermediate to high (Table 2). In *S. meliloti*, the genes encoding phosphotransacetylase and acetate kinase are induced by phosphate deficiency and are controlled by the *pho* regulon (Summers et al. 1999). Moreover, 2-OGDH genes (*odhAB*) were downregulated in PbI condition while genes coding for carbohydrate-binding proteins (P.riograndensis_final_346, P.riograndensis_final_635, P.riograndensis_final_4161) were upregulated, reinforcing the statement that bacteria change their metabolic channeling of glucose

Discussion

to perform PS [106]. In the case of *P. riograndensis* SBR5, it is suggested that the metabolic flux towards the TCA cycle is reduced in PbI condition (Chapter 2.4, Figures 4 and 5).

An operon comprising motility-related genes was downregulated under PS conditions (PbI; *P.riograndensis_final_6162-6164*) similarly to *Burkholderia multivorans* [106], and the loss of motility could be confirmed *in vivo* (Chapter 2.4). This can be due to the fact that P is not readily available for utilization by SBR5 in the first hours of growth (Chapter 2.4) and this element is essential in bacterial motility. Inorganic phosphate is part of the nucleoside adenosine triphosphate (ATP) which is referred to the chemical energy transfer highly demanded in motility factors [107]. For instance, the energetic cost of flagellar synthesis is particularly high in *B. subtilis* [108]. In *P. riograndensis* SBR5, the gene *P.riograndensis_final_6164* code for a flagellin protein, which in *B. subtilis* is the protein monomer composing the flagellar filament [109]. The assembly of the flagellum is an energy-expensive process primarily because of the estimated thousands of flagellin subunits that are required to assemble a single filament [110]. To support the high structural demand, flagellin genes were expressed from strong promoters and flagellin proteins are translated from near-consensus RBS [111,112], which is confirmed in SBR5, where the RBS sequence 5'GGGAGG assigned to *P.riograndensis_final_6164* is similar to the consensus RBS sequence 5'aGGaGg (Chapter 2.2). Lastly, the function of a gene *P.riograndensis_final_5412* which was upregulated under PbI condition still needs to be investigated, this phosphate-binding protein coding gene was upregulated in PbI condition, but not expressed in the transcriptome landscape analysis (Table 2).

Table 2. Gene transcription abundancies (RPKM) of genes probably related to PS process in SBR5 in the cultivation conditions of the transcriptome landscape analysis (TLA; Chapter 2.2), PbI or PbS conditions (Chapter 2.4). Transcript abundance is considered low for transcripts with RPKM values < 100, intermediate with RPKM between 100 and 1,000 and high for transcripts with RPKM between 1,000 and 10,000.

Locus	Gene ID	Product	RPKM		
			TLA	PbI	PbS
<i>P.riograndensis_final_2307</i>	<i>phoR</i>	Signal transduction histidine kinase	25	25	23
<i>P.riograndensis_final_2308</i>	<i>phoP</i>	Alkaline phosphatase synthesis transcriptional regulatory protein PhoP	42	87	74
<i>P.riograndensis_final_3645</i>	<i>pstB2</i>	Phosphate import ATP-binding protein PstB 2	2	17	6
<i>P.riograndensis_final_3646</i>	<i>yqgI</i>	Probable ABC transporter permease protein YqgI	7	8	3
<i>P.riograndensis_final_3647</i>	<i>yqgH</i>	Probable ABC transporter permease protein YqgH	2	11	1
<i>P.riograndensis_final_3648</i>	<i>pstS</i>	Phosphate-binding protein PstS	13	53	8
<i>P.riograndensis_final_3937</i>	-	<i>Putative phosphotransacetylase</i>	429	959	1,242
<i>P.riograndensis_final_4369</i>	<i>ackA</i>	Acetate kinase	536	324	407

Discussion

P.riograndensis_final_6464	-	Alkylphosphonate utilization operon protein PhnA	407	7	58
P.riograndensis_final_6601	-	<i>Glucose dehydrogenase</i>	14	16	22
P.riograndensis_final_731	-	Alkaline phosphatase-like protein	16	75	52
P.riograndensis_final_635*	-	<i>Carbohydrate/starch-binding protein</i>	41	235	32
P.riograndensis_final_346*		<i>Carbohydrate Binding protein</i>	11	13	1
P.riograndensis_final_4161*	-	<i>Carbohydrate/starch-binding protein</i>	1,075	11,718	539
P.riograndensis_final_6162 [†]	-	Flagellar capping protein	28	6	111
P.riograndensis_final_6163 [†]	-	<i>FlaG protein</i>	50	1	83
P.riograndensis_final_6164 [†]	-	Flagellin	99	147	2,725
P.riograndensis_final_5412*	-	Phosphate binding protein	0	32	1
P.riograndensis_final_476 [†]	<i>odhA</i>	2-Oxoglutarate dehydrogenase E1 component	245	199	1,377
P.riograndensis_final_475 [†]	<i>odhB</i>	Dihydrolypoyllysine-residue succinyltransferase component of 2-oxoglutarate dehydrogenase complex	158	247	1,766

Genes significantly upregulated* or downregulated[†] in P*s*I condition accordingly to DESeq analysis (Chapter 2.4).

Altogether, the results in Chapter dd indicate that *P. riograndensis* SBR5 is indeed a promising PSB candidate among *Paenibacillus* species. However, the full PS performance by SBR5 should be tested in terms of P contribution to plants, in either greenhouse or field conditions. However, the genetic and physiological basis of the PS process in SBR5 should be further investigated. The results obtained in this research are preliminary but important first step on the full exploration of the PS potential of SBR5. The extensive material on genome and genome-wide transcriptome data, tools for inducible gene expression and data on gene expression under PS conditions established here enables future work on *P. riograndensis* SBR5 characterization not only concerning PS, but also to other important aspects of plant growth promotion.

3.5. Final Remarks

P. riograndensis SBR5 is a facultatively aerobic and endospore forming bacterium which exhibits plant growth promoting characteristics [2,113,114]. Here, the complete genome sequence and a genome-wide transcriptome analysis of this organism were presented for the first time. The database generated in the present thesis was valuable for the development of gene expression tools for *P. riograndensis* SBR5 and *P. polymyxa* DSM-365. The genetic toolbox developed in the present thesis was used to characterize the functionality of the TPP riboswitch of *P. riograndensis* SBR5 and to establish a biotin prototrophic strain. The presence of cis-regulatory elements predicted in the genome SBR5 on the basis of the available databases was

confirmed by the transcriptional analysis. This finding is the first step in the investigation on regulatory elements in this organism.

My thesis leaves a solid background for future exploration of agriculturally relevant features of *P. riograndensis* SBR5 and other *Paenibacillus* species. The two plasmid inducible system opens doors for the development of a knockout/knockdown system that greatly facilitates the characterization studies. For example, the CRISPRi-dCas9 system developed by Cleto et al. [51] requires the use of two plasmids [51].

The effort done in the present thesis serves as groundwork for the characterization of plant growth promoting features of *P. riograndensis*. However, a further investigation is necessary. The PS process for instance still needs to be studied in depth; my findings showed that SBR5 possibly changes its metabolic channeling of glucose to perform PS. Finally, thanks to the progress in the study of plant growth promoting features and PS activity of SBR5, characterization of the genome and transcriptome, and development of gene expression tools, it is reinforced that SBR5 is a promising candidate as a crop inoculant.

3.6. References

1. Beneduzi A, Campos S, Ambrosini A, de Souza R, Granada C, Costa P, et al. Genome Sequence of the Diazotrophic Gram-Positive Rhizobacterium *Paenibacillus riograndensis* SBR5^T. *J Bacteriol.* 2011;193:6391–2.
2. Fernandes GDC, Trarbach LJ, Campos SB De, Beneduzi A, Passaglia LMP. Alternative nitrogenase and pseudogenes: unique features of the *Paenibacillus riograndensis* nitrogen fixation system. *Res Microbiol.* 2014;165:571–80.
3. Timmusk S, Behers L, Muthoni J, Muraya A, Aronsson A-C. Perspectives and challenges of microbial application for crop improvement. *Front. Plant Sci.* 2017;8:49.
4. Weilharter A, Mitter B, Shin M V, Chain PSG, Nowak J, Sessitsch A. Complete genome sequence of the plant growth-promoting endophyte *Burkholderia phytofirmans* strain PsJN. *J. Bacteriol.* 2011;193:3383–4.
5. Duan J, Jiang W, Cheng Z, Heikkila JJ, Glick BR. The complete genome sequence of the plant growth- promoting bacterium *Pseudomonas* sp . UW4. *PLoS ONE.* 2013;8:e58640.
6. Wang X, Luo C, Chen Z. Genome sequence of the plant growth-promoting rhizobacterium *Bacillus* sp. strain 916. *J. Bacteriol.* 2012;194:5467–8.

Discussion

7. He P, Hao K, Blom J, Rückert C, Vater J, Mao Z, et al. Genome sequence of the plant growth promoting strain *Bacillus amyloliquefaciens* subsp. *plantarum* B9601-Y2 and expression of mersacidin and other secondary metabolites. *J. Biotechnol.* 2013;164:281–91.
8. Bruto M, Prigent-Combaret C, Muller D, Moënne-Loccoz Y. Analysis of genes contributing to plant-beneficial functions in plant growth-promoting rhizobacteria and related proteobacteria. *Sci. Rep.* 2014;4:6261.
9. Xie J, Shi H, Du Z, Wang T, Liu X, Chen S. Comparative genomic and functional analysis reveal conservation of plant growth promoting traits in *Paenibacillus polymyxa* and its closely related species. *Sci. Rep.* 2016;6:21329.
10. Bruijn I De, Kock MJD De, Yang M, Waard P De, Beek TA Van, Raaijmakers JM. Genome-based discovery , structure prediction and functional analysis of cyclic lipopeptide antibiotics in *Pseudomonas* species. *Mol. Microbiol.* 2007;63:417–28.
11. Bower S, Perkins JB, Yocum RR, Howitt CL, Rahaim P, Pero J. Cloning, sequencing, and characterization of the *Bacillus subtilis* biotin biosynthetic operon. *J. Bacteriol.* 1996;178:4122–30.
12. Irla M, Neshat A, Brautaset T, Rückert C, Kalinowski J, Wendisch VF. Transcriptome analysis of thermophilic methylotrophic *Bacillus methanolicus* MGA3 using RNA-sequencing provides detailed insights into its previously uncharted transcriptional landscape. *BMC Genomics.* 2015;16:73.
13. Pfeifer-Sancar K, Mentz A, Rückert C, Kalinowski J. Comprehensive analysis of the *Corynebacterium glutamicum* transcriptome using an improved RNAseq technique. *BMC Genomics.* 2013;14:888.
14. Irla M, Heggeset, Tonje M. B. Nærdal I, Paul L, Tone H, Le SB, Brautaset T, et al. Genome-based genetic tool development for *Bacillus methanolicus*: theta- and rolling circle-replicating plasmids for inducible gene expression and application to methanol-based cadaverine production. *Front. Microbiol.* 2016;7:1481.
15. Yoshida N, Sato M. Plasmid uptake by bacteria: a comparison of methods and efficiencies. *Appl. Microbiol. Biotechnol.* 2009;83:791–8.
16. Aune TEV, Aachmann FL. Methodologies to increase the transformation efficiencies and the range of bacteria that can be transformed. *Appl. Microbiol. Biotechnol.* 2010;85:1301–13.
17. Yoshida N, Ikeda T, Yoshida T, Sengoku T, Ogawa K. Chrysotile asbestos fibers mediate transformation of *Escherichia coli* by exogenous plasmid DNA. *FEMS Microbiol. Lett.*

Discussion

2001;195:133–7.

18. Tan H, Fu L, Seno M. Optimization of bacterial plasmid transformation using nanomaterials based on the Yoshida effect. *Int. J. Mol. Sci.* 2010;11:4962–72.
19. Landrigan PJ, Nicholson WJ, Suzuki Y, Ladou J. The Hazards of Chrysotile Asbestos: a critical review. *Ind. Health.* 1999;37:271–80.
20. Mann S, Burkett SL, Davis SA, Fowler CE, Mendelson NH, Sims SD, et al. Sol-gel synthesis of organized matter. *Chem. Mater.* 1997;4756:2300–10.
21. Patil AJ, Li M, Dujardin E, Mann S. Novel bioinorganic nanostructures based on mesolamellar intercalation or single-molecule wrapping of DNA using organoclay building blocks. *Nano Lett.* 2007;7:2660–5.
22. Yang L, Choi SK, Shin HJ, Han HK. 3-Aminopropyl functionalized magnesium phyllosilicate as an organoclay based drug carrier for improving the bioavailability of flurbiprofen. *Int. J. Nanomedicine.* 2013;8:4147–55.
23. Demanèche S, Jocteur-monrozier L, Simonet P. Evaluation of biological and physical protection against nuclease degradation of evaluation of biological and physical protection against nuclease degradation of clay-bound plasmid DNA. *Appl. Env. Microbiol.* 2001;67:293–9.
24. Li Z, Briggs BR, Sheridan PP, Shields MS. An anion-exchange method to concentrate dissolved DNA from aquifer water. *J. Microbiol. Methods.* 2013;93:1–8.
25. Romanowski G, Lorenz M, Wackernagel W. Adsorption of plasmid DNA to mineral surfaces and protection against DNase I. *Appl. Env. Microbiol.* 1991;57:1057–61.
26. Choi HA, Lee YC, Lee JY, Shin HJ, Han HK, Kim GJ. A simple bacterial transformation method using magnesium- and calcium-aminoclays. *J. Microbiol. Methods.* 2013;95:97–101.
27. Kim S, Lee YC, Cho DH, Lee HU, Huh YS, Kim GJ, et al. A simple and non-invasive method for nuclear transformation of intact-walled *Chlamydomonas reinhardtii*. *PLoS ONE.* 2014;9:1–9.
28. Bach E, Fernandes GDC, Maria L, Passaglia P. How to transform a recalcitrant *Paenibacillus* strain: From culture medium to restriction barrier. *J. Microbiol. Methods.* Elsevier B.V.; 2016;131:135–43.
29. Nguyen HD, Nguyen QA, Ferreira RC, Ferreira LCS, Tran LT, Schumann W. Construction of plasmid-based expression vectors for *Bacillus subtilis* exhibiting full structural

Discussion

- stability. *Plasmid*. 2005;54:241–8.
30. Rygus T, Hillen W. Inducible high-level expression of heterologous genes in *Bacillus megaterium* using the regulatory elements of the xylose-utilization operon. *Appl. Microbiol. Biotechnol.* 1991;35:594–9.
 31. Zhang L, Fan F, Palmer LM, Lonetto MA, Petit C, Voelker LL, et al. Regulated gene expression in *Staphylococcus aureus* for identifying conditional lethal phenotypes and antibiotic mode of action. *Gene*. 2000;255:297–305.
 32. Kim L, Mogk A, Schumann W. A xylose-inducible *Bacillus subtilis* integration vector and its application. *Gene*. 1996;181:71–6.
 33. D’Urzo N, Martinelli M, Nenci C, Brettoni C, Telford JL, Maione D. High-level intracellular expression of heterologous proteins in *Brevibacillus choshinensis* SP3 under the control of a xylose inducible promoter. *Microb. Cell Fact.* 2013;12:12.
 34. Altschup SF, Gish W, Miller W, Myers E, Lipman D. Basic local alignment search tool. *J. Mol. Biol.* 1990;215:403–10.
 35. Heggeset TMB, Krog A, Balzer S, Wentzel A, Ellingsen TE, Brautaset T. Genome sequence of thermotolerant *Bacillus methanolicus*: features and regulation related to methylotrophy and production of L-lysine and L-glutamate from methanol. *Appl. Environ. Microbiol.* 2012;78:5170–81.
 36. Irla M, Neshat A, Winkler A, Albersmeier A, Heggeset TMB, Brautaset T, et al. Complete genome sequence of *Bacillus methanolicus* MGA3, a thermotolerant amino acid producing methylotroph. *J. Biotechnol.* 2014;188:110–1.
 37. Ochsner AM, Müller JEN, Mora CA, Vorholt JA. In vitro activation of NAD-dependent alcohol dehydrogenases by Nudix hydrolases is more widespread than assumed. *FEBS Lett.* 2014;588:2993–9.
 38. Pátek M, Nešvera J. Sigma factors and promoters in *Corynebacterium glutamicum*. *J. Biotechnol.* 2011;154:101–13.
 39. Solovyev V, Salamov A. Automatic annotation of microbial genomes and metagenomic sequences. *Metagenomics and its applications in agriculture, biomedicine and environmental studies*. Nova Science Publishers; 2011. p. 61–78.
 40. Luo Y, Zhang L, Barton KW, Zhao H. Systematic identification of a panel of strong constitutive promoters from *Streptomyces albus*. *ACS Synth. Biol.* 2015;4:1001–10.
 41. Liao Y, Huang L, Wang B, Zhou F, Pan L. The global transcriptional landscape of *Bacillus*

Discussion

- amyloliquefaciens* XH7 and high-throughput screening of strong promoters based on RNA-seq data. *Gene*. 2015;571:252–62.
42. Wang J, Ai X, Mei H, Fu Y, Chen B, Yu Z, et al. High-throughput identification of promoters and screening of highly active promoter-5'-UTR DNA region with different characteristics from *Bacillus thuringiensis*. *PLoS ONE*. 2013;8:1–11.
 43. Zhu D, Liu F, Xu H, Bai Y, Zhang X, Saris PEJ, et al. Isolation of strong constitutive promoters from *Lactococcus lactis* subsp. *lactis* N8. *FEMS Microbiol. Lett. Letters*. 2015;362:fnv107.
 44. Batchelor E, Silhavy TJ, Goulian M. Continuous control in bacterial regulatory circuits. *J. Bacteriol*. 2004;186:7618–25.
 45. Kim S Bin, Timmusk S. A simplified method for gene knockout and direct screening of recombinant clones for application in *Paenibacillus polymyxa*. *PLoS ONE*. 2013;8:e68092.
 46. Wang L, Zhang L, Liu Z, Zhao D, Liu X, Zhang B, et al. A minimal nitrogen fixation gene cluster from *Paenibacillus* sp . WLY78 enables expression of active nitrogenase in *Escherichia coli*. *PLoS Genet*. 2013;9:e1003865.
 47. Abd El Daim IA, Häggblom P, Karlsson M, Stenström E, Timmusk S. *Paenibacillus polymyxa* A26 Sfp-type PPTase inactivation limits bacterial antagonism against *Fusarium graminearum* but not of *F. culmorum* in kernel assay. *Front. Plant Sci*. 2015;6:368.
 48. Datsenko KA, Wanner BL. One-step inactivation of chromosomal genes in *Escherichia coli* K-12 using PCR products. *Proc. Natl. Acad. Sci. USA*. 2000;97:6640–5.
 49. Zarschler K, Janesch B, Zayni S, Schaffer C, Messner P. Construction of a gene knockout system for application in *Paenibacillus alvei* CCM 2051^T, exemplified by the S-layer glycan biosynthesis initiation enzyme WsfP. *Appl. Env. Microbiol*. 2009;75:3077–85.
 50. Tong Y, Charusanti P, Zhang L, Weber T, Lee SY. CRISPR-Cas9 based engineering of actinomycetal genomes. *ACS Synth. Biol*. 2015;4:1020–9.
 51. Cleto S, Jensen JK, Wendisch VF, Lu TK. *Corynebacterium glutamicum* metabolic engineering with CRISPR interference (CRISPRi). *ACS Synth. Biol*. 2016;5:375–85.
 52. Generoso WC, Gottardi M, Oreb M, Boles E. Simplified CRISPR-Cas genome editing for *Saccharomyces cerevisiae*. *J. Microbiol. Methods*. 2016;127:203–5.
 53. Mozafar A, Oertli JJ. Thiamin (vitamin B1): translocation and metabolism by soybean seedling. *J. Plant Physiol*. 1993;142:438–45.

Discussion

54. Oertli JJ. Exogenous application of vitamins as regulators for growth and development of plants—a review. *Z. Pflanzenernähr. Bodenkd.* 1987;150:375–91.
55. Streit W, Joseph C, Phillips D. Biotin and other water-soluble vitamins are key growth factors for alfalfa root colonization by *Rhizobium meliloti* 1021. *Mol. Plant. Microbe Interact.* 1996;9:330–8.
56. Marek-Kozaczuk M, Skorupska A. Production of B-group vitamins by plant growth-promoting *Pseudomonas fluorescens* strain 267 and the importance of vitamins in the colonization and nodulation of red clover. *Biol. Fertil. Soils.* 2001;33:146–51.
57. Dahm H, Rózycki H, Strzelczyk E, Li C. Production of B-group vitamins by *Azospirillum* spp. grown in media of different pH at different temperatures. *Zentralbl. Mikrobiol.* 1993;148:195–203.
58. Strzelczyk E, Dahm H, Pachlewski R. B-group vitamins production by mycorrhizal fungi in response to pH (in vitro studies). *Plant Soil.* 1991;137:237–41.
59. Revillas JJ, Rodelas B, Pozo C, Martinez-Toledo M V, Gonzalez LJ. Production of B-Group vitamins by two *Azotobacter* strains with phenolic compounds as sole carbon source under diazotrophic and adiazotrophic conditions. *J. Appl. Microbiol.* 2000;89:486–93.
60. Deryło M, Skorupska A. Enhancement of symbiotic nitrogen fixation by vitamin-secreting fluorescent *Pseudomonas*. *Plant Soil.* 1993;154:211–7.
61. Rodelas B, Salmerón V, Martinez-Toledo M V., González-López J. Production of vitamins by *Azospirillum brasilense* in chemically-defined media. *Plant Soil.* 1993;153:97–101.
62. Gloeckler R, Ohsawa I, Speck D, Ledoux C, Bernard S, Zinsius M, et al. Cloning and characterization of the *Bacillus sphaericus* genes controlling the bioconversion of pimelate into dethiobiotin. *Gene.* 1990;87:63–70.
63. Lin S, Cronan JE. Closing in on complete pathways of biotin biosynthesis. *Mol. Biosyst.* 2011;1811–21.
64. Entcheva P, Phillips DA, Streit WR. Functional analysis of *Sinorhizobium meliloti* genes involved in biotin synthesis and transport. *Appl. Env. Microbiol.* 2002;68:2843–8.
65. Hatakeyama K, Kohama K, Vertès AA, Kobayashi M, Kurusu Y, Yukawa H. Genomic organization of the biotin biosynthetic genes of coryneform bacteria: Cloning and sequencing of the *bioA-bioD* genes from *Brevibacterium flavum*. *DNA Seq.* 1993;4:177–84.
66. Serebriiskii IG, Vassin VM, Tsygankov YD. Two new members of the bio B superfamily:

Discussion

- cloning, sequencing and expression of bio B genes of *Methylobacillus flagellatum* and *Corynebacterium glutamicum*. *Gene*. 1996;175:15–22.
67. Peters-Wendisch P, Götter S, Heider SAE, Reddy GK, Nguyen AQ, Stansen KC, et al. Engineering biotin prototrophic *Corynebacterium glutamicum* strains for amino acid, diamine and carotenoid production. *J. Biotechnol.* 2014;192:346–54.
 68. Streit WR, Phillips DA. Recombinant *Rhizobium meliloti* strains with extra biotin synthesis capability. *Appl. Env. Microbiol.* 1996;62:3333–8.
 69. Streit W, Entcheva P. Biotin in microbes, the genes involved in its biosynthesis, its biochemical role and perspectives for biotechnological production. *Appl. Microbiol. Biotechnol.* 2003;61:21–31.
 70. Azaizeh HA, Neumann G, Marschner H. Effects of thiamine and nitrogen fertilizer form on the number of N₂-fixing and total bacteria in the rhizosphere of maize plants. *Z. Pflanzenernähr. Bodenkd.* 1996;159:183–8.
 71. Dakora FD, Phillips DA. Root exudates as mediators of mineral acquisition in low-nutrient environments. *Plant Soil.* 2002;245:35–47.
 72. Rovira A, Harris J. Plant root excretions in relation to the rhizosphere effect. *Plant Soil.* 1961;14:199–214.
 73. Breaker RR. Riboswitches and the RNA world. *Cold Spring Harb. Perspect. Biol.* 2012;4:a003566.
 74. Kubodera T, Watanabe M, Yoshiuchi K, Yamashita N, Nishimura A, Nakai S, et al. Thiamine-regulated gene expression of *Aspergillus oryzae thiA* requires splicing of the intron containing a riboswitch-like domain in the 5'-UTR. *FEBS Lett.* 2003;555:516–20.
 75. Sudarsan N, Barrick J, Breaker R. Metabolite-binding RNA domains are present in the genes of eukaryotes. *RNA.* 2003;9:644–7.
 76. Bocobza S, Adato A, Mandel T, Shapira M, Nudler E, Aharoni A. Riboswitch-dependent gene regulation and its evolution in the plant kingdom. *Genes Dev.* 2007;21:2874–9.
 77. Berens C, Groher F, Suess B. RNA aptamers as genetic control devices: the potential of riboswitches as synthetic elements for regulating gene expression. *Biotechnol. J.* 2015;10:246–57.
 78. Lünse CE, Scott FJ, Suckling CJ, Mayer G. Novel TPP-riboswitch activators bypass metabolic enzyme dependency. *Front. Chem.* 2014;2:53.
 79. Du Q, Wang H, Xie J. Thiamin (vitamin B1) biosynthesis and regulation: a rich source of

Discussion

- antimicrobial drug targets? *Int. J. Biol. Sci.* 2011;7:41–52.
80. Schyns G, Potot S, Geng Y, Perkins JB. Isolation and characterization of new thiamine-deregulated mutants of *Bacillus subtilis*. *J. Bacteriol.* 2005;187:8127–36.
81. Palacios OA, Bashan Y, De-Bashan LE. Proven and potential involvement of vitamins in interactions of plants with plant growth-promoting bacteria-an overview. *Biol. Fertil. Soils.* 2014;50:415–32.
82. Leonardi R, Roach PL. Thiamine biosynthesis in *Escherichia coli*: In vitro reconstitution of the thiazole synthase activity. *J. Biol. Chem.* 2004;279:17054–62.
83. Melnick J, Lis E, Park J, Kinsland C, Mori H, Baba T, et al. Identification of the two missing bacterial genes involved in thiamine salvage: thiamine pyrophosphokinase and thiamine kinase. *J. Bacteriol.* 2004;186:3660–2.
84. Rodionov DA, Mironov AA, Gelfand MS. Conservation of the biotin regulon and the BirA regulatory signal in Eubacteria and Archaea. *Genome Res.* 2002;12:1507–16.
85. Seldin L, Rosado AS, William D, Cruz DA, Nobrega A, Elsas JANDVAN, et al. Comparison of *Paenibacillus azotofixans* strains isolated from rhizoplane, rhizosphere, and non-root-associated soil from maize planted in two different Brazilian soils. *Appl. Environ. Microbiol.* 1998;64:3860–8.
86. Hu X, Chen J, Guo J, Hangzhou X. Two phosphate- and potassium-solubilizing bacteria isolated from Tianmu Mountain, Zhejiang, China. *World J. Microbiol. Biotechnol.* 2006;22:983–90.
87. Berge O, Guinebretière M, Achouak W, Normand P, Heulin T. *Paenibacillus graminis* sp. nov. and *Paenibacillus odorifer* sp. nov., isolated from plant roots, soil and food. *Int. J. Syst. Evol. Microbiol.* 2017;4:607–16.
88. Narayan S, Swarnalee D, Anil D. Plant growth-promoting chitinolytic *Paenibacillus elgii* responds positively to tobacco root exudates. *J. Plant Growth Regul.* 2010;29:409–18.
89. Marra LM, Oliveira SM De, Ademar P, Ferreira A. Biological nitrogen fixation and phosphate solubilization by bacteria isolated from tropical soils. *Plant Soil.* 2012;357:289–307.
90. Wang Y, Shi Y, Li B, Shan C, Ibrahim M, Jabeen A, et al. Phosphate solubilization of *Paenibacillus polymyxa* and *Paenibacillus macerans* from mycorrhizal and non-mycorrhizal cucumber plants. *Afr. J. Microbiol. Res.* 2012;6:4567–73.
91. Pandya M, Rajput M, Rajkumar S. Exploring plant growth promoting potential of non

Discussion

- rhizobial root nodules endophytes of *Vigna radiata*. *Microbiology*. 2015;84:80–9.
92. Gügi B, Orange N, Hellio F, Burini JF, Guillou C, Leriche F, et al. Effect of growth temperature on several exported enzyme activities in the psychrotrophic bacterium *Pseudomonas fluorescens*. *J. Bacteriol.* 1991;173:3814–20.
93. Song OR, Lee SJ, Lee YS, Lee SC, Kim KK, Choi YL. Solubilization of insoluble inorganic phosphate by *Burkholderia cepacia* DA23 isolated from cultivated soil. *Braz. J. Microbiol.* 2008;39:151–6.
94. Thaller MC, Berlutti F, Schippa S, Iori P, Passariello C, Rossolini GM. Heterogeneous patterns of acid phosphatases containing low-molecular-mass polypeptides in members of the family *Enterobacteriaceae*. *Int. J. Syst. Evol. Microbiol.* 1995;45:255–61.
95. Richardson AE, Hadobas PA. Soil isolates of *Pseudomonas* spp. that utilize inositol phosphates. *Can. J. Microbiol.* 1997;43:509–16.
96. Ohtake H, Wu H, Imazu K, Anbe Y, Kato J, Kuroda A. Bacterial phosphonate degradation, phosphite oxidation and polyphosphate accumulation. *Resour. Conserv. Recy.* 1997;66:611–20.
97. McGrath JW, Wisdom GB, McMullan G, Larkin MJ, Quinn JP. The purification and properties of phosphonoacetate hydrolase, a novel carbon-phosphorus bond-cleavage enzyme from *Pseudomonas fluorescens* 23F. *Eur. J. Biochem.* 1995;234:225–30.
98. Qi Y, Kobayashi Y, Hulett FM. The *pst* operon of *Bacillus subtilis* has a phosphate-regulated promoter and is involved in phosphate transport but not in regulation of the *pho* regulon. *J. Bacteriol.* 1997;179:2534–9.
99. Atalla A, Schumann W. The *pst* operon of *Bacillus subtilis* is specifically induced by alkali stress. *J. Bacteriol.* 2003;185:5019–22.
100. Metcalf WW, Wanner BL. Mutational analysis of an *Escherichia coli* fourteen-gene operon for phosphonate degradation, using *TnpA*' elements. *J. Bacteriol.* 1993;175:3430–42.
101. Shahid M, Hameed S. Root colonization and growth promotion of sunflower (*Helianthus annuus* L.) by phosphate solubilizing *Enterobacter* sp. Fs-11. *World J. Microbiol. Biotechnol.* 2012;28:2749–58.
102. Vyas P, Gulati A. Organic acid production in vitro and plant growth promotion in maize under controlled environment by phosphate-solubilizing fluorescent *Pseudomonas*. *BMC Microbiol.* 2009;9:174.
103. Chen YP, Rekha PD, Arun AB, Shen FT, Lai W, Young CC. Phosphate solubilizing bacteria

Discussion

- from subtropical soil and their tricalcium phosphate solubilizing abilities. *Appl. Soil Ecol.* 2006;34:33–41.
104. Werra P De, Pe M, Keel C, Maurhofer M. Role of gluconic acid production in the regulation of biocontrol traits of *Pseudomonas fluorescens* CHA0. *Appl. Env. Microbiol.* 2009;75:4162–74.
105. Wendisch VF, Spies M, Reinscheid DJ, Schnicke S, Sahm H, Eikmanns BJ. Regulation of acetate metabolism in *Corynebacterium glutamicum*: transcriptional control of the isocitrate lyase and malate synthase genes. *Arch. Microbiol.* 1997;168:262–9.
106. Zeng Q, Wu X, Wang J, Ding X. Phosphate solubilization and gene expression of phosphate-solubilizing bacterium *Burkholderia multivorans* WS-FJ9 under different levels of soluble phosphate. *J. Microbiol. Biotechnol.* 2017;27:844–55.
107. Paul K, Erhardt M, Hirano T, Blair DF, Hughes KT. Energy source of flagellar type III secretion. *Nature.* 2008;451:489–92.
108. Mukherjee S, Kearns DB. The structure and regulation of flagella in *Bacillus subtilis*. *Annu. Rev. Genet.* 2014;48:319–40.
109. Yonekura K, Maki-Yonekura S, Namba K. Complete atomic model of the bacterial flagellar filament by electron cryomicroscopy. *Nature.* 2003;424:643–50.
110. Macnab RM. Genetics and biogenesis of bacterial flagella. *Annu. Rev. Genet.* 1992;26:131–58.
111. Guttenplan SB, Shaw S, Kearns DB. The cell biology of peritrichous flagella in *Bacillus subtilis*. *Mol. Microbiol.* 2013;87:211–29.
112. Guttenplan SB, Kearns DB. Regulation of flagellar motility during biofilm formation. *FEMS Microbiol. Rev.* 2013;37:849–71.
113. Bach E, Seger GD dos S, Fernandes G de C, Lisboa BB, Passaglia LMP. Evaluation of biological control and rhizosphere competence of plant growth promoting bacteria. *Appl. Soil Ecol.* 2016;99:141–9.
114. Beneduzi A, Costa PB, Melo IS, Bodanese-zanettini MH, Passaglia LMP. *Paenibacillus riograndensis* sp. nov ., a nitrogen- fixing species isolated from the rhizosphere of *Triticum aestivum*. *Int. J. Syst. Evol. Microbiol.* 2010;60:128–33.

4. APPENDIX

Supplementary material to “Magnesium-aminoclay-based transformation of Paenibacillus riograndensis and Paenibacillus polymyxa and development of tools for inducible gene expression”.

Table S1. Sequence of oligonucleotides used in this study.

Oligonucleotides	Sequence (5' – 3')
<i>Protein fusion plasmids</i>	
bbpREcm ^R fw	taaaagccagtcattaggcctatc
bbpREcm ^R rv	tatgagataatgccgactgtac
gfcM ^R fw	aaagtacagtcggcattatctc ataattttgtagagctcatccatgc
gfcM ^R rv	gataggcctaatactgactggcttt aatgagtaaaggagaagaacttttcac
crim ^R fw	aaagtacagtcggcattatctc ataactactggaacaggtggggc
crim ^R rv	gataggcctaatactgactggcttt aatggatagcactgagaacgtcatcaag
mChcm ^R fw	aaagtacagtcggcattatctc ataataagcaccggaggagtgacgacc
mChcm ^R rv	gataggcctaatactgactggcttt aatggcgagtagcgaagacgttatcaaaag
<i>Constitutive expression plasmids</i>	
bbpREfw	gcagccaagcttggcgtaatcatg
bbpRErv	gatccatatggtaccgccatagg
pgapfw	catgattacgccaagcttggctg ccgaatcgctcgctattattttaac
pgaprv	tgaatagttcctcctagatttcg
gfp ^R gapfw	aacgaaatctaggaggaaactattca atgagtaaaggagaagaacttttc
ppykfw	catgattacgccaagcttggctg caatgacacagcgtcgactaaagac
ppykrv	taggtttcctccggtttttcgttc
gfp ^R pykfw	gaacg aaaaaacgga ggaaaacct aatgagtaaaggagaagaacttttc
ptuffw	catgattacgccaagcttggctg cactcaaaagcagccaagacaag
ptufrv	gaacagttcctcctaatgt
gfp ^R ptuffw	acccacattaaggaggaaactgtt catgagtaaaggagaagaacttttc
gfpRErv	cctatggcgggtaccatattggat ctattttgtagagctcatccatg
<i>Inducible expression plasmids</i>	
<i>Mannitol inducible</i>	
bbpRE-gfp ^R UVfw	atgattgaacaagaggtaccggtagaa
bbpRE-gfp ^R UVrv	ctgcagccaagcttggcgtaatcatggtcatagctg
M1fw	tacgccaagcttggctg cagggggcgccgagcggaaaagtatg
M1rv	ggtacctctgttcaatcatt taaaatgccccctatgtagtgaatgg
M3fw	tacgccaagcttggctg cagaaccaggagcctttttatt
M3rv	ggtacctctgttcaatcatt ataataaacctccctgctttt
bbpRM2-gfp ^R UVfw	ggatccatatggtaccgccatagg
bbpRM2-gfp ^R UVrv	atgtactacctcctaaggaaatttaaaaaaac

Appendix

bioWAFDBIpEKEX3fw **gtttttttaaattccttaggaggtacat**atgcaagaagaacttttatagtg
 bioWAFDBIpEKEX3rv **cctatggcgggtaccat**atggatcctattcaaaagtcaccggcagctcc
Xylose inducible
 bbEcoRVpTEfw atctaaaaatcaaaggggaaatgg
 bbEcoRVpTErv atcactagttggaccattgtcatttccc
 cripTEfw **atgacaaatgg**tccaaactagtgatggatagcactgagaacgtcatcaag
 cripTErv **cccattcccccttgatttt**agatctactggaacaggtggggc
 mChpTEfw **atgacaaatgg**tccaaactagtgattaaagcaccggggagtgacgacc
 mChpTErv **cccattcccccttgatttt**agatggcgagtagcgaagacgttatcaag

Overlaps in bold.

Table S2. GfpUV and Crimson fluorescence of *P. riograndensis* cells co-expressing pRE with pTE (EE), pRM2-*gfpUV* with pTE (RE), pRE with pTX-*crimson* (ET) or pRM2-*gfpUV* with pTX-*crimson* (RT) cultivated with the addition of 0, 25 or 50 mM of xylose and mannitol to the growth medium. The table shows means and standard deviations of biological triplicates.

Strain	Mean fluorescence intensity							
	EE		RE		ET		RT	
plasmids	pRE, pTE		pRM2- <i>gfpUV</i> , pTE		pRE, pTX- <i>crimson</i>		pRM2- <i>gfpUV</i> , pTX- <i>crimson</i>	
	GfpUV fluorescence							
0 mM inducer	0.23	± 0.09	0.60	± 0.11	0.33	± 0.10	0.42	± 0.07
25 mM inducer	0.24	± 0.04	0.62	± 0.32	0.40	± 0.19	0.60	± 0.13
50 mM inducer	0.22	± 0.05	2.22	± 0.05	0.43	± 0.13	1.60	± 0.17
	Crimson fluorescence							
0 mM inducer	0.40	± 0.29	0.21	± 0.09	0.34	± 0.05	0.28	± 0.23
25 mM inducer	0.32	± 0.20	0.20	± 0.10	0.44	± 0.17	0.32	± 0.28
50 mM inducer	0.28	± 0.16	0.20	± 0.13	2.09	± 0.15	1.19	± 0.21

Appendix

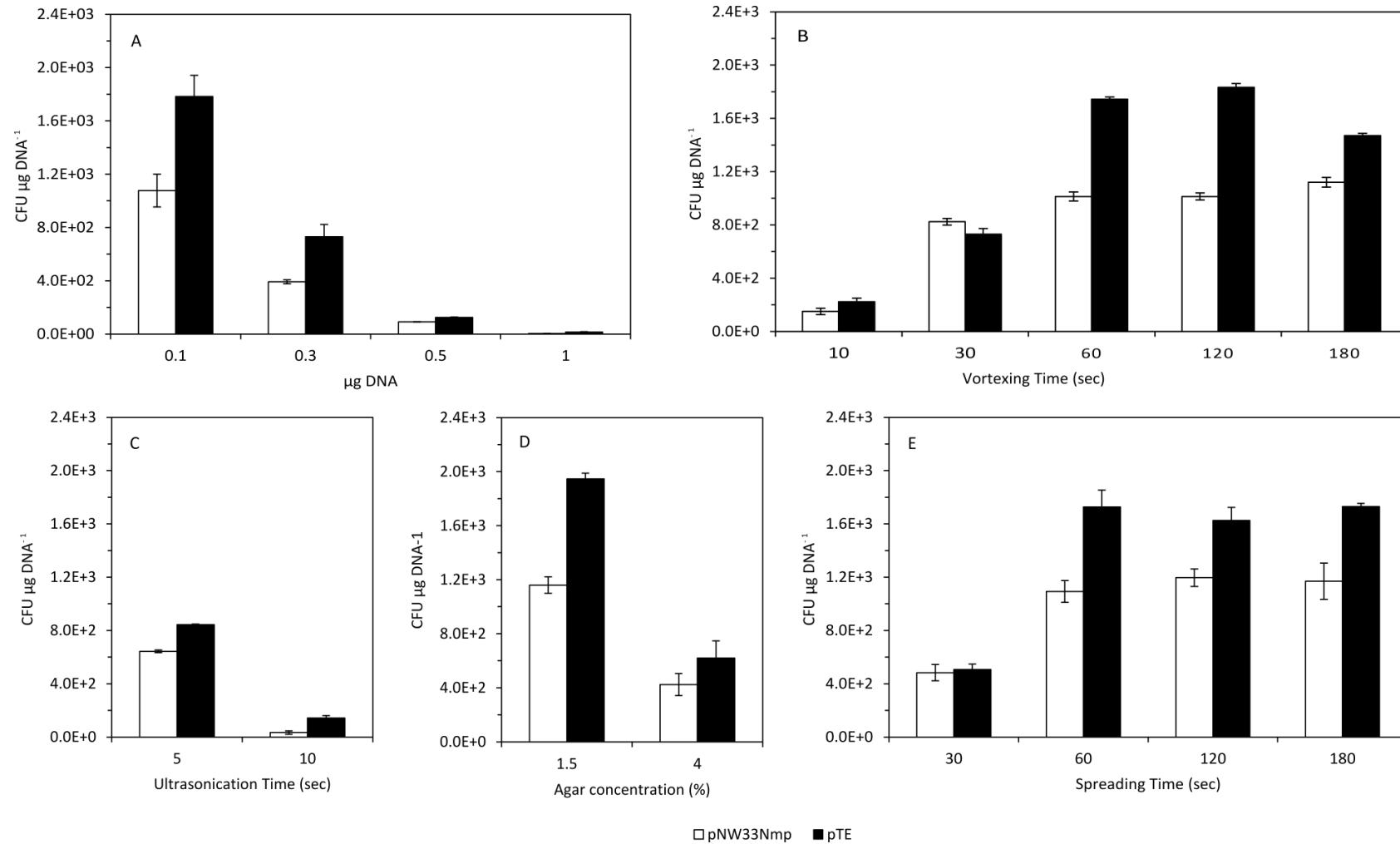


Figure S1. Transformation efficiency (CFU $\mu\text{g DNA}^{-1}$) of *P. riograndensis* using the magnesium aminoclay method at different parameters. The amount of DNA of plasmids pNW33Nmp or pTE (A), mixing time of the cells with magnesium aminoclay and plasmids by vortexing (B) or ultrasonication (C), and the friction force by varying agar concentration (D) or spreading time (E) on the plate were analyzed. Means and standard deviations of triplicates are shown.

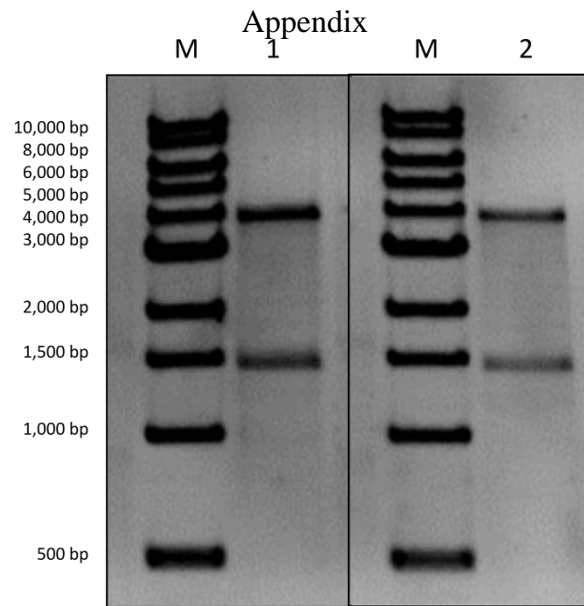


Figure S2. Electrophoresis gel image of plasmid pNW33Nmp restricted with the enzyme *AclI*. The plasmid DNA was derived either from *P. riograndensis* SBR5(pNW33Nmp) (1) or from *E. coli* transformed with plasmid DNA isolated from the *P. riograndensis* SBR5(pNW33Nmp) (2). M-molecular weight marker.

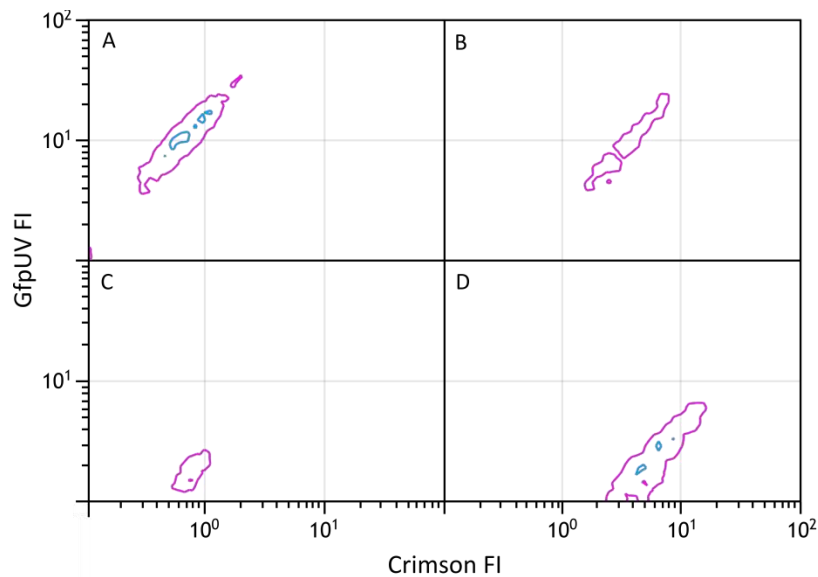


Figure S3. Reporter gene expression analysis of *P. riograndensis* cells carrying two compatible expression vectors. GfpUV and Crimson fluorescence was analysed by FACS scanning of populations of 3,000 *P. riograndensis* cells carrying the two compatible plasmids pRM2-*gfpUV* and pTX-*crimson*. Cells were cultivated in the absence of inducers (C), in the presence of 50 mM xylose (A), 50 mM mannitol (D) a mixture of 50 mM xylose and 50 mM mannitol (B).

Appendix

Supplementary material to “Differential gene expression of phosphate solubilizing-bacterium *Paenibacillus riograndensis* SBR5 cultivated in two distinct phosphate sources”.

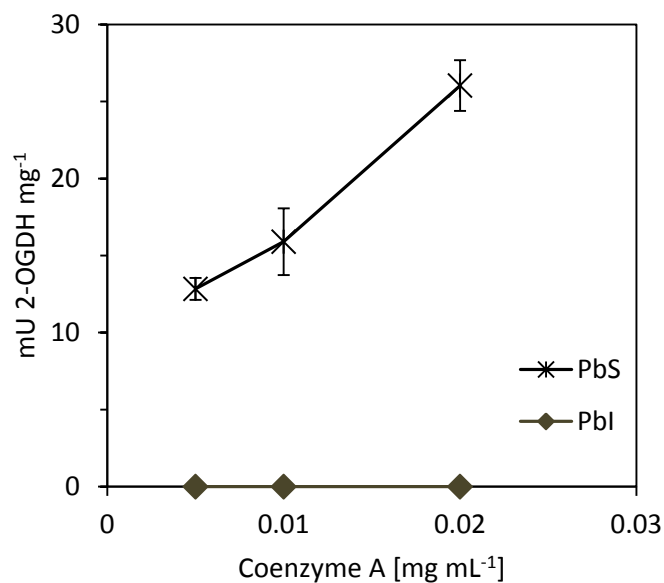


Figure S1. 2-Oxoglutarate dehydrogenase (2-OGDH) specific activities (mU 2OGDH mg⁻¹) in crude extracts of *P. riograndensis* SBR5 cultivated in PVK broth (PbI) in comparison to cultivation in PVK broth having NaH₂PO₄ as P source (PbS). The activity of 2-oxoglutarate dehydrogenase was measured dependently of the concentration of CoA (mg mL⁻¹)

Acknowledgements

I thank:

Prof. Dr. Volker F. Wendisch for accepting me in his group and for the supervision and patience during the past years.

Dr. Petra Peters-Wendisch and Dr. Marta Irla for the constructive critique of this thesis.

Dr. Irla, for the whole “Marta treatment” through the writing process and also through my life.

CAPES and Science without Borders Program for funding me.

Members of Dr. Jörn Kalinowski group for the help during genomic/transcriptomic analysis.

Gagi, Jaide, Marta, João, Fernando and Samanta (my favorite gaúcha ever) for being my “Bielefeld family”.

Spanish speakers (including Marta and Guido) for the hilarious moments and for making me feel closer to home.

All my “PhD” colleagues from Genpro: Marta, Lenny, Christian, João, Guido, Benno, Daniel, Gagi, Eli, Melanie, Kareen, Sabine, Fernando, Nadja, Marius, Jonas, Jojo, Anh, Ahmed, Elvira, Pierre, Carlos, Jaide, Hiro, Dorit, Stephi, Marina and Samanta.

Mila, Irene, Susanne, Sabine and Lucy for the support inside the lab and Petra K for the support outside the lab.

Fernando, por el apoyo, lealtad y PACIENCIA en el tiempo que hemos pasado.

Minha família, especialmente minha mãe, por estar comigo a cada segundo da minha vida mesmo estando separados por um oceano.

